DOE/MC/11076-2448
(DE88005703)

Characterization of DOE reference oil shales: Mahogany Zone, Parachute Creek Member, Green River Formation Oil Shale, and Clegg Creek Member, New Albany Shale

Miknis, F.P.; Robertson, R.E.

Sep 1987

Western Research Inst., Laramie, WY (USA)

DISCLAIMER

This report was prepared as an account of work sponsored by an agency of the United States Government. Neither the United States Government nor any agency thereof, nor any of their employees, makes any warranty, express or implied, or assumes any legal liability or responsibility for the accuracy, completeness, or usefulness of any information, apparatus, product, or process disclosed, or represents that its use would not infringe privately owned rights. Reference herein to any specific commercial product, process, or service by trade name, trademark, manufacturer, or otherwise does not necessarily constitute or imply its endorsement, recommendation, or favoring by the United States Government or any agency thereof. The views and opinions of authors expressed herein do not necessarily state or reflect those of the United States Government or any agency thereof.

This report has been reproduced directly from the best available copy.

Available from the National Technical Information Service, U. S. Department of Commerce, Springfield, Virginia 22161.

Price: Printed Copy A05
Microfiche A01

Codes are used for pricing all publications. The code is determined by the number of pages in the publication. Information pertaining to the pricing codes can be found in the current issues of the following publications, which are generally available in most libraries: *Energy Research Abstracts (ERA); Government Reports Announcements* and Index *(GRA* and I); *Scientific and Technical Abstract Reports (STAR);* and publication NTIS-PR-360 available from NTIS at the above address.

Printed in the United States of America
USDOE Office of Scientific and Technical Information
Oak Ridge, Tennessee

DOE/MC/11076-2448
(DE88005703)
Distribution Category UC-123

CHARACTERIZATION OF DOE REFERENCE OIL SHALES: MAHOGANY ZONE, PARACHUTE CREEK MEMBER, GREEN RIVER FORMATION OIL SHALE, AND CLEGG CREEK MEMBER, NEW ALBANY SHALE

By
Francis P. Miknis
Raymond E. Robertson
Coprincipal Investigators

September 1987

Work Performed Under Cooperative Agreement
DE-FC21-86MC11076

For
U.S. Department of Energy
Office of Fossil Energy
Morgantown Energy Technology Center
Laramie Project Office
Laramie, Wyoming

By
Western Research Institute
Laramie, Wyoming

TABLE OF CONTENTS

LIST OF TABLES

LIST OF TABLES (Continued)

LIST OF FIGURES

LIST OF FIGURES (Continued)

SUMMARY

Measurements have been made on the chemical and physical properties of two oil shales designated as reference oil shales by the Department of Energy. One oil shale is a Green River Formation, Parachute Creek Member, Mahogany Zone Colorado oil shale from the Exxon Colony mine and the other is a Clegg Creek Member, New Albany shale from Kentucky. Material balance Fischer assays, carbon aromaticities, thermal properties, and bulk mineralogic properties have been determined for the oil shales. Kerogen concentrates were prepared from both shales. The measured properties of the reference shales are comparable to results obtained from previous studies on similar shales. The western reference shale has a low carbon aromaticity, high Fischer assay conversion to oil, and a dominant carbonate mineralogy. The eastern reference shale has a high carbon aromaticity, low Fischer assay conversion to oil, and a dominant silicate mineralogy.

Chemical and physical properties, including ASTM distillations, have been determined for shale oils produced from the reference shales. The distillation data were used in conjunction with API correlations to calculate a large number of shale oil properties that are required for computer models such as ASPEN. There was poor agreement between measured and calculated molecular weights for the total shale oil produced from each shale. However, measured and calculated molecular weights agreed reasonably well for true boiling point distillate fractions in the temperature range of 204-399°C (400-750°F). Similarly, measured and calculated viscosities of the total shale oils were in disagreement, whereas good agreement was obtained on distillate fractions for a boiling range up to 315°C (600°F). Thermal and dielectric properties were determined for the shales and shale oils. The dielectric properties of the reference shales and shale oils decreased with increasing frequency of the applied frequency.

INTRODUCTION

In 1984 the Department of Energy (DOE) made an assessment of its oil shale program based on information from industry, the Fossil Energy Research Working Group, a National Research Council review of safety issues related to synthetic fuels development, a review of available oil shale data, and an examination of the existing DOE oil shale program. This led to a restructuring of the DOE oil shale program. An integral part of the restructured program involves the measurement of fundamental chemical and physical properties of reference oil shales.

The DOE reference oil shale program began in October 1985, when Terra Tek, Inc. of Salt Lake City, Utah was awarded a DOE contract for the establishment and maintenance of an oil shale sample bank. Work sponsored by DOE on oil shales is to be conducted on oil shales in the reference shale program, the idea being that data obtained from different research programs on the reference shales will be more consistent and more readily correlated with other oil shale data.

Under the DOE reference shale program, two oil shales per year will be acquired and characterized over a five-year period. A total of ten oil shales will be acquired; five will be from the western United States deposits, and five will be from deposits in the eastern United States. The shales selected will be as representative as possible of what may likely be used in future oil shale development.

Fundamental chemical and physical properties of the first pair of reference oil shales have been acquired. The measurements fall into three general categories: 1) chemical and physical properties of organic matter, 2) mineralogic properties, and 3) chemical and physical properties of shale oils produced from the reference shales. The results of these various measurements are the subject of this report.

PROPERTIES OF ORGANIC MATTER

Oil Shale Samples

The reference shales were sent to WRI from Terra Tek during the first quarter of FY 87. The western reference shale is a Mahogany zone, Parachute Creek Member, Green River Formation oil shale obtained from the Exxon Colony mine located near Parachute, Colorado. The eastern reference shale is a Clegg Creek member, New Albany shale obtained from the Knieriem quarry, which is located approximately 16 miles south of the Ohio river at Louisville, Kentucky. Both of the reference oil shales have been described in detail (Owen 1987).

The oil shale that was received from Terra Tek had a top size of approximately 3/4 in. The material was further reduced in size by grinding, and then riffled to obtain representative sample material for the respective property measurements tasks. Additional sample preparation of the representative material was made, commensurate with the analytical requirements of the tasks.

Material Balance Fischer Assay

Probably the single most important piece of information about an oil shale is its potential to produce oil during heating. The Fischer assay (American Society for Testing and Materials, Method D-3904-80) is the traditional method for determining the oil potential of an oil shale. In brief, the Fischer assay consists of heating a 100-g sample of oil shale to 500°C (932°F) at a rate of 12°C/min and maintaining this temperature for another 40 minutes. The hydrocarbon vapors that distill from the sample condense to form a shale oil. This material is collected, its volume and weight recorded, and specific gravity determined. From these measurements the oil potential is reported in either weight percent or gallons of oil per ton of shale. In a material balance Fischer assay (MBFA) developed by the Western Research Institute, the elemental compositions of the products are determined as well.

MBFA results for the reference shales are reported in Table 1 of Appendix A. Gas compositional data are given in Table 2. The conversion of organic matter to gas, oil, and residue products can be determined from these data (Table 3). The greater conversion of organic carbon to oil for the western reference shale is clearly evident from the data in Table 3. The differences in conversion of organic carbon to oil, gas, and residue products are related to the carbon structure of the original organic matter.

Carbon Aromaticity Measurements

Modern analytical techniques make it possible to determine some of the chemical structural features of the kerogen. The most significant of these are cross polarization (CP), magic-angle spinning (MAS), ^{13}C nuclear magnetic resonance (NMR) techniques (Miknis et al. 1979). The CP/MAS ^{13}C NMR techniques provide a direct, nondestructive measurement of the organic carbon distribution in oil shales. In particular the fractions of aromatic and aliphatic carbons can be determined. These carbon types represent the major carbon fractions in oil shales, and their relative amounts largely determine the conversion behavior of oil shales. Highly aliphatic oil shales have high conversions to oil (Miknis et al. 1982a) while highly aromatic oil shales produce greater residue carbon (Miknis et al. 1982b).

Solid-state ^{13}C NMR measurements were made on the reference shales, and liquid-state ^{13}C NMR measurements were made on the MBFA shale oils (Table 4). The carbon aromaticity values of the shales are compatible with their conversion data in Table 3. In addition, the shale oil aromaticity values are similar to results of previous work for similar shales (Netzel and Miknis 1982; Miknis et al. 1986).

NMR Measurements of Shale Oil Carbon Types

A practical procedure was developed (Netzel 1987) and used in this study whereby the fraction of carbon types--primary (CH_3), secondary (CH_2), tertiary (CH), and quaternary (C)--can be quantitatively determined using DEPT (Distortionless Enhancement by Polarization

Transfer (Bendall and Pegg 1983)), and QUAT (Quaternary Only Carbon Spectra (Bendall et al. 1982)) pulse sequences. The DEPT/QUAT technique is preferable to other spin-echo techniques because less time is required for data acquisition and reduction.

The carbon and hydrogen distributions calculated from the ^{13}C DEPT and QUAT spectra of the eastern and western shale oils are given in Table 5. The normalized hydrogen type distribution data were calculated using the carbon type distribution data. The structural parameters listed in Table 6 were calculated from the DEPT and QUAT spectra, and are compared with data obtained directly from conventional ^{1}H and ^{13}C NMR spectra. The agreement between the two methods is very good considering the possible sources of error involved in obtaining quantitative NMR data. There are noticeable differences in the quaternary and tertiary aromatic carbon distributions, and in the secondary aliphatic carbon distributions in the two shale oils. These differences basically reflect the fact that the eastern oil shale has more aromatic carbon than the western oil shale.

Oxygen Determination by Neutron Activation Analysis

Samples of raw shale, MBFA spent shale, and MBFA shale oils were sent to an outside laboratory (IRT Corporation, San Diego, CA) for direct oxygen determination by neutron activation analysis. Each sample, along with an oxygen standard, was irradiated with 14 MeV neutrons, and counted for ^{16}N induced activity on a single pulse-height analyzer using a pair of 5-in. x 5-in. NaI(Tl) scintillation crystals. The oxygen concentration was determined by comparing the intensity of the 6.13 MeV gamma-ray photopeak of ^{16}N in the sample with that of the oxygen standard. The basic nuclear reaction for the process is $^{16}O(n,p)^{16}N$.

Oxygen determinations were made in triplicate for the raw and spent shales except for the raw eastern shale, while single samples of oils were analyzed (Table 7). The reported values are for total oxygen and included contributions from organic and inorganic sources. For the raw and spent shales, it is not possible to determine the amount of organic oxygen. However, the oxygen values for the shale oils are organic oxygen values, and these can be compared with the values obtained by subtracting the sum of the carbon, hydrogen, sulfur, and nitrogen weight percent values in each oil (Table 1) from 100%, i.e. using oxygen by difference.

There is close agreement between the direct and by difference oxygen values for the western reference shale oil. However, the agreement between the two values for the eastern shale oil is not as good.

Kerogen Concentrates

It is difficult to characterize the organic matter in raw shales because the bulk of oil shale is inorganic matter. Even a simple determination of the elemental composition (carbon, hydrogen, nitrogen, oxygen, and sulfur) is compromised by contributions from inorganic sources of these elements. To obtain the elemental composition of the organic matter, it is necessary to remove the mineral matter, without altering the composition of the kerogen.

Most kerogen concentration schemes involve four steps: removal of bitumen, decomposition of carbonate rocks, destruction of silicates, and destruction of pyrites. It is desirable to carry out these steps with as little chemical alteration of the kerogen as possible. If kerogen functional groups are drastically altered during concentration, subsequent studies of properties will give questionable results.

The procedures used for the first three steps are fairly straightforward and are based on work by Durand and Nicaise (1980) and Orr (1986). Pyrite removal requires drastic chemical treatment (Orr 1986). In general, pyrite concentrates with the organic matter when acid digestion procedures are used to concentrate the organic matter.

A concentration procedure not involving successive attack on mineral species was attempted for purposes of comparison with orthodox procedures. In this procedure (Siskin et al. 1987), kerogen is desorbed from mineral surfaces by a hot ammonium sulfate solution while carbonates are decomposed. The desorbed kerogen then is concentrated by flotation.

The first step in the conventional concentration of kerogen is bitumen removal. Two 75-g aliquots of each reference shale were separately extracted for 24 hours in a Soxhlet extractor using benzene-methanol, 3:2 v/v. After 24 hours, bitumen was recovered by solvent evaporation, and residual shale samples were dried. Yield data for this procedure are provided in Table 8.

The dried shale samples from which bitumen had been extracted were then treated with hydrochloric acid to dissolve carbonates. For each sample, two acid treatments were performed in accordance with the procedure recommended by Durand and Nicaise (1980). After drying, each shale sample was again extracted with benzene-methanol (3:2, v/v) in a Soxhlet extractor for 24 hours to obtain residual soluble materials. An additional 1.47% and 0.57% soluble materials were removed from the western and eastern shales, respectively.

Yields of kerogen concentrate are seen to be fairly repeatable for each shale (Table 9). More material is lost from the Eastern shale by HCl treatment than would be predicted by considering how small the amounts of mineral carbonates are in this shale.

Results for the debitumenized, decarbonated shales are fairly consistent. The western shales lose significant amounts of material from HCl extraction and bitumen removal. Hence, residual materials are relatively rich in organic carbon compared with the parent shale (Table 9). Mineral carbon is absent, which shows that the HCl procedure is effective for removing carbonate minerals. There is little acid-soluble material present in the eastern reference shale so little enrichment of organic carbon content in the decarbonated-debitumenized shales is observed.

The residual shales that were treated to remove bitumen and mineral carbonates were further treated with 70% hydrofluoric acid (HF) to remove silicates (Orr 1986). This procedure is dangerous. It is strongly recommended that only experienced laboratory personnel perform this phase of the kerogen concentration procedure. This procedure leaves a residual material consisting of kerogen, pyrite, and other minerals inaccessible to HF. Yields of kerogen concentrates from the HF treatment of the reference shales are shown in Table 9.

For the western reference shale, the yield of kerogen and pyrite correspond well with the organic carbon content and pyrite content of the original shale. The eastern shale is known to have large amounts of pyrite. Pyrite and some other minerals may have escaped exhaustive reaction with HF.

The ammonium sulfate procedure of Siskin et al. (1987) was used to obtain a kerogen concentrate of the western reference shale. This procedure yielded float and sink fractions, both of which were analyzed (Table 9). Both fractions probably contained some residual ammonium sulfate. The organic carbon was greatly concentrated into the float fraction by this procedure.

The two reference shales were evaluated for concentration of kerogen by two methods. A method utilizing successive treatments by HCl and HF provides good yields of kerogen from the western reference shale and seems to be fairly reproducible. The method is somewhat less successful with the eastern reference shale, but does remove most non-pyritic minerals. The method is tedious and dangerous.

The method of Siskin et al. (1987) is quick and safe, but does not appear to provide anything but a crude kerogen concentrate. However, improvements may be possible with this procedure. In particular, it may prove to be a method of pyrite removal for some shales. On the other hand, the concentrated kerogen may not be truly representative of the whole kerogen, i.e., there may have been a fractionation of kerogen itself, which does not occur in the orthodox acid-treatment procedure.

Thermal Properties

Heating Values

Gross heating values were determined on the reference shales using a standard ASTM procedure (D-3286). The results are reported in Table 4. Measurements were made on the raw shales and the spent shales from the MBFA tests. The heating value for the western shale is slightly less than that of the eastern shale. This is probably due to the contribution from the endothermic carbonate decomposition of the western shale. The heating value of the spent shale is greater for the eastern shale because of the greater residue carbon on the spent shale. Heating values for the shale oils were calculated using the Boie equation (Ringen et al. 1979).

Enthalpy of Retorting of Oil Shale Using a Dropping Calorimeter

The object of this procedure is to measure the total enthalpy required to heat oil shale from ambient temperature, 25°C (77°F), to a selected retorting temperature of 500°C (932°F). The enthalpy of retorting is a function of (a) kerogen bonding energy, (b) bitumen bonding energy, (c) specific heat energy of the inorganic phase, (d) specific heat energy of the organic phase (kerogen and bitumen), (e) energy to remove bound water, (f) energy of reaction of organic phase, (g) decomposition energy of certain carbonates.

A detailed discussion of these contributions to heat of retorting was recently published by Camp (1987). He was able to show a good correlation between predicted heat capacitance and actual heat capacitance as a function of temperature. Shaw (1947) measured the retorting energy as a function of temperature for a wide range of shale grades as shale was heated from 25° to 232°C (77 to 450°F). Using a gas flow technique, Wise et al. (1971) measured the energy of retorting raw shales and the heat required to heat spent shales. The temperature range investigated by these authors was between 25° and 500°C (77 to 932°F). Recently Mraw and Keweshan (1984, 1986) used a ballistic calorimeter at 500°C (932°F) to determine the heat of retorting of shale samples separated from raw shale using a sink-float technique. They used quantities of shale in the 40-100 mg range. Carley (1975) surveyed the literature for heat of retorting of oil shale and reported heats of retorting for five different shale richnesses over a temperature range between 65° and 450°C (149° and 842°F). Carley developed equations with four constants that fit quite well with data reported by Shaw.

Camp (1987) attempted to relate the contribution of the organic portion of oil shale to the specific heat of retorting (1) to the hydrogen and carbon content and (2) to the individual mineral contributions. The common western oil shale minerals--quartz, dolomite, calcite, sodium and potassium feldspars--have specific heats near 0.24 cal/g which have been shown to be approximately the specific heat of a spent shale. The organic and inorganic contributions discussed herein are for a mean temperature between 25° and 500°C (77° and 932°F).

Two types of containers were used to measure the specific heat of retorting. Initially the shale samples were contained in a thin-walled aluminum capsule. This allowed for either retorting in air or in an inert gas atmosphere such as nitrogen. In a second phase of the work the shale sample was contained in a stainless steel screen cylinder. Also for this phase a purge tube was connected to the reaction tube so the atmosphere surrounding the sample could be controlled and the emitted product gases immediately removed.

The specific heat of a sample of oil shale bitumen was determined with the ballistic calorimeter using a stainless steel cylinder (5 mm diameter and 80 mm long) with the bottom end closed and the top partially closed with a Teflon door.

The initial temperature was required for all samples whose specific heats or heats of retorting were to be determined. The initial temperature for the specific heat data of retorting was ambient temperature. After thermal equilibrium was assured, the sample was dropped into the ballistic calorimeter. The energy absorbed or released is detected by a thermopile, amplified, and recorded. A calibration was required to calculate actual energy changes. Both quartz and aluminum of known specific heats were used for this purpose.

The heat requirements for retorting a 35/48 mesh western and a eastern oil shale under flowing nitrogen are given in Table 10. A comparison of the specific heats for the western reference shale obtained from this study with results from other studies is given in Table 11. A disagreement was noted for the heat of retorting of the raw western oil shale with data for other western oil shales of comparable organic content and temperature range. Reported values varied between 0.32 and 0.37 cal/g-°C. The value of 0.43 cal/g-°C in this report is slightly higher than the highest reported value. This value and the other reported data were obtained under a nitrogen atmosphere.

A good correlation between reported data and these data are noted for spent shales. The values between 0.24 and 0.26 cal/g-°C are in the region typical of minerals. Therefore the differences in raw oil shale data are probably due to sample treatment or origin rather than instrumentation.

Bound Water

Several attempts were made to determine the energy requirement to release bound water in shale. The experiments were conducted with a differential scanning calorimeter-thermal gravimetric analyzer (DSC-TGA) instrument. The most promising experiments were several sets in which two riffled shale samples were used for each experiment. Each experiment involved heating one shale sample to a subpyrolysis temperature and then cooling it back to room temperature. Then differential DSC-TGA data were acquired using both the heated and unheated samples. This was done to determine water loss by difference. In all cases, the release of bound water occurred over a wide temperature range and was so small that it could not be measured with any reasonable degree of confidence.

Mineralogic Properties

Mineralogic Characterization of Reference Shales

The bulk and clay mineralogies of the raw and retorted reference shales were determined by X-ray diffraction (XRD). Since this technique is qualitative rather than quantitative, peak height data provided in this report should be used as estimates of relative abundance of minerals within a given sample. Minerals present in minor amounts may be difficult to identify due to mineralogic complexity of oil shales and to the presence of one or more dominant mineral phases. In order to minimize problems related to sample complexity, slow scans were used to improve accuracy, and multiple runs were performed to increase precision.

Bulk samples were ground to a -325 mesh (45 microns) and slurry mounted with absolute ethanol onto glass slides for mounting in the Scintag PAD V X-ray diffraction instrument. Samples were scanned at a rate of 0.5 degrees 2-theta/minute to obtain maximum intensities from peaks of less abundant minerals. Ten replicate determinations of each sample were scanned at 2 degrees 2-theta/minute to check the repeatability of the technique. The Joint Committee for Powder Diffraction Standards (JCPDS) value for the primary peak for each mineral, and the average and range of values obtained from repetitive runs are given in Tables 12 (western) and 13 (eastern). To minimize effects of instrument variation and sample preparation, 2-theta values were corrected using the d101 (100% intensity) quartz peak as an internal reference (Zen 1956). Remnant differences between actual and theoretical peak locations may be attributed to instrument error, minute sample differences, and preparation technique.

The fine fraction (<2 microns), consisting primarily of clay minerals, was isolated by gravimetric separation and prepared for XRD analysis after the method of Drever (1973). Three potassium-saturated and three magnesium-saturated samples were prepared for each shale and were scanned from 2 to 30 degrees 2-theta. Potassium-saturated samples were then ashed at 550°C (1022°F) for one hour and rescanned to determine whether kaolinite and/or chlorite were present. Magnesium-saturated samples were glycolated overnight and rescanned to detect peak shift due to expanding clay minerals.

Quantitative analysis of the reference shales was not successful. Relative intensity ratios for each individual mineral compared to a standard would need to be prepared prior to quantitative XRD analysis. Because of the mineralogic complexity of oil shales and cation substitution in natural samples, the use of standard mineral references would be difficult, and isolation of oil shale mineral phases and calculation of relative intensity ratios was beyond the scope of this project.

Minerals identified in western reference shale, listed in order of decreasing abundance, were

Mineral	Composition
Quartz	SiO_2
Ankerite	$(Ca, Mg, Fe)(CO_3)_2$
Calcite	$CaCO_3$
Dawsonite	$NaAlCO_3(OH)_2$
Na-feldspar	$NaAlSi_3O_8$
K-feldspar	$KAlSi_3O_8$
Mg-siderite	$(Fe, Mg)CO_3$

Pyrite	FeS_2
Augite	$Ca(Fe, Mg)Si_2O_6$
Pyrrhotite	Fe_{1-xS}
Akermanite/gehlenite	$Ca_2MgSi_2O_7$
Periclase	$(Mg, Fe)O$

Dawsonite, Mg-siderite, and pyrite were present only in raw western reference shale, whereas augite, pyrrhotite, akermanite/gehlenite, and periclase were minerals generated during the Fischer assay. Mineralogical changes caused by retorting included: decomposition of carbonates, alteration of sulfides, and formation of higher temperature silicates and oxides. A more detailed summary of mineral reactions occurring during the retorting of oil shale is given by Mason et al. (1984). X-ray diffractograms of raw and spent western reference shale are shown in Figures 1-3.

Minerals identified in eastern reference shale, listed in order of decreasing abundance, were

Mineral	Composition
Quartz	SiO_2
Illite	K-Al-Si-O-H
Smectite	$(Na, Ca)-(Al, Mg)-SI-O \cdot xH_2O$
Pyrite	FeS_2
Na-feldspar	$NaAlSi_3O_8$
Kaolinite	Al-Si-O-H
Chlorite	Mg-Fe-Al-Si-O-H
K-feldspar	$KAlSi_3O_8$
Calcite	$CaCO_3$
Pyrrhotite	Fe_{1-xs}
Augite	$Ca(Fe, Mg)Si_2O_6$
Akermanite/gehlenite	$Ca_2MgSi_2O_7/Ca_2Al(Al, Si)_2O_7$

Pyrrhotite, augite, and akermanite/gehlenite are minerals generated as a result of increased temperatures and are present only in the spent shales. The major changes observed from retorting were decreased relative amounts of calcite, alteration of sulfides, and formation of high temperature silicates. Bulk mineral XRD traces (Figures 4-6) demonstrate that silicate minerals are the dominant mineral phases in eastern reference shales. Clay mineral identification procedures show the presence of illite, illite-smectite mixed layer clay, kaolinite, and chlorite.

In contrasting and comparing eastern and western reference shales, eastern reference shales are dominated by silicate minerals especially clay minerals and quartz, while western reference shales contain both carbonate and silicate minerals in moderate abundances. However, in western reference shales, clay minerals constitute only a minor fraction of the total mineral assemblage. Clay minerals contained in the eastern reference shales are abundant and diverse in type, while clay minerals in western reference shales were limited in abundance and type (only illite was detected). Western reference shale contained abundant ankerite (ferroan dolomite isotype), calcite, Mg-siderite, and dawsonite, while calcite was the only carbonate mineral detected in the eastern reference shale. Particle sizes for both references shale types are very small; however, only the eastern reference shale could be considered a true shale. Western reference shale should be considered to be a kerogenaceous marlstone.

Major and Minor Trace Elements

An understanding of the fate of major and minor trace elements during oil shale retorting is necessary for the development of short term (eg. air and water quality) and long term (spent shale leaching) environmental mitigation strategies. To establish baseline data on the distribution of major and minor trace elements during oil shale retorting, the spent shales and shale oils generated from the MBFA, along with the raw oil shales were analyzed for major and minor trace elements (Table 14). Two instruments were used for this purpose: a) a Jarrell-Ash 1100 Series inductively coupled plasma (ICP) spectrometer equipped with a Digital PDP M/23 computer and b) a Perkin Elmer 5000 atomic absorption (AA) spectra photometer equipped with a Perkin Elmer 500 heated graphite atomizer, a Perkin Elmer AS-40 autosampler, and a Perkin Elmer 3600 data station.

EPA quality control reference solutions were analyzed after all instrument calibrations to verify the accuracy of the calibrations and the performance of the instrument. Standard Reference Materials (SRMS), obtained from the National Bureau of Standards were prepared and analyzed with each batch of sample whenever possible to evaluate the accuracy of the analytical procedures being used.

Three methods of sample preparation were used in this work. A lithium metaborate fusion method (Bosshart et al. 1980) was used to prepare the raw and spent shale samples for major trace element determinations by ICP. An acid digestion procedure, described by Bosshart et al. (1980), was used to prepare the solid samples for minor trace element determinations by ICP or AA. The Parr bomb combustion method (Nadkarni 1981) was used for the determination of the trace elements in the shale oils.

The trace element data (Table 14) reaffirm previous observations that all the elements of interest remain in the spent shale (see for example Johnson 1986). Differences in the major trace element data between the shales simply reflect their differences in mineralogy. For example, the high calcium and magnesium values of the western shale reflect its carbonate mineralogy, while high silicon and iron values for the eastern shale reflect the silicate mineralogy and high pyrite contents of these shales. The eastern shales also have greater concentrations of the minor trace elements than the western shales. It has been suggested (Leventhal and Kepferle 1981; Spiewek et al. 1981) that leaching of these elements from the spent shale of a retorting operation would constitute a valuable source of strategic metals.

PROPERTIES OF REFERENCE SHALE OILS

The chemical and physical properties of shale oils differ considerably from the properties of conventional sources of petroleum. In order to best utilize synthetic fuels derived from oil shales, it is important to characterize their chemical and physical properties. Shale oils usually have a lower H/C ratio and higher heteroatom content than other petroleum sources. In addition, the higher temperature processes used to generate shale liquids produce olefins as a result of thermal cracking of the kerogen and bitumen.

Shale oils were produced from the reference shales for use in this study as described by Merriam et al. (1987). Oil was produced from both the eastern and western reference shales using the Paraho Batch Pilot Plant, demulsified as described by Robertson (1983), and composited. Enough oil was generated from each shale to obtain the desired data for characterization.

Physical Properties Calculations

Characterization of the shale oils requires determining many physical properties. ASPEN is a computer model that simulates various process conditions by using feedstock chemical and physical property information. ASPEN requirements were assumed to be a reasonable set of properties for characterization. These properties included molecular weight, critical temperature, critical pressure, critical volume, critical compressibility factor, Benedict-Webb-Rubin orientation parameter, Watson characterization factor, liquid molar volume, enthalpy of vaporization, ideal gas heat capacity, isobaric liquid heat capacity, acentric factor, fugacity, enthalpy, solubility parameter, viscosity, surface tension, thermal conductivity, liquid vapor pressure, boiling points, and heat of combustion. The results of these calculations are shown in Table 15. The correlation methods used to determine these properties are given in Appendix B.

The majority of oil physical property correlations available today have been developed for normal paraffinic crude oils. Shale oil properties can differ greatly from petroleum properties, and therefore the use of correlations designed for petroleum may give erroneous results. Comparison of some measured properties with correlation results can help determine the validity of using these correlations for shale oils.

Many of the correlation procedures require specific gravity and average boiling points for input. A true boiling point (TBP) distillation (ASTM D-2892) was performed on the western and eastern reference shale oils (Tables 16 and 17). The TBP distillation was then used to approximate an ASTM D-86 distillation (Figures 7 and 8) which allows the determination of the volumetric, mean, molal, and cubic average boiling points. The properties listed earlier were then calculated using American Petroleum Institute (API) and other published correlations (Table 15).

Measured and correlation determined properties could then be compared. Molecular weight is one property that was measured and calculated by correlation. The average correlation molecular weight for the whole western reference shale oil was 290 while the laboratory value was 380. The eastern oil showed similar results with a laboratory value of 270 and a correlation value of 218. Because this was not considered very good agreement, the molecular weight of each TBP distillation fraction was also measured and determined by correlation (Table 18). Correlation and laboratory values for both oils agree reasonably well in the 204-399°C (400-750°F) range but not as well at both temperature extremes (Figures 9 and 10).

Viscosity is another property that was both measured and calculated. The western reference shale oil has a viscosity of 53 centipoise according to the laboratory while correlation results show 18.7 centipoise at 38°C (100°F). Eastern reference shale oil has a viscosity of 31.9 centipoise according to the laboratory while correlation results show 7.5 centipoise at 38°C (100°F). Correlation and laboratory values for the western reference shale oil fractions show good agreement up to the 315°C (600°F) boiling range (Figure 11). The eastern reference shale oil fraction viscosity values agree with correlation values up to the 260°C (500°F) boiling range (Figure 12). However, the curves do show similar shapes, and therefore the correlation may be modified to improve the agreement. Actual viscosity values are given for both oils in Table 19.

Heats of vaporization were calculated for both whole oils over a range of temperatures from the boiling point to the critical temperature and plotted (Figures 13 and 14, Tables 20 and 21). The thermal conductivity correlation available from API is merely a function of temperature and does not account for molecular type or weight and, therefore, thermal conductivity was not determined. Vapor pressure was calculated over a range of temperatures and is given in Figure 15.

Plots of the molecular weight of the fractions for the two oils show very minor differences (Figure 16) while plots of H/C ratios (Figure 17) vary greatly. This implies that the oils are different, but that molecular weight is not a good indicator of those differences. Therefore, molecular weight would not be a good property to use to determine other properties accurately which depend upon chemical structure. However, many of the API correlations do use molecular weight for estimating properties.

Some properties of shale oil are similar enough to those of petroleum fluids that the API standard correlations work reasonably well. However, other shale oil properties should be measured to determine which properties do not parallel petroleum fluids. Correlations could then be modified to account for differences in shale oil, or new correlations could be developed. Without physical measurements to reinforce the correlation results, the correlations are suspect and it would be worthwhile to undertake such measurements to test the correlations at some point in the future.

Thermal Conductivity

Thermal conductivity data were acquired for both reference shale oils as part of the information required for the ASPEN computer code. These measurements were made using a standard thermal conductivity comparator apparatus (Tye 1969). The laboratory apparatus contained a stack of three elements: two Pyrex 7740 reference standards and the test material, including the containment vessel. Pyrex 7740 was used for a standard because its thermal conductivity as a function of temperature is known. Pyrex 7740 served as the top and bottom reference standard while the test sample was aligned in the middle.

For the measurement of the thermal conductivity of liquids, a cylindrical containment vessel was used. The two ends of the vessel were capped by copper discs which were fitted with O-rings to contain the liquid. The liquid was added to the top of the vessel, and the top cap was installed so there would be no risk of introducing any air bubbles into the container. The two caps were then moved downward to be even with the top and bottom edges of the cylinder. Two materials were used for containment vessels: acrylic and polycarbonate. First acrylic was tried. It was discovered that the internal pressures in the vessel at elevated temperature were sufficient to cause the acrylic to deform and the O-ring seals to fail because of the increased cylinder diameter. The polycarbonate vessel did not appear to deform; however, the higher temperatures were avoided.

The apparatus was calibrated with a Pyrex 7740 standard in place of the test sample in the middle of the stack. For liquid measurements, a laboratory-grade material of known conductivity was introduced in the containment vessel and tested. For this work, glycerine was used for the calibration fluid.

A comment on the preparation of the Western oil shale sample is in order. Since the room temperature consistency of the glycerine-shale sample was gel-like, it was necessary to elevate the temperature of the sample somewhat to allow it to be poured and handled. This was done quickly by heating a small, covered sample in a microwave and immediately pouring the liquid sample into the containment vessel. The measured thermal conductivities for the two samples are given in Table 22.

Field Ionization Mass Spectroscopic Analyses of Composite Eastern and Western Reference Shale Oils

Field ionization mass spectra were acquired for both the eastern and western shale oil composites. Field ionization mass spectrometric methods employ low ionizing potentials so that, if properly tuned, only molecular ions are observed in the spectrum. Further, the configuration of the spectrometer emitter allows relatively high molecular weight materials to be volatilized into the mass spectral beam. Volatilization is increased further and controlled by a temperature program which is applied to the emitter. The resulting spectrum for a mixture is essentially a molecular weight distribution plot. The data can be manipulated to give number average, weight average, or any other average molecular weight value. This method, like any method which depends upon volatility, is limited by the point at which cracking rather than volatilization occurs. The cracking temperature is easily detected by the appearance of new lower molecular weight species in the mass spectrum.

The mass spectral data for the two reference shale oils are shown in Figures 18 (eastern shale oil) and 19 (western shale oil). The data show that the number average and weight average molecular weights for the eastern shale oil are calculated to be 330 and 436, based on a uniform response of the mass spectrometer to oil species. For the western shale oil the number and weight averages are 486 and 647. For comparison, the vapor phase osmometry molecular weight values, which are number average values, are 270 AMU and 380 AMU for the eastern and western oils, respectively.

Comparisons of ASTM Distillation Methods

The distillation data for the ASTM D-86, D-1160, and D-2892 distillations of the composite eastern and western shale oils are given in Tables 23, 16, and 17. The distillation mid-point data for each cut of the ASTM D-2892 (True Boiling Point) distillations were observed to correlate quite well with the D-86 distillation end point data over the temperature range where both the D-2892 and D-86 distillations proceeded. However, the eastern shale oil began to distill at approximately 100°F (24°C) lower by the D-86 method than by the D-2892 method. In the cases of both eastern and western shale oils by the D-86 method, which is conducted only at atmospheric pressure, the distillations were terminated at approximately 650°F (326°C) because of cracking. Somewhat surprisingly, the D-1160 distillation did not correlate well with the D-2892 method, even though both of these are conducted at atmospheric temperature to about 650°F (326°C) and then both are continued under vacuum. For the western shale oil, the D-1160 distillation was generally the same profile as that obtained from the D-2892, but the D-1160 end points occurred at higher temperatures than did either the mid- or end-point temperatures of the D-2892 method for the same percent volumes distilled. The D-1160 distillation of eastern shale oil from 5% distilled to the cracking temperature occurred over the narrow range of 86°F (16°C), and the data do not correlate with either of the other two methods.

In summary, it appears that the 15 theoretical plate ASTM 2892 (True Boiling Point) distillation is relatively well duplicated by the rapid and inexpensive D-86 method for the atmospheric pressure portion of distillation. For higher boiling (>650°F(326°C)/atm) materials, the rapid D-1160 method does not appear to correlate with the true boiling point method.

Chromatographic Separation of Shale Oils

Reference shale oils generated by Fischer assay were further characterized using techniques of elution chromatography. The separation scheme is shown in Figure 20. The asphaltenes are first removed with pentane. The petrolenes of the crude shale oil are then passed through anion and cation resins to remove strong and weak acids and strong and weak bases which are then recovered from the resins. The material that passes through the resins is chromatographed on grade 12 silica gel with elution by pentane (saturates/olefins), benzene (aromatics), and 2:1 (v/v) benzene-methanol (neutral heteroatomic compounds). The saturate/olefin fraction is then chromatographed on silver nitrate treated silica gel to give a saturated fraction (pentane) and an olefin fraction [1:3 (v/v); benzene-pentane]. The greatest differences between the two oils appear in the saturate, olefin, and aromatic compound classes, which parallels the differences in the structure of the original kerogen. The results of the chromatographic separations are given in Table 24.

DIELECTRIC PROPERTIES OF OIL SHALES AND SHALE OILS

The dielectric capacity is most easily defined as the capacity of a non-conductor material to retain imposed electrical charge. This capacity varies with temperature and usually varies with the frequency of the imposed electrical potential. Further, it is often presented as a constant, the dielectric constant, which is a ratio of the capacity of the material to retain imposed charge to the retention of charge in a vacuum. Under the influence of an alternating electrical potential, the ability of a material to store charge often decreases with increasing frequency because of the inability of polar or polarized molecules to rotate as fast in the field changes, but the reverse of this phenomena may occur at resonance frequencies. In addition to the loss of real storage capacity under the influence of an alternating field of increasing frequency, there is an imaginary part of the dielectric response which is most simply defined as the attenuation of the electrical wave, or the loss caused by work being performed on the material by the alternating field.

A vast amount of experimental data exists on other heterogeneous materials such as glasses and polymers. Numerous explanations have been advanced to attempt to fit these experimental data to empirical dielectric functions. The classic case of the theoretical study of dielectric response is the single relaxation time model of Debye. The original Debye model treats the system as if it were composed of noninteracting dipoles. The dipoles are free to rotate except where there are frictional torques opposing their motion.

In heterogenous materials such as glasses, polymers, and oil shale materials, one does not expect the experimental data to fit the simple Debye relaxation time model. It is therefore natural to attempt to model the dielectric response as several relaxations, each obeying a Debye type behavior. This type of behavior is best explained by Williams and Watts (1970) and later by Williams et al. (1971). This form was used in later work to study the dielectric response of polyatomic liquids. It was shown that the general behavior of a dielectric such as oil shale exhibits a decrease in the dielectric constant as frequency increases.

An apparatus was assembled to perform dielectric property measurements. The solid sample holder is a shielded open circuit coaxial transmission line. The liquid sample holder is an open transmission line. The outer conductor of the sample holder extends beyond the terminated inner conductor. This introduces some discontinuity capacitance which is accounted for during calibration and measurements.

Dielectric measurements of capacitance can be performed over a wide range of frequencies (1-1000 MHz) and at elevated temperatures (up to 300°C (572°F). A computer program was written which solves the admittance equations using a Newton interaction scheme to obtain the dielectric constants.

The liquid sample holder was used to determine the dielectric constants of an eastern shale oil and a western shale oil. The liquid sample holder was calibrated by measuring the dielectric constant of air. As can be seen in Figures 21 and 22, the calibration is quite good. The calibration tends to be best at lower frequencies, reaches a maximum deviation at around 500 MHz, and then improves again at higher frequencies.

The liquid measurements of the eastern shale oil are given in Figures 23 and 24. The general behavior is a decrease of both the real and imaginary parts of the dielectric constant as a function of increasing frequency.

The measurements of the liquid western shale oil are given in Figures 25 and 26. Again it is seen that the general behavior is a decrease of both the real and imaginary parts of the dielectric constant as a function of increasing frequency.

All of the measurements show the normal trend to decrease as a function of increasing frequency. The real part of the dielectric constant of the eastern oil is slightly higher than the real part of the western shale. One reason for this is that the eastern shale contains less water than the western shale. Also the imaginary part of the dielectric constant of the eastern shale oil is slightly higher than that of the western oil. This is primarily because of the slightly higher water content in the eastern oil.

The solid sample holder reproduces the dielectric constant of air very well as shown in Figures 26 and 27. The measurements on the solid samples of western shale show generally a decrease of dielectric constant with increasing frequency. However, the real part increases at around 800 MHz. This increase must be related to a resonant frequency of water which occurs at 915 MHz. The shift of the resonant peaks from 915 MHz is caused by the binding of the water molecules to the matrix which effectively increases the mass of the molecule and changes the resonant frequency. Figures 29-32 show the dielectric properties of two western shale samples. These differ slightly because of minor differences in water content in the two shale samples. Although more than 100 attempts were made using a variety of techniques, these attempts were not successful in producing an eastern shale core sample that could be used in the dielectric cell. In all cases the core sample collapsed during the coring operation. Therefore, no data are given for the eastern shale. The high temperature dielectric properties of the western reference shale core are given in Figures 33 and 34.

CONCLUSIONS

The properties of the reference shales are comparable to the properties of other western and eastern oil shales. Western oil shales from the Green River Formation typically have high conversions to oil because of their low carbon aromaticities and hydrogen richness. Eastern oil shales have low conversion to oil because of their higher carbon aromaticity and low hydrogen content.

Carbon-containing minerals dominate the mineralogy of the western oil shale while silicates and clay minerals are predominant in the eastern reference shale. These minerals are indicative of the lacustrine and near shore to shallow marine depositional environments of the western and eastern shales.

Standard API and other published correlations do not appear to be adequate for predicting properties of shale oils. Poor agreement was obtained between calculated and measured molecular weights. Consequently, calculated properties that make use of molecular weight data, such as solubility parameters, would be expected to be in disagreement with measured results.

In general, the dielectric properties of the reference oil shales and shale oils have significant real values and have much smaller imaginary values at low frequency (1-2 MHZ). As expected, the dielectric constants of shales and oils decrease as the frequency of the applied field increases.

Thermal properties of the reference oil shales and shale oils are in relatively good agreement with other published values.

ACKNOWLEDGMENTS

The principal investigators wish to acknowledge the following WRI personnel for their contributions: Verne E. Smith, overall coordination and management of the project; David Goertz, material balance Fischer assay; Dr. Dan Netzel, liquid state NMR; Dr. Jan Branthaver, kerogen concentrates; Dr. Keith Ensley and Mark Scott, thermal properties; Shawn Sullivan and Charles Mones, correlation calculations; Robert Bosshart, Norman Merriam for production of the crude oil. Other analytical data were acquired by the Analytical Services Division of WRI. Solid state ^{13}C NMR measurements were provided by Professor G. E. Maciel of Colorado State University. Distillations were performed by Litton Co. of Core Labs, Houston. Thermal conductivity was determined by Professor William Lindberg of The University of Wyoming. Dielectric property determinations were conducted by associates of Professor Ramarao Inguva of the University of Wyoming. Mass spectra were acquired by Dr. Ripudaman Malhotra of SRI International, Menlo Park, CA. This work was supported by the United States Department of Energy under cooperative agreement number DE-FC21-86MC11076.

DISCLAIMER

REFERENCES

Adler, S. B., and K. R. Hall. "Use Correlation for Oil Properties," Hydrocarbon Processing, 1985, 64(11), 71-75.

American Society for Testing and Materials. ASTM Standard D 3904-80.

API. "Technical Data Book: Petroleum Refining," American Petroleum Institute: New York, 1978.

Bendall, M. R., and D. T. Pegg. "Complete Accurate Editing of Decoupled ^{13}C Spectra Using a DEPT and a Quaternary-Only Sequence," J. Magn. Reson., 1983, 53, 272-296.

Bendall, M. R., D. T. Pegg, D. M. Doddrell, S. R. Johns, and R. I. Willing. "Pulse Sequence for the Generation of a ^{13}C Subspectrum of Both Aromatic and Aliphatic Quaternary Carbons," J. Chem. Soc., Chem Comm., 1982, 1138-1140.

Bosshart, R. E., A. A. Price, and C. T. Ford. "Evaluation of the Effect of Coal Cleaning on Fugitive Elements: Part II, Analytical Methods," Pittsburgh, PA, March 1980, Bituminous Coal Research, Inc. Report L-1083.

Brule, M. R., C. T. Lin, L. L. Lee, and K. E. Starling. "Multiparameter Corresponding-States Correlation of Coal-Fluid Thermodynamic Properties." Am. Inst. Chem. Eng. J., 1982, 28, 616-625.

Camp, D. W. "Oil Shale Heat-Capacity Relations and Heats of Pyrolysis and Dehydration," 20th Oil Shale Symposium Proceedings, Golden, CO, 1987.

Carley, J. F. "Heat of Kerogen Decomposition and Improved Enthalpy-Temperature Relationships for Raw and Spent Colorado Oil Shales," July 1975, unpublished report.

Cook, E. W. "Thermal Analysis of Oil Shales," Quart. Colo. Sch. Mines, 1970, 65, 133-140.

Drever, J. I. "The Preparation of Oriented Clay Mineral Specimens for X-Ray Diffraction Analysis by a Filter Membrane Peel Technique," Amer. Min., 1973, 58, 553-554.

Durand, B., and G. Nicaise. "Procedures for Kerogen Isolation", in "Kerogen" B. Durand, Ed.; Editions Technip: Paris, 1980, Ch. 2.

Johnson, L. S. "Selected Elemental Distributions as Determined by Reference Retorting of Oil Shale," Laramie, WY, July 1986, DOE Report DOE/FE/60177-2292.

Kesler, M. G., and B.I. Lee. "Improved Predictions of Enthalpy of Fractions," Hydrocarbon Process., 1976, 53, 153-158.

Leventhal, J. S., and R. C. Kepferle. "Geochemistry and Geology of Strategic Metals and Uranium in Devonian Shales of the Eastern Interior United States," Symposium on Synthetic Fuels from Oil Shale II Proceedings, Institute of Gas Technology, Nashville, TN, 1981, 73-96.

McCain, W. D. The Properties of Petroleum Fluids, Pennwell Publishing Company: Tulsa, OK, 1973, 125.

Mason, G. M., L. K. Spackman, and H. W. Leimer, "Mineralogic Characterization of a Chattanooga Shale Core from Central Tennessee," 1984 Eastern Oil Shale Symposium Proceedings, Lexington, KY, 1984.

Merriam, N. W., C. Y. Cha, S. Sullivan. "Production of Spent Shales by Simulation of Surface Oil Shale Retorting Processes," August 1987, U.S. DOE Contract DE-FC21-83FE60177.

Miknis, F. P., S. Sullivan, and G. Mason. "Characterization of Interim Reference Shales," Laramie, WY, March 1986, DOE report DOE/FE/60177-2221.

Miknis, F. P., V. J. Bartuska, and G. E. Maciel. "Cross Polarization ^{13}C NMR with Magic-Angle Spinning: Some Applications to Fossil Fuels and Polymers," Amer. Lab, 1979, 11, 19.

Miknis, F. P., D. A. Netzel, J. W. Smith, M. A. Mast, and G. E. Maciel. "^{13}C NMR Measurements of the Genetic Potential of Oil Shales," Geochim et Cosmochim Acta, 1982a, 46, 977-984.

Miknis, F. P., N. M. Szeverenyi, and G. E. Maciel. "Characterization of the Residual Carbon in Retorted Oil Shales by Solid State ^{13}C NMR," Fuel, 1982b, 61, 341-345.

Mraw, S. C., and C. F. Keweshan. "Calvet-type Calorimeter for the Study of High-Temperature Process II New Ballistic Method for the Enthalpy of Vaporization of Organic Materials at High Temperatures," J. Chem. Thermo., 1984, 16, 873.

Mraw, S. C., and C. F. Keweshan. "Calorimetric Determination of the Heat of Retorting Oil Shales to 773 K," Fuel, 1986, 65, 54-57.

Nadkarni, R. A. "Determination of Volatile Elements in Coal and Other Organic Materials by Oxygen Bomb Combustion," Am. Lab, 1981,

Netzel, D. A. The Quantitation of Carbon Types Using the DEPT/QUAT NMR Pulse Sequences: Application to Fossil Fuel Derived Oils, Anal. Chem., 1987, 59, 1775-1779.

Netzel, D. A., and F. P. Miknis. "An NMR Study of Eastern and Western Shale Oils Produced by Pyrolysis and Hydropyrolysis," Fuel, 1982, 61, 1101-1109.

Orr, W. H. "Kerogen/Asphaltene/Sulfur Relationships in Sulfur-Rich Monterey Oils," Org. Geochem, 1986, 10, 499-516.

Owen, L. B. "DOE Oil Shale Reference Sample Bank, Quarterly Report Jan - March 1987," Salt Lake City, UT, March 1987, Terra Tek Inc. Report TR87-89.

Reid, R. C., J. M. Prausnitz and T. K. Sherwood. The Properties of Gases and Liquids, 3rd ed.; McGraw-Hill, New York, 1977.

Riazi, M. R., and T. E. Daubert. "Simplify Property Predictions," Hydrocarbon Process., 1980, 59, 115-116.

Ringen, S., J. Lanum, and F. P. Miknis. "Calculating Heating Values from Elemental Compositions at Fossil Fuels," Fuel, 1979, 58, 69.

Robertson, R. E. "Application of Petroleum Demulsification Technology to Shale Oil Emulsions," Liquid Fuels Technology, (1983), 1(4), 325-333.

Shaw, R. J. "Specific Heat of Colorado Oil Shales, 1947, U. S. Bur. Mines Report of Investigations 4151.

Siskin, M., G. Brons, and J. F. Payack. "Disruption of Kerogen - Mineral Interactions in Oil Shales," Energy and Fuels, 1987, 1, 248-252.

Spiewek, I., T. M. Gilliam, and M. D. Silverman. "Development of Process for Recovery of Minerals from Eastern Shale," Symposium on Synthetic Fuels from Oil Shale II Proceedings, Institute of Gas Technology, Nashville, TN, 1981.

Twu, C. H. "An Internally Consistent Correlation for Predicting the Critical Properties and Molecular Weights of Petroleum and Coal-Tar Liquids," Fluid Phase Equilibria, 1984, 16, 137-150.

Tye, R. P., ed. Thermal Conductivity, Vol. 2, Ch. 6, Academic Press, New York, NY, 1969.

Williams, G., and D. C. Watts. "Non-Symmetrical Dielectric Relaxation Behavior Arising from a Simple Empirical Decay Function," Trans. Farad. Soc., 1970, 66, 80-85.

Williams, G., D. C. Watts, S. B. Dev, and A. M. North. "Further Considerations of Non-Symmetrical Dielectric Relaxation Behavior Arising from a Simple Empirical Decay Function," Trans. Farad. Soc., 1971, 67, 1323-1335.

Wise, R. L., R. C. Millwer, and H. W. Sohns. "Heat Contents of Some Green River Oil Shales," 1971, U. S. Bur. Mines Report of Investigations 7482.

Zen, E-An. "Correlation of Chemical Composition and Physical Properties of Dolomite," American Journal of Science, 1956, 254, 51-60.

APPENDIX A: TABLES AND FIGURES

Table 1. **Material Balance Fischer Assay Results for Reference Shales**

Product Spent Shale	wt %	Gal/ton	Specific Gravity	% Ash	Mineral Carbon wt %	C wt %	H wt %	N wt %	S wt %
Western Reference Oil Shale									
Oil	10.24	27.50	-	-	-	83.2	12.2	1.7	0.7
Gas	4.60	-	-	-	-	41.4	7.0	-	4.8
Spent Shale	83.50	-	-	78.63	4.9	8.8	0.2	0.5	1.1
Water	1.62	3.88	-	-	-	-	11.1	-	-
Raw Shale	100.00	-	-	66.90	4.2	18.0	1.9	0.6	1.3
% Recovery	99.96	-	-	98.14	97.42	98.8	101.4	89.7	94.1
Eastern Reference Shale									
Oil	5.67	14.38	-	-	-	84.5	10.6	1.2	1.6
Gas	3.16	-	-	-	-	39.5	12.4	-	40.5
Spent Shale	89.54	-	-	87.12	0.22	8.7	0.4	0.9	4.5
Water	1.20	2.87	-	-	-	-	11.1	-	-
Raw Shale	100.0	-	-	78.38	0.25	13.9	1.4	0.4	5.8
% Recovery	99.57	-	-	99.52	78.8	99.7	104.9	114.1	92.6

Table 2. Material Balance Fischer Assay Gas Analyses

Component	Weight %	
	Western Shale	Eastern Shale
H_2	0.73	0.060
CO	0.166	0.057
CH_4	0.236	0.343
CO_2	2.829	0.285
C_2H_4	0.050	0.045
C_2H_6	0.148	0.213
H_2S	0.234	1.356
C_3H_6	0.082	0.067
C_3H_8	0.089	0.104
C_4+	0.693	0.630

Table 3. Organic Carbon Conversion in Reference Shales

Product	% Conversion	
	Western	Eastern
Oil	61.7	35.1
Gas	13.8	9.1
Residue	23.7	55.8

Table 4. Other Properties of Oil Shale and Shale Oil

Property	Western	Eastern
Heating Value, Btu/lb		
Raw Shale	2607	2859
Spent Shale	370	1587
Shale Oil[a]	18650	18100
Molecular Weight - Shale Oil[b]	295	275
Carbon Aromaticity		
Raw Shale	0.259	0.450
Shale Oil	0.236	0.420
Proton Aromaticity		
Shale Oil	0.043	0.110

[a] Calculated from the Boie equation,

$$H_g(\text{Btu/lb}) = 151.2\ (C) + 499.7\ (H) + 27\ (N) + 45\ (S) - 47.7\ (O)$$

[b] VPO in chloroform

Table 5. Carbon and Hydrogen-Type Distribution for Western and Eastern Reference Shale Oils from Carbon-13 DEPT Experiments

	Atom % Carbon-Type		Atom % Hydrogen-Type	
	WSO[a]	ESO[b]	WSO	E
Quaternary (C)				
Aromatic	14.8	25.4		
Olefinic				
Aliphatic	0.3	0.6		
Tertiary (CH)				
Aromatic	7.6	14.1	4.4	10.1
Olefinic	1.0	0.2	0.6	0.10
Aliphatic	2.5	9.5	1.4	6.8
Secondary (CH_2)				
Olefinic	1.6	0.4	1.9	0.6
Aliphatic	57.9	34.6	66.7	49.6
Primary (CH_3)				
Aliphatic	14.5	15.3	25.1	32.8

---

[a] Western reference shale oil
[b] Eastern reference shale oil

Table 6. Average Structural Parameters of Shale Oils by Nuclear Magnetic Resonance

Parameter	WSO[a]	ESO[b]
Atomic H/C Ratio		
Combustion	1.76	1.51
DEPT	1.73	1.40
Hydrogen Aromaticity		
Direct	.0434	.1095
DEPT	.0438	.1010
Hydrogen Olefinic		
Direct	.0289	.0175
DEPT	.0240	.0074
Hydrogen Aliphatic		
Direct	.2360	.8729
DEPT	.9322	.8916
Carbon Aromaticity		
Direct	.9276	.4201
DEPT	.2493	.4008
Carbon Olefinic (1-alkene only)		
Direct	.0262	NM[c]
DEPT	.0256	.0061

[a] Western reference shale oil
[b] Eastern reference shale oil
[c] Not measured

Table 7. Summary of Neutron Activation Analyses for Oxygen (Wt %)

Sample		Oxygen wt %		
		Raw Shale	Spent Shale	Shale Oil
Western	1	33.9	36.9	2.30
	2	35.8	37.8	2.21[a]
	3	35.9	37.4	
	Avg	35.2	37.4	
Eastern	1	33.6	36.6	1.60
	2	34.3	36.9	2.10[a]
	3	--	36.5	
	Avg	34.0	36.7	

[a] By difference value

Table 8. Yields of Bitumen from Reference Shales

Shale	Sample	Bitumen Yield, wt %
Western	1	1.92
Western	2	1.99
Eastern	1	0.58
Eastern	2	0.56

Table 9. Yields and Elemental Analyses of Oil Shale Concentrates

Sample	Shale	Treatment	Yield, Wt % of Starting Shale	Mineral C, wt %	Total C, wt %	H wt %	N wt %	S wt %
OW	Western	Raw Shale	100	4.2	18.0	1.9	0.6	1.3
OE	Eastern	Raw Shale	100	0.3	13.9	1.4	0.4	5.8
1W	Western	HCl	53.02	<0.1	27.4	3.6	0.8	1.4
2W	Western	HCl	53.27	<0.1	26.0	3.3	0.9	1.5
1E	Eastern	HCl	89.41	<0.1	15.2	1.5	0.3	NM[a]
2E	Eastern	HCl	89.89	<0.1	14.2	1.4	0.3	6.0
1W	Western	HCl/HF	20.5	<0.1	64.4	8.2	2.3	3.5
2W	Western	HCl/HF	20.5	<0.1	70.8	9.0	2.5	4.1
1E	Eastern	HCl/HF	29.6	<0.1	36.3	3.6	1.4	NM
2E	Eastern	HCl/HF	32.4	<0.1	43.4	4.0	1.4	19.7
Float	Western	NH_4SO_4	32.3	1.0	36.1	4.8	2.4	3.5
Sink	Western	NH_4SO_4	65.1	1.7	6.5	1.4	1.4	7.8

[a] Not measured

Table 10. Heat of Retorting of Reference Oil Shales at 500°C

	Enthalpy of Retorting for 475°C Temperature Change, cal/g	Enthalpy in Specific Heat Units, Cal/g-°C
Western		
Raw	204	0.43 ± .01[a]
Spent	123	0.26 ± .02[a]
Eastern		
Raw	171	0.36 ± .02[a]
Spent	114	0.24 ± .02[a]

[a] Arithmetic mean based on four determinations

Table 11. Comparison of Specific Heat Data for Colorado Oil Shale

		Specific Heat, cal/g-°C[a]			
Material	This Study	Camp (1987)	Mraw and Keweshan (1986)	Wise et al. (1970)	Cook (1970)
Raw Shale	0.43	0.38	0.37	0.32	0.35
Spent Shale	0.26	0.26	NM[b]	0.20	0.26

[a] For retorting temperature of 500°C with sample initially at 25°C
[b] Not measured

Table 12. Minerals Determined in Western Reference Shale by X-Ray Diffraction[a]

	Quartz	Ankerite	Calcite	Dawsonite	Na-feldspar	K-feldspar	Mg-siderite	Pyrite
Raw Western Reference Shale								
JCPDS Value	26.65	30.80	29.40	15.62	27.94	27.68	32.00	33.04
Mean	NM[c]	30.76	29.48	15.62	27.96	27.61	32.11	33.00
Minimum	NM	30.76	29.48	15.61	27.94	27.58	32.10	33.01
Maximum	NM	30.77	29.50	15.64	27.97	27.65	32.14	33.10

	Quartz	Ankerite	Calcite	Na-feldspar	K-feldspar	Augite[b]	Pyrrhotite[b]	Akermanite/ gehlenite[b]	Illite
Spent Western Reference Shale									
JCPDS	26.65	30.80	29.40	27.94	27.68	29.82	43.65	31.12/ 31.28	8.84
Mean	NM	30.76	29.51	27.96	27.62	29.91	43.52	31.22	8.83
Minimum	NM	30.74	29.49	27.95	27.55	29.84	43.39	31.17	8.66
Maximum	NM	30.77	29.52	27.87	27.67	30.00	43.66	31.27	8.93

Note:

[a] Minerals are ranked in general order of decreasing abundance.
[b] Augite, akermanite/gehlenite, and pyrrhotite formed during retorting.
[c] Not measured

Table 13. Minerals Determined in Eastern Reference Shale by X-Ray Diffraction[a]

	Quartz	Illite	Smectite	Pyrite	Na-feldspar	Kaolinite/ Chlorite	K-feldspar	Calcite
Raw Eastern Reference Shale								
JCPDS Value	26.65	8.84	19.84	33.04	27.94	12.51	27.68	29.40
Mean	--	8.83	19.85	33.05	27.94	12.51	27.75	29.46
Minimum	--	8.81	19.82	33.04	27.88	12.47	27.68	29.45
Maximum	--	8.84	19.88	33.06	27.97	12.56	27.79	29.47

	Quartz	Illite	Pyrrhotite[b]	Augite[b]	Na-feldspar	Smectite	Kaolinite/ Chlorite	Pyrite	K-feldspar	Akermanite[b]
Spent Eastern Reference Shale										
JCPDS Value	26.65	8.84	43.65	29.82	27.94	19.84	12.51	33.04	27.513	1.12-31.28
Mean	--	8.83	43.85	29.93	27.93	19.81	12.51	33.04	27.52	31.24
Minimum	--	8.82	43.83	29.91	27.88	19.79	12.49	33.02	27.46	31.19
Maximum	--	8.84	43.87	29.95	29.95	19.85	12.52	33.08	27.57	31.29

Note:

[a] Minerals ranked in general orders of decreasing abundance.

[b] Augite, akermanite, and pyrrhotite are formed during retorting.

Table 14. Major and Minor Trace Elemental Distributions

	Western Reference Shale			Eastern Reference Shale		
Element	Raw	Spent	Oil	Raw	Spent	Oil
Major[a]						
Al	4.16	4.99		6.11	6.37	
Ca	8.87	10.20		0.86	0.91	
Fe	2.45	2.94	<1.5 ppm	6.66	6.96	< 23.4 ppm
K	1.58	1.86	<400 ppm	2.91	3.04	<423 ppm
Mg	2.56	2.99		0.80	0.82	
Mn	0.03	0.04	<1.6 ppm	0.03	0.03	< 1.8 ppm
P	0.14	0.18	<0.8 ppm	0.04	0.03	< 84 ppm
Na	1.68	2.01		0.35	0.37	
Si	14.8	17.67		28.47	29.4	
Ti	0.16	0.19		0.38	0.39	
Ba	0.04	0.05	<1.6 ppm	0.04	0.04	< 1.7
Sr	0.06	0.07	<0.4 ppm	0.09	0.09	< 1.4 ppm
Minor[b]						
Be	<2.2	<1.9	<0.8	<2.2	<1.8	< 0.83
Cd	.82	.75	<0.8	.43	.74	< 0.83
Co	14	16.0	<0.8	43.4	46.1	<0.83
Cr	35.6	40.5	11.0	76.4	79.1	20.7
Cu	75.0	83.7	1.8	89.9	96.0	2.8
Li	145	159	<1.4	35.2	35.7	<1.3
Mo	21	23.1	<0.8	178	194	< 0.84
Ni	24.8	28.2	1.8	103	110	5.0
Pb	3.5	50	<0.4	74	93	<.5
V	117	137	<1.6	199	212	< 1.8
Zn	84.2	103.4		127	147	

[a] All values are percent unless shown otherwise.
[b] All values are ppm.

Table 15. Physical Properties of Reference Shale Oils from Correlations

Physical Property & Correlation Source	Western Reference Shale Oil	Eastern Reference Shale Oil
Molecular Weight		
Adler, Hall (1985)	300	225
API Tech. Data Book (1985)	305	217
Kesler, Lee (1976)	336	256
Riazi, Daubert (1980)	271	201
Twu (1984)	270	191
Average	296	218
Critical Temperature		
API Tech. Data Book (1985)	1519°R	1495°R
Brule, Lin, Lee, Starling (1982)	1496°R	1442°R
Kesler, Lee (1976)	1490°R	1440°R
Riazi, Daubert (1980)	1472°R	1392°R
Twu (1984)	1512°R	1456°R
Average	1498°R	1445°R
Critical Pressure		
Kesler, Lee (1976)	215 psia	344 psia
Riazi, Daubert (1980)	206 psia	307 psia
Twu (1984)	229 psia	365 psia
Average	217 psia	339 psia
Critical Volume		
Brule, Lin, Lee Starling (1982)	0.062132 ft^3/lb	0.054566 ft^3/lb
Riazi, Daubert (1980)	0.055130 ft^3/lb	0.057330 ft^3/lb
Twu (1984)	0.054464 ft^3/lb	0.047457 ft^3/lb
Average	0.057242 ft^3/lb	0.053118 ft^3/lb
Benedict-Webb-Rubin Orientation Parameter		
Brule, Lin, Lee, Starling (1982)	0.7351	0.5336
Critical Compressibility		
Ideal Gas Law	0.000773	0.001161
Watson Characterization Factor		
API Tech. Data Book (1985)	11.5	10.4
Kesler, Lee (1976)	11.5	10.4

Table 15. Physical Properties of Reference Shale Oils from Correlations (Continued)

Physical Property & Correlation Source	Western Reference Shale Oil	Eastern Reference Shale Oil
Pitzer Acentric Factor		
Reid, Prausnitz, Sherwood (1977)	0.81	0.55
Kesler, Lee (1976)	0.83	0.55
Liquid Molar Volume at 68°F, 1 atm		
Riazi, Daubert (1980)	0.016298 ft^3/lb	0.015556 ft^3/lb
At Normal Boiling Point		
Reid, Prausnitz, Sherwood (1977)	0.022773 ft^3/lb	0.020753 ft^3/lb
Ideal Gas Heat Capacity at 0°F		
Riazi, Daubert (1980)	88.5 Btu/lb-mole °F	60.8 Btu/lb-mole-°F
Isobaric Liquid Heat Capacity at 0°F		
API Tech. Data Book (1985)	111.8 Btu/lb-°F	72.3 Btu/lb-°F
Kesler, Lee (1976)	85.1 Btu/lb-°F	52.9 Btu/lb-°F
Average	98.5 Btu/lb-°F	62.6 Btu/lb-°F
Enthalpy of Vaporization at Normal Boiling Point		
Riazi, Daubert (1980)	25,591 Btu/lb-mole	22,683 Btu/lb-mole
Adler, Hall (1985)	27,450 Btu/lb-mole	24,750 Btu/lb-mole
Average	26,521 Btu/lb-mole	23,717 Btu/lb-mole
Liquid Enthalpy at 77°F,1 atm		
API Tech. Data Book (1985)	96.5 Btu/lb	80.2 Btu/lb
Kesler, Lee (1976)	102.0 Btu/lb	88.4 Btu/lb
Average	99.3 Btu/lb	84.3 Btu/lb
Fugacity		
API Tech. Data Book (1985)		
a) at 77°F, 100 psia	5.62×10^{-8} psia	6.91×10^{-6} psia
b) at 500°F, 100 psia	0.7112 psia	5.2 psia
c) at 1000°F, 100 psia	124.9 psia	89.6 psia

Table 15. Physical Properties of Reference Shale Oils from Correlations (Continued)

Physical Property & Correlation Source	Western Reference Shale Oil	Eastern Reference Shale Oil
Liquid Vapor Pressure		
API Tech. Data Book (1985)		
a) 100°F	0.00 psia	0.00 psia
b) 200	0.00	0.01
c) 300	0.01	0.11
d) 400	0.10	0.95
e) 500	0.79	4.84
f) 600	3.87	16.89
g) 700	13.36	45.42
h) 800	36.13	101.80
i) 900	82.50	201.66
Solubility Parameter		
API Tech Data Book (1985)	8.86	10.00
Dynamic Viscosity		
API Tech. Data Book (1985)		
a) at 100°F	18.7 cp	7.5 cp
b) at 210°F	3.8 cp	2.2 cp
Kinematic Viscosity		
API Tech. Data Book (1985)		
a) at 100°F	20.4 cs	7.7 cs
b) at 210°F	4.1 cs	2.3 cs
Surface Tension		
API Tech. Data Book (1985)	34.6 Dynes/cm	37.4 Dynes/cm
Mean Average Boiling Point		
API Tech. Data Book (1985)	1167°R	1048°R
Volumetric Average Boiling Point		
API Tech. Data Book (1985)	1224°R	1126°R
Molal Average Boiling Point		
API Tech. Data Book (1985)	1128°R	986°R

Table 15. Physical Properties of Reference Shale Oils from Correlations (Continued)

Physical Property & Correlation Source	Western Reference Shale Oil	Eastern Reference Shale Oil
Cubic Average Boiling Point		
API Tech. Data Book (1985)	1206°R	1101°R
Heat of Combustion		
Gross		
Adler, Hall (1985)	19,200 Btu/lb	18,800 Btu/lb
API Tech. Data Book (1985)	18,922 Btu/lb	18,492 Btu/lb
Net		
API Tech. Data Book (1985)	17,817 Btu/lb	17,472 Btu/lb

Table 16. True Boiling Point Distillation Data (ASTM D-2892) and Elemental Analysis for Western Reference Shale Oil Distillate Fractions and the Whole Oil

Distillation Range, °F	Volume %	API 60/60	Carbon wt %	Hydrogen wt %	Nitrogen wt %	Sulfur wt %
IBP - 405	4.96	45.2	84.6	13.4	0.4	1.0
405 - 461	4.97	39.2	84.4	13.2	0.7	0.9
461 - 512	4.91	34.8	84.6	12.7	0.9	1.0
512 - 573	4.94	31.1	85.4	12.7	1.3	1.0
573 - 621	4.96	30.3	84.5	12.7	1.2	0.9
621 - 690	4.96	27.3	85.6	12.5	1.5	0.9
690 - 725	4.99	26.6	85.3	12.8	1.3	0.8
725 - 740	4.97	26.0	85.5	12.8	1.3	0.7
740 - 775	4.90	21.2	85.2	12.8	1.2	0.7
775 - 800	4.88	20.2	85.7	12.8	1.2	0.7
800 - 835	4.90	18.7	84.4	12.7	1.4	0.7
835 - 863	4.94	17.6	85.2	12.5	1.4	0.7
863 - 896	4.98	16.2	85.6	12.3	1.6	0.7
896 - 933	4.89	15.1	85.1	11.9	1.9	0.8
933 - 965	4.89	14.2	85.2	11.7	2.1	0.9
965 - 1000	4.87	13.5	85.6	11.5	2.3	0.8
Bottoms	20.06	8.9	85.9	10.9	2.5	0.8
Whole Oil	100	22.8	84.6	12.1	2.0	0.9

Table 17. True Boiling Point Distillation Data (ASTM D-2892) and Elemental Analysis for Eastern Reference Shale Oil Distillate Fractions and the Whole Oil

Distillation Range, °F	Volume %	API 60/60	Carbon wt %	Hydrogen wt %	Nitrogen wt %	Sulfur wt %
IBP - 300	7.08	NM[a]	NM	NM	NM	NM
300 - 381	5.58	37.5	82.1	12.4	0.1	1.7
381 - 447	4.98	32.1	83.0	12.0	.1	2.1
447 - 464	4.96	28.4	83.2	11.8	.1	2.1
464 - 497	4.81	24.7	82.8	11.3	0.2	2.3
497 - 532	4.97	22.6	84.7	10.9	0.5	2.4
532 - 567	5.03	20.2	84.4	11.0	0.4	2.1
567 - 630	4.84	18.2	84.2	10.9	0.6	2.0
630 - 640	5.01	15.5	85.0	10.4	0.6	2.0
640 - 650	4.95	16.3	84.5	10.2	0.8	2.1
650 - 774	5.30	12.1	84.6	10.2	1.8	1.7
774 - 796	5.22	11.4	86.1	10.3	2.0	2.0
796 - 838	5.25	10.3	85.3	10.1	1.7	2.0
838 - 870	5.21	8.3	85.8	9.9	1.8	1.9
870 - 910	4.75	6.5	85.7	9.7	1.9	1.8
Bottoms	22.49	-3.8	85.7	8.4	1.9	2.6
Whole Oil	100	13.2	82.0	10.4	1.0	5.2

[a] Not measured

Table 18. Molecular Weight of Fractions of Reference Shale Oils

Reference Shale Oil	Boiling Range, °F	Molecular Weight from Correlation	Molecular Weight from Laboratory
Western Reference Shale Oil	IBP - 405	145	160
	405 - 461	176	170
	461 - 512	196	195
	512 - 573	219	210
	573 - 621	247	240
	621 - 690	278	260
	690 - 725	312	320
	725 - 740	329	330
	740 - 775	339	340
	775 - 800	360	350
	800 - 835	382	360
	835 - 863	407	380
	863 - 896	432	410
	896 - 933	464	440
	933 - 965	498	460
	965 - 1000	535	480
	Bottoms	734	740
Eastern Reference Shale Oil	300 - 381	141	160
	381 - 447	163	160
	447 - 464	177	180
	464 - 497	184	185
	497 - 532	195	200
	532 - 567	209	220
	567 - 630	231	235
	630 - 640	246	250
	640 - 650	253	240
	650 - 774	285	295
	774 - 796	336	310
	796 - 838	358	330
	838 - 870	383	355
	870 - 910	409	390
	Bottoms	527	800

Table 19. Viscosities of Fractions of Reference Shale Oils

Reference Shale Oil	Boiling Range °F	Correlation Viscosity at 100°F, cp	Laboratory Viscosity at 100°F, cp	Correlation Viscosity at 210°F, cp
Western	IBP - 405	0.8	1.5	0.4
Reference	405 - 461	1.5	2.4	0.7
Shale Oil	461 - 512	2.2	3.0	0.9
	512 - 573	3.5	4.8	1.3
	573 - 621	5.2	6.6	1.7
	621 - 690	9.1	9.8	2.5
	690 - 725	14.3	19.6	3.3
	725 - 740	18.9	24.1	3.9
	740 - 775	33.0	28.9	5.1
	775 - 800	48.3	NM[a]	6.2
	800 - 835	80.9	NM	7.9
	835 - 863	140.3	NM	10.0
	863 - 896	272.4	NM	13.0
	896 - 933	592.9	NM	17.4
	933 - 965	1481.	NM	24.2
	965 - 1000	3667.	NM	32.8
Eastern	300 - 381	1.0	2.1	0.5
Reference	381 - 447	1.6	2.5	0.7
Shale Oil	447 - 464	2.1	3.0	0.9
	464 - 497	2.4	3.9	1.1
	497 - 532	2.7	5.1	1.2
	532 - 567	5.1	7.5	1.8
	567 - 630	7.8	11.5	2.3
	630 - 640	11.4	18.3	2.8
	640 - 650	12.8	17.5	2.9
	650 - 774	37.8	127.0	4.7
	774 - 796	165.7	211.3	8.5
	796 - 838	368.8	409.5	11.0
	838 - 870	1064.1	2330.	14.2
	870 - 910	15241.	11900.	27.5

[a] Not measured for this fraction

Table 20. Heats of Vaporization for the Western Reference Shale Oil Between the Boiling Point and the Critical Temperature

Temperature, °F	Heat of Vaporization, Btu/lb-mole
707	26521.0
717	26120.9
727	25715.2
737	25303.4
747	24885.5
757	24461.2
767	24030.1
777	23592.0
787	23146.6
797	22693.4
807	22232.0
817	21762.0
827	21282.8
837	20793.9
847	20294.5
857	19784.0
867	19261.3
877	18725.6
887	18175.6
897	17610.0
907	17027.0
917	16424.7
927	15800.5
937	15151.6
947	14473.8
957	13762.3
967	13010.2
977	12208.0
987	11341.8
997	10389.9
1007	9314.7
1017	8041.0
1027	6368.0
1037	2861.8

Table 21. Heats of Vaporization for the Eastern Reference Shale Oil Between the Boiling Point and the Critical Temperature

Temperature, °F	Heat of Vaporization, Btu/lb-mole
588	23717.0
598	23441.1
608	23161.2
618	22877.1
628	22588.7
638	22295.8
648	21998.4
658	21696.3
668	21389.2
678	21077.1
688	20759.8
698	20436.9
708	20108.4
718	19773.8
728	19433.0
738	19085.7
748	18731.4
758	18369.8
768	18000.5
778	17623.0
788	17236.7
798	16841.0
808	16435.3
818	16018.5
828	15590.0
838	15148.4
848	14692.5
858	14220.7
868	13731.1
878	13221.3
888	12688.3
898	12128.4
908	11536.5
918	10905.7
928	10226.4
938	9483.9
948	8654.6
958	7695.4
968	6511.9
978	4793.6

Table 22. Thermal Conductivities of Reference Shale Oils

Material	Thermal Conductivity (W/m-K)		
	25°C	50°C	75°C
Eastern Oil Shale	0.273[a]	0.292[a]	
	0.280[b]	0.303[b]	0.322[b]
Western Oil Shale	0.263[a]	0.289[a]	

[a] Containment vessel of acrylic
[b] Containment vessel of polycarbon

Table 23. ASTM D-86 and D-1160 Distillation Data

Composite Western Shale Oil

D-86	
---IBP °F	346
---5	414
---10	472
---20	581
---30	655, Cracked
---40	
---50	
---60	
---70	
---80	
---90	
---95	
---End Point	700
---Recovery, %	37.0
---Residue, %	62.5
---Loss, %	0.5

D-1160 (Vacuum)	
---IBP °F	455
---5	531
---10	576
---20	669
---30	743
---40	800
---50	838
---60	894
---70	966
---80	1038, Cracked
---90	
---95	
---End Point	1038
---Recovery, %	80.0
---Residue, %	20.0
---Loss, %	0.0

Composite Eastern Shale Oil

D-86	
---IBP °F	209
---5	214
---10	356
---20	462
---30	540
---40	601
---50	639
---60	Cracked
---70	
---80	
---90	
---95	
---End Point	658
---Recovery, %	60.0
---Residue, %	39.5
---Loss, %	0.5

D-1160 (Vacuum)	
---IBP °F	380
---5	496
---10	540
---20	Cracked
---30	
---40	
---50	
---60	
---70	
---80	
---90	
---95	
---End Point crackpoint	502
---Recovery, %	20.0
---Residue, %	80.0
---Loss, %	0.0

Table 24. Chromatographic Analyses of Reference Shale Oils[a]

	Asphaltenes	Strong Acids	Strong Bases	Weak Acids	Weak Bases	Saturates	Olefins	Aromatics	Neutral Hetero-Compounds
Western	1.4	21.8	19.4	6.6	5.6	14.8	17.5	13.3	1.0
Eastern	3.6	26.5	9.4	7.0	7.5	5.7	7.0	35.0	1.8

[a] All values are percent of total starting material.

Legend for Figures 1 - 6:

CL = chlorite
I = illite
K = kaolinite
S = smectite
Q = quartz
F = feldspars
C = calcite

A = augite
A/G = akermanite/gehlenite
P = pyrite
PR = pyrrhotite
MG = Mg-siderite
D = dawsonite
AN = ankerite

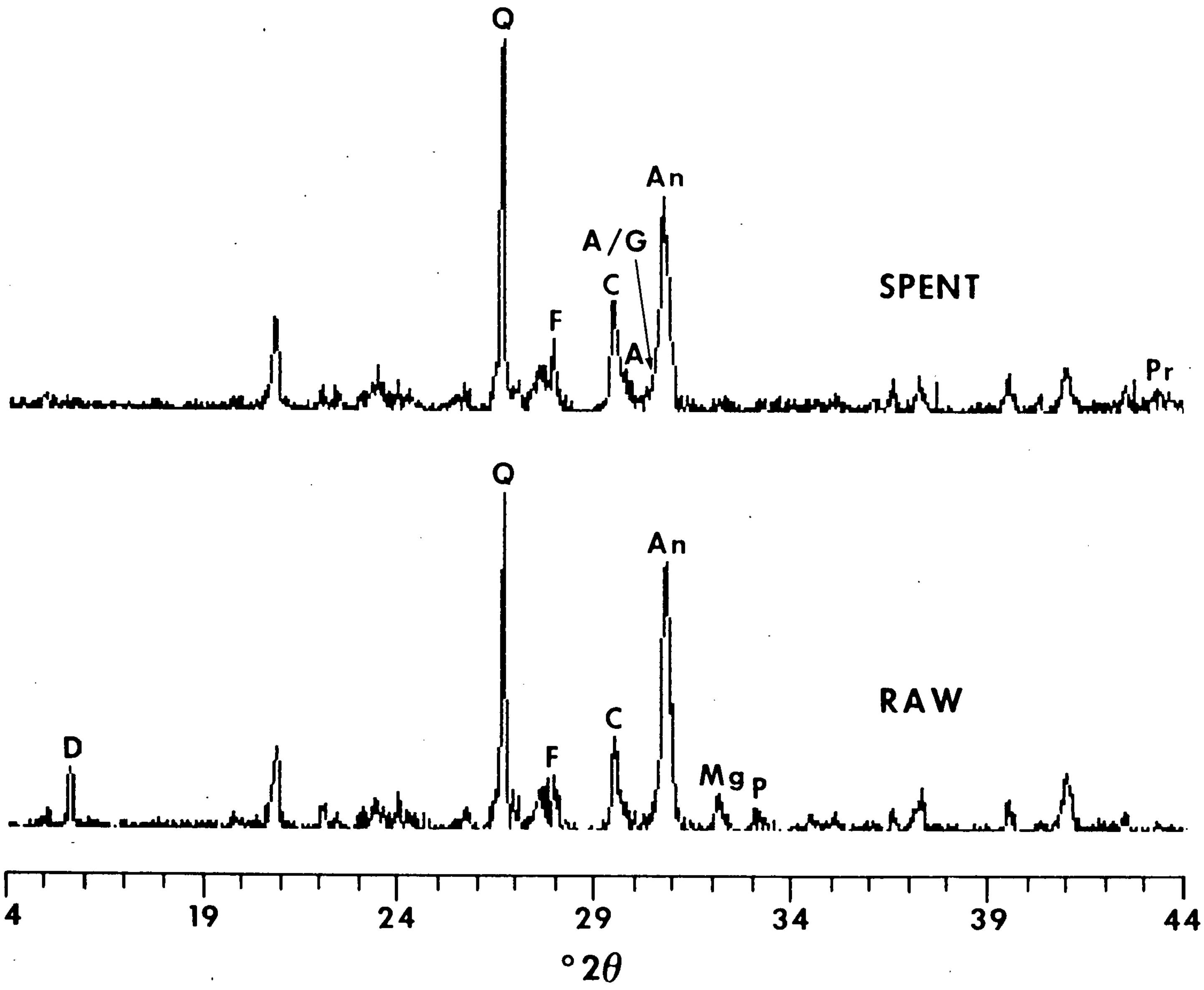

Figure 1. Comparison of X-Ray Diffraction Patterns for Raw and Spent Western Reference Shale (See legend on p. 48)

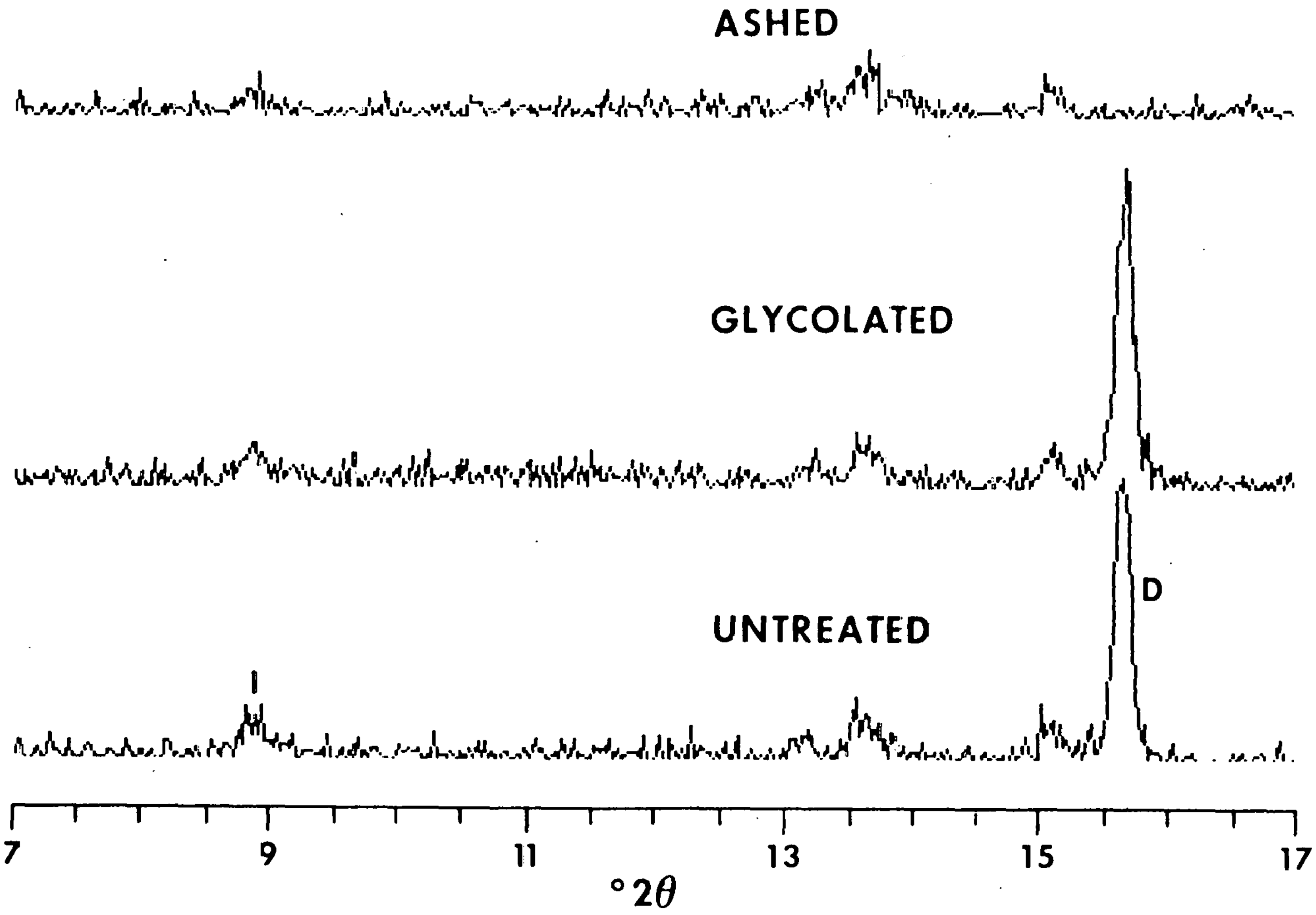

Figure 2. X-ray Diffraction Patterns Showing Clays Present in Raw Western Reference Shale and Changes Produced by Ashing and Glycolating (See legend on p. 48)

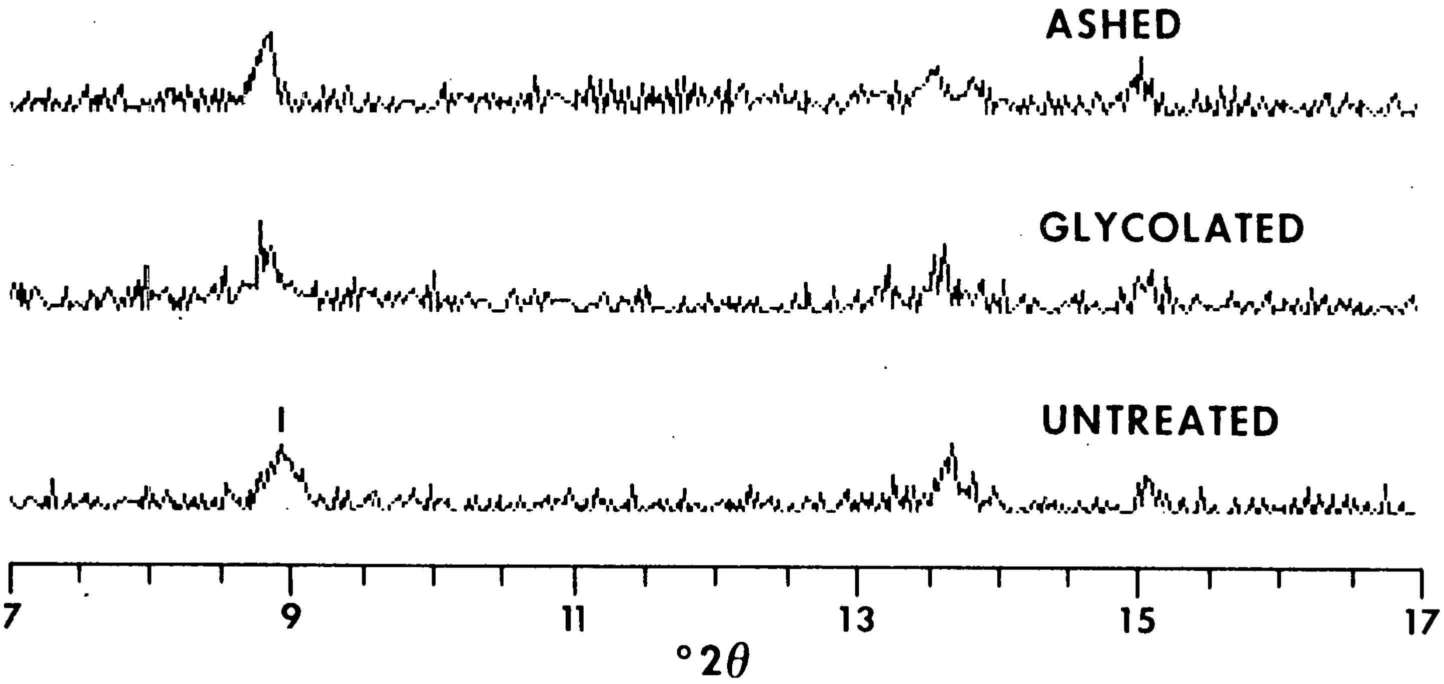

Figure 3. X-Ray Diffraction Patterns Showing Clays Present in Spent Western Reference Shale and Changes Produced by Ashing and Glycolating (See legend on p. 48)

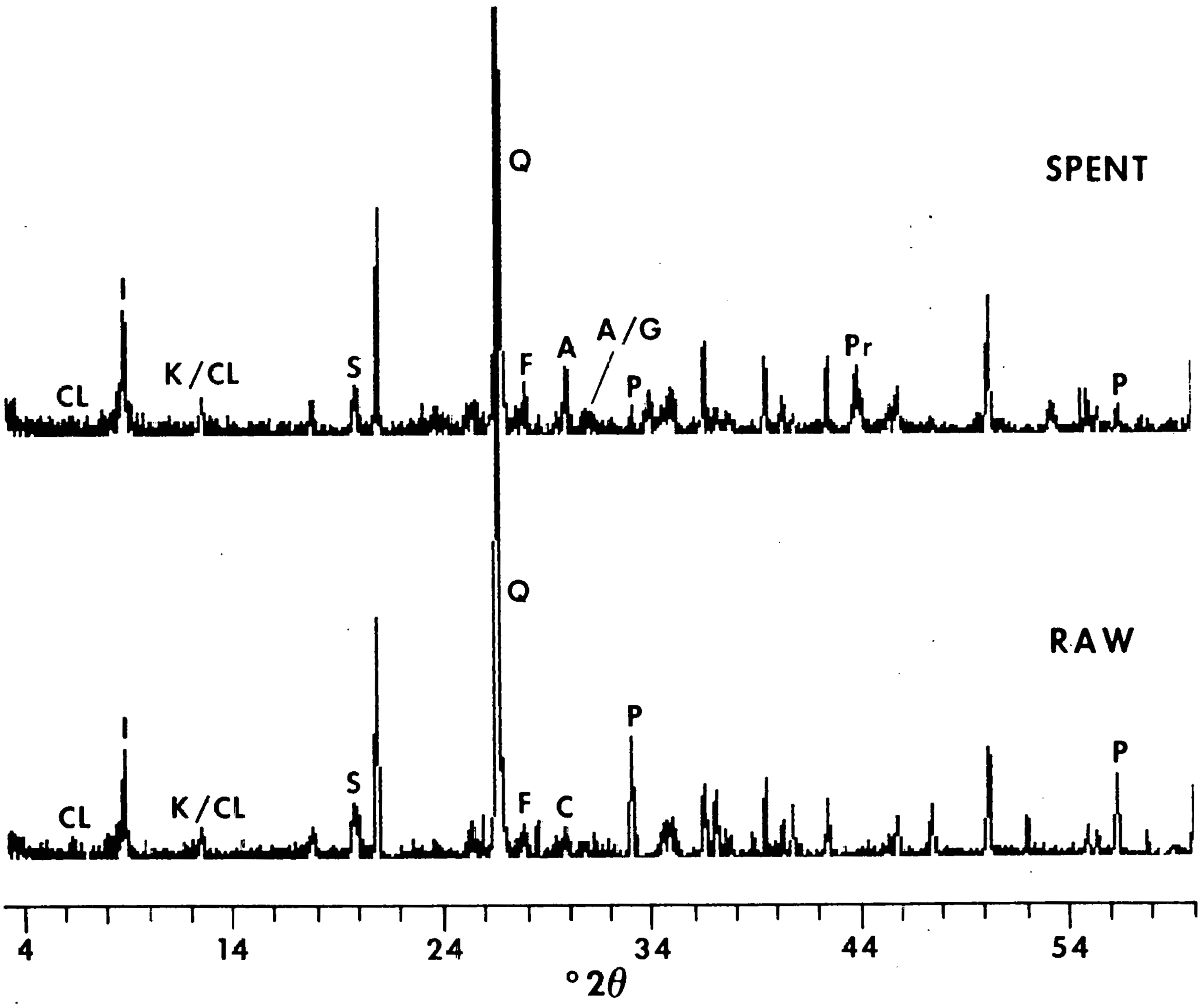

Figure 4. Comparison of X-Ray Diffraction Patterns for Raw and Spent Eastern Reference Shale (See legend on p. 48)

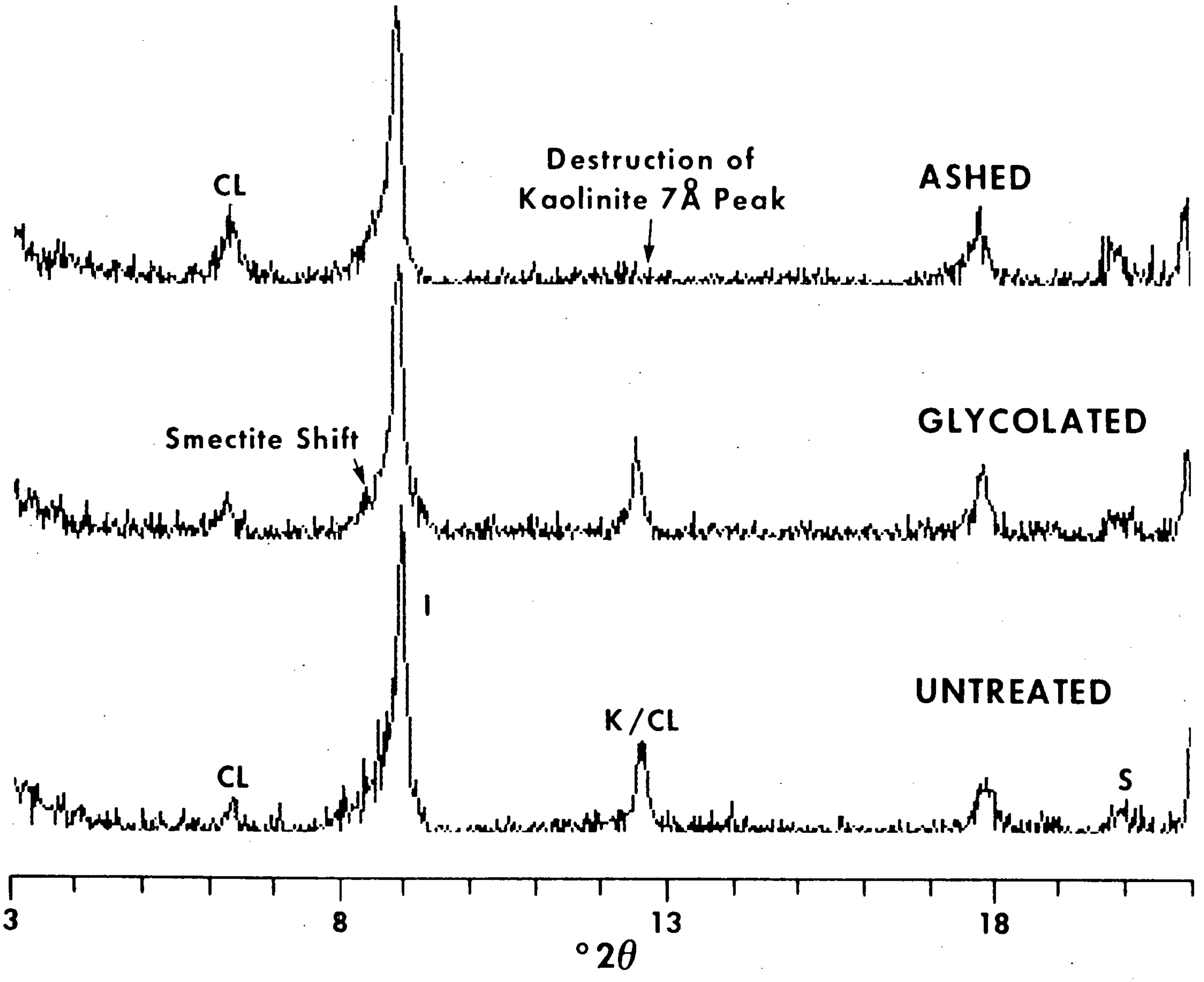

Figure 5. X-Ray Diffraction Patterns Showing Clays Present in Raw Eastern Reference Shale and Changes Produced by Ashing and Glycolating (See legend on p. 48)

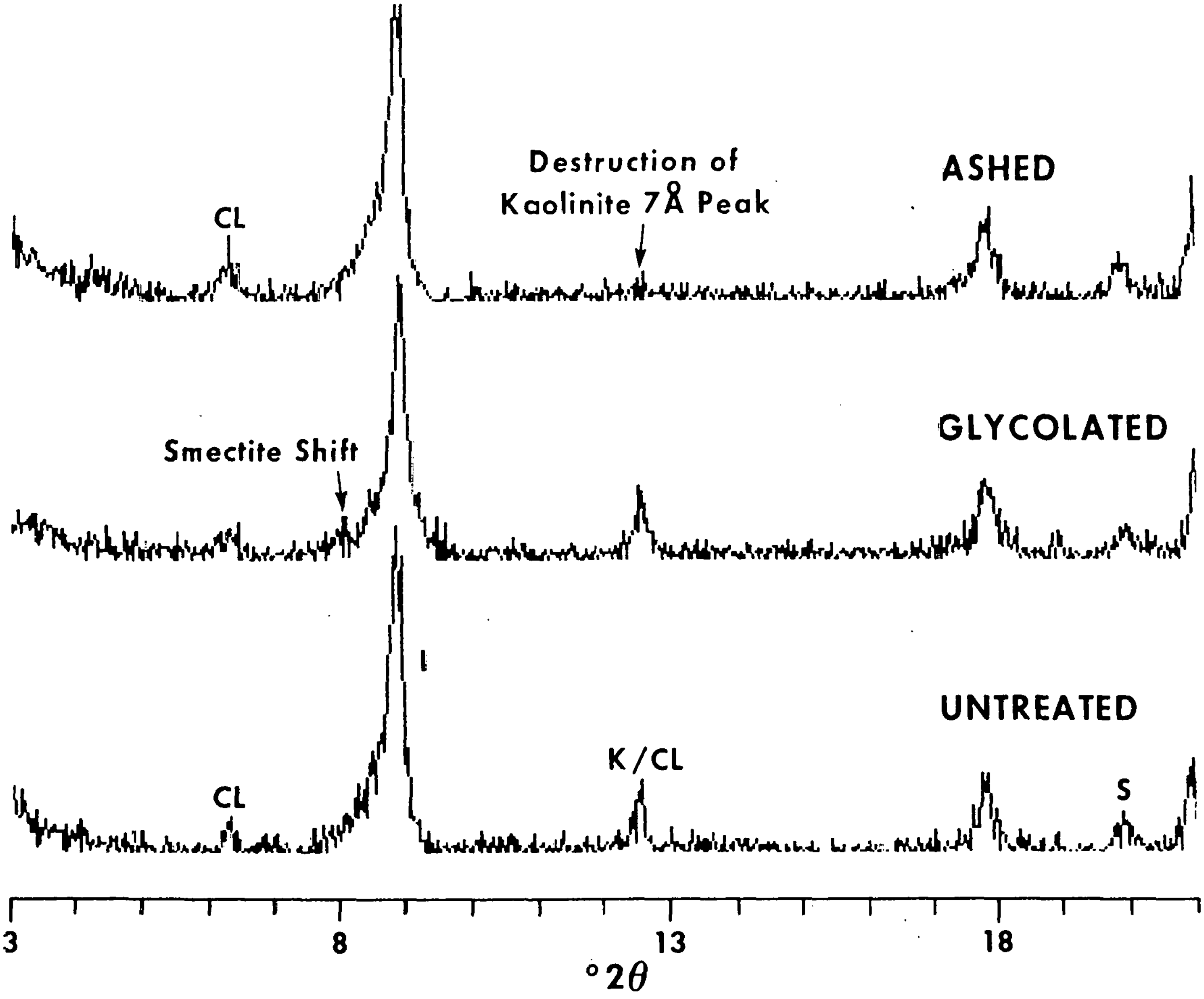

Figure 6. X-Ray Diffraction Patterns Showing Clays Present in Spent Eastern Reference Shale and Changes Produced by Ashing and Glycolating (See legend on p. 48)

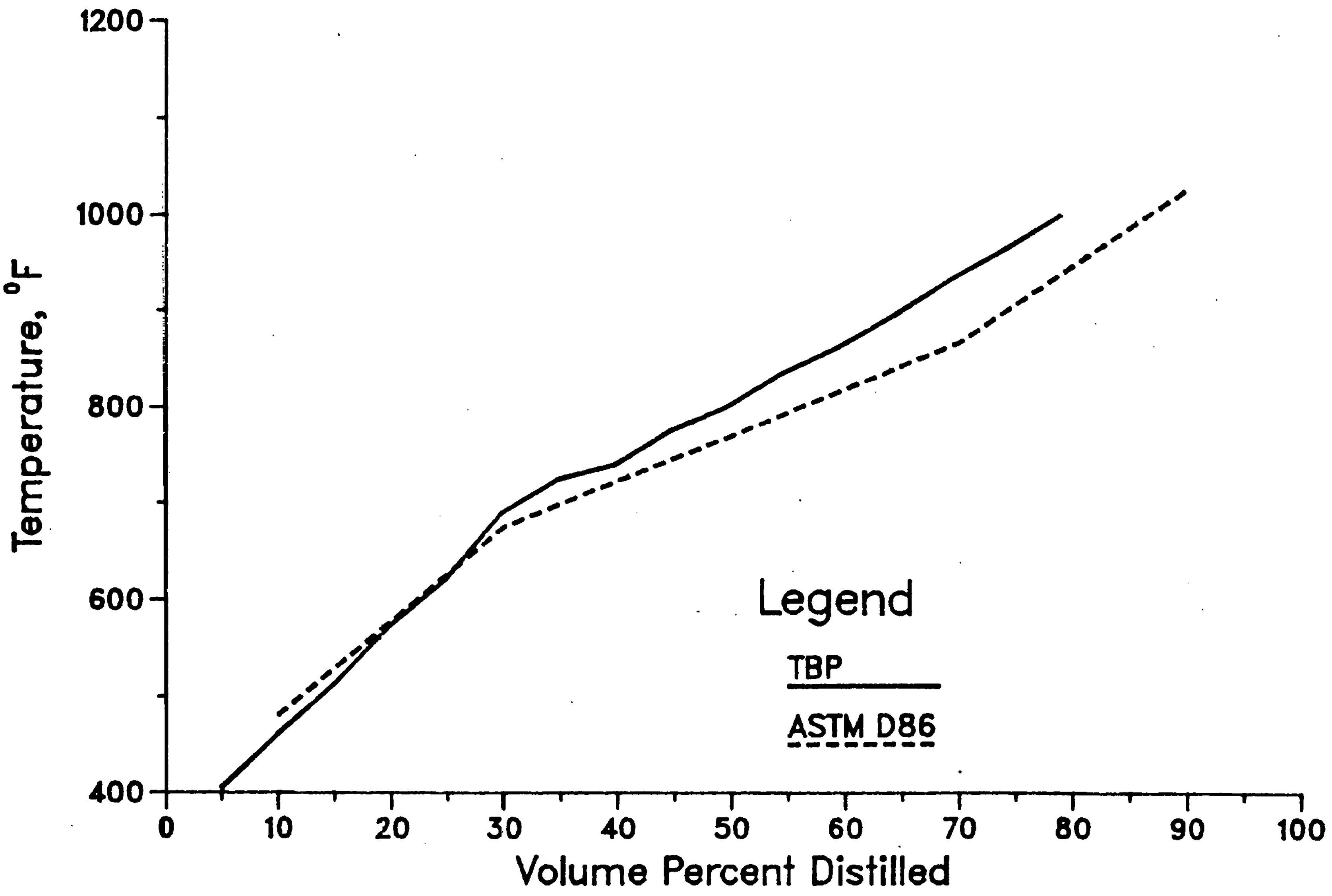

Figure 7. Distillation Curves for Western Reference Shale Oil

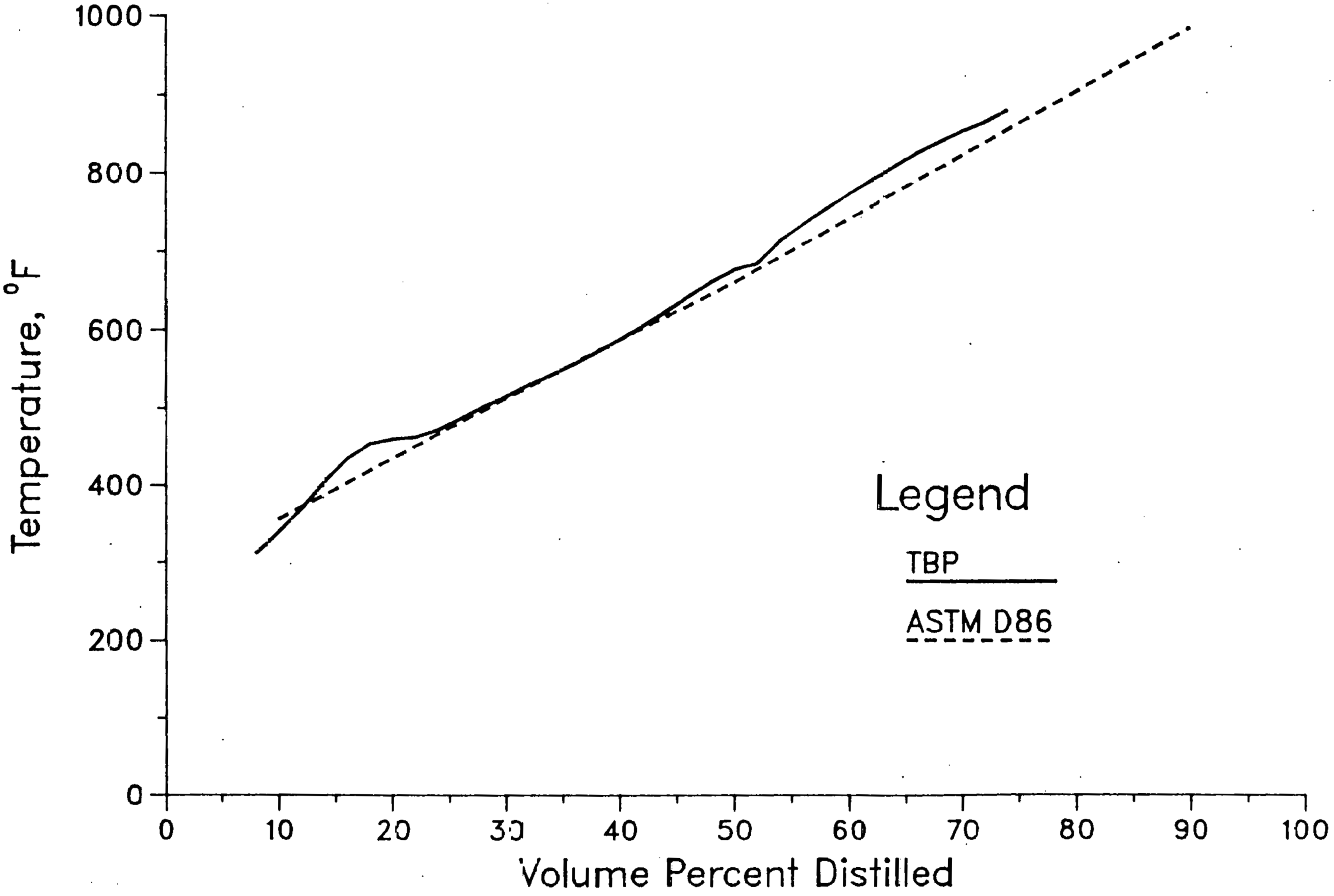

Figure 8. Distillation Curves for Eastern Reference Shale Oil

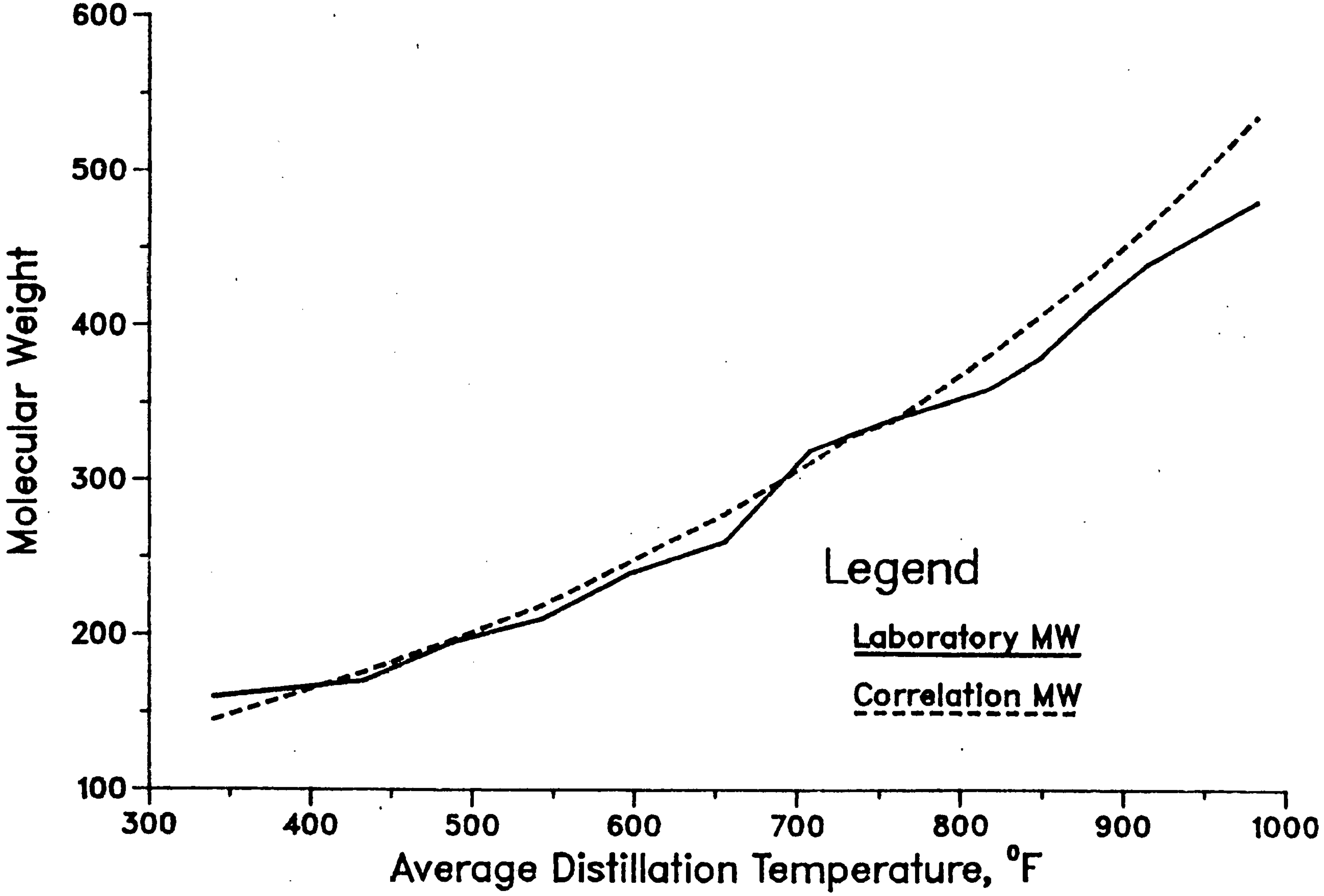

Figure 9. Laboratory and Correlation Molecular Weights for Western Reference Shale Oil Fractions

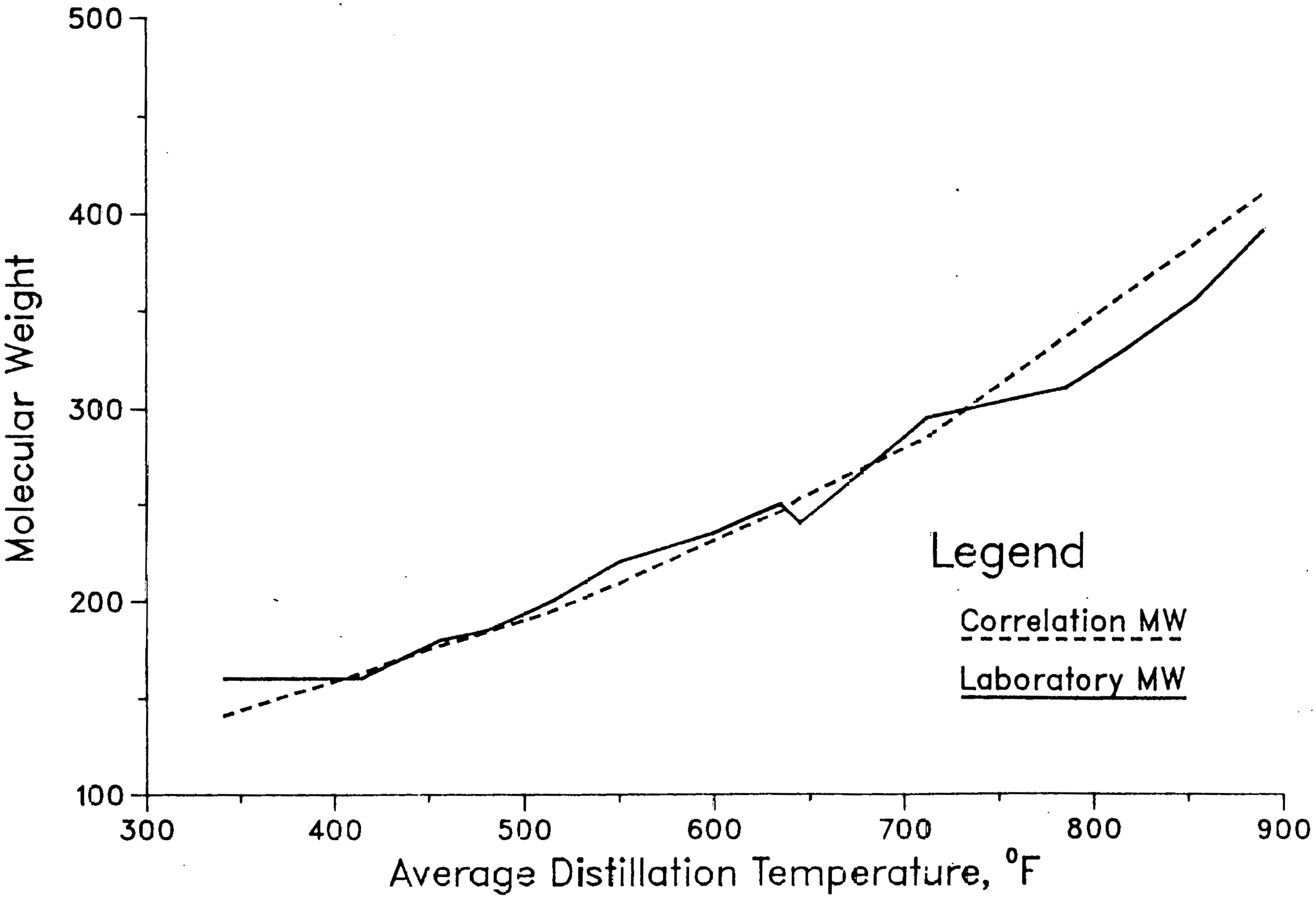

Figure 10. Laboratory and Correlation Molecular Weights for Eastern Reference Shale Oil Fractions

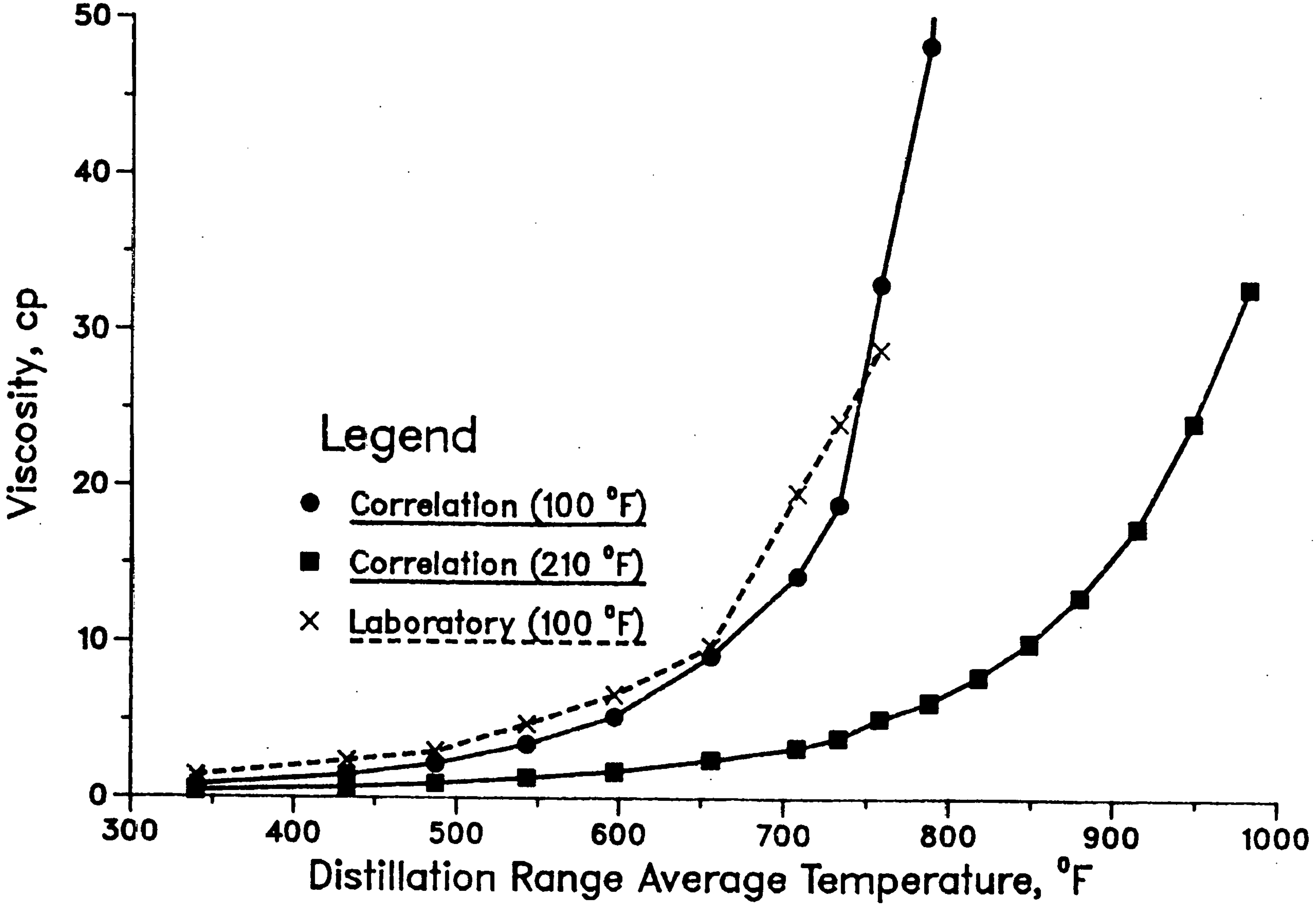

Figure 11. Comparison of Laboratory and Correlation Viscosities for Western Reference Shale Oil Fractions

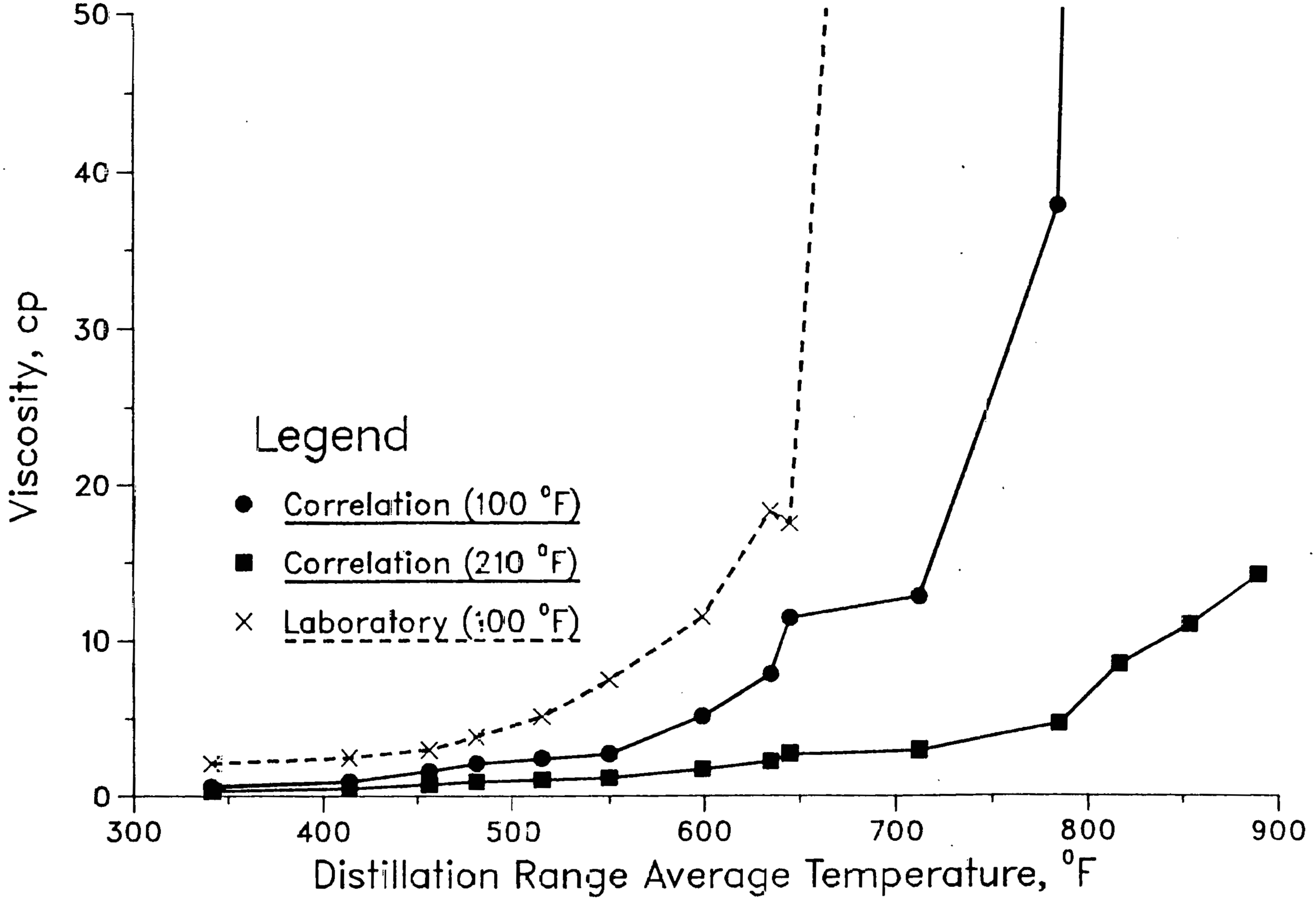

Figure 12. Comparison of Laboratory and Correlation Viscosities for Eastern Reference Shale Oil Distillation Fractions

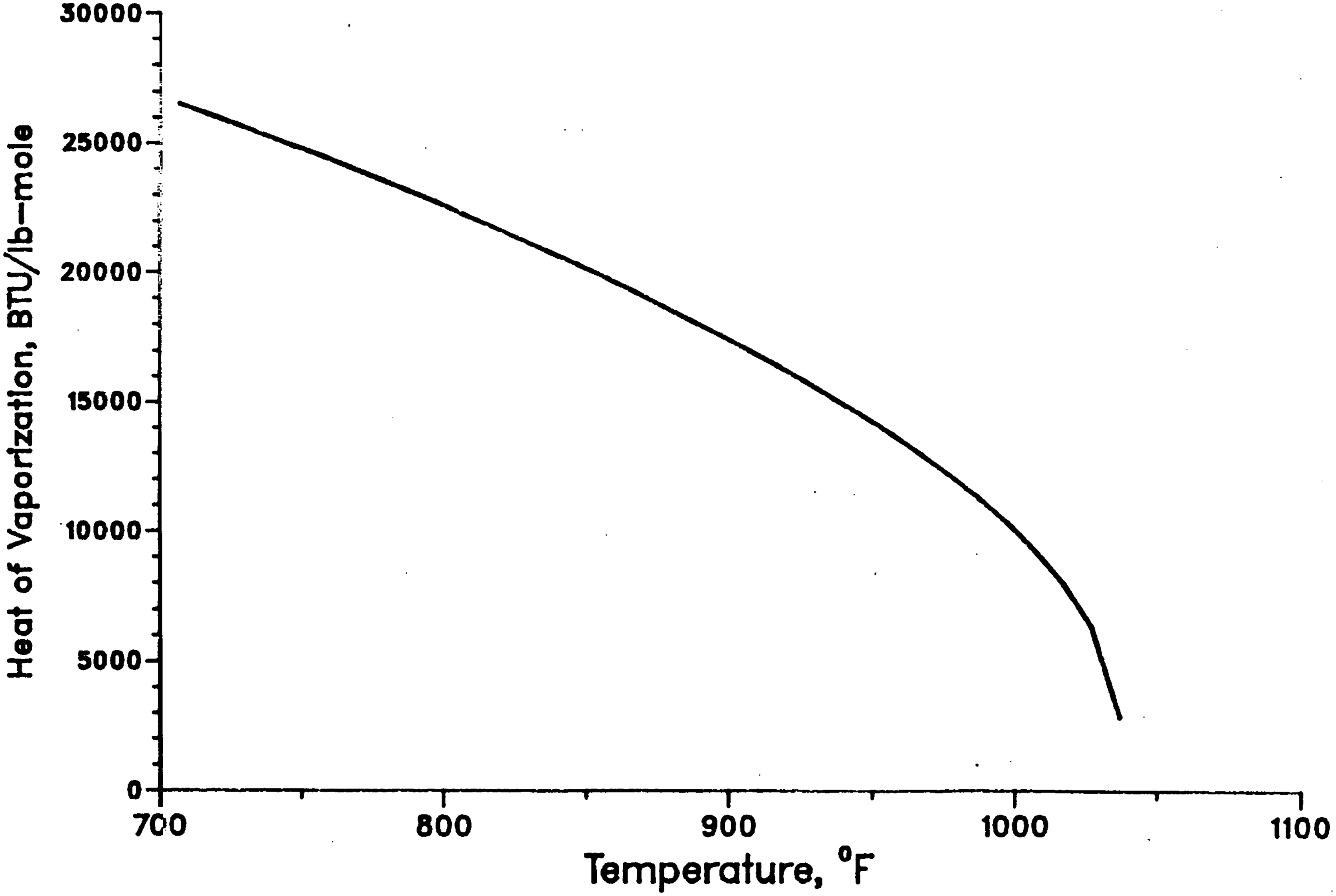

Figure 13. Heat of Vaporization vs. Temperature for Western Reference Shale Oil

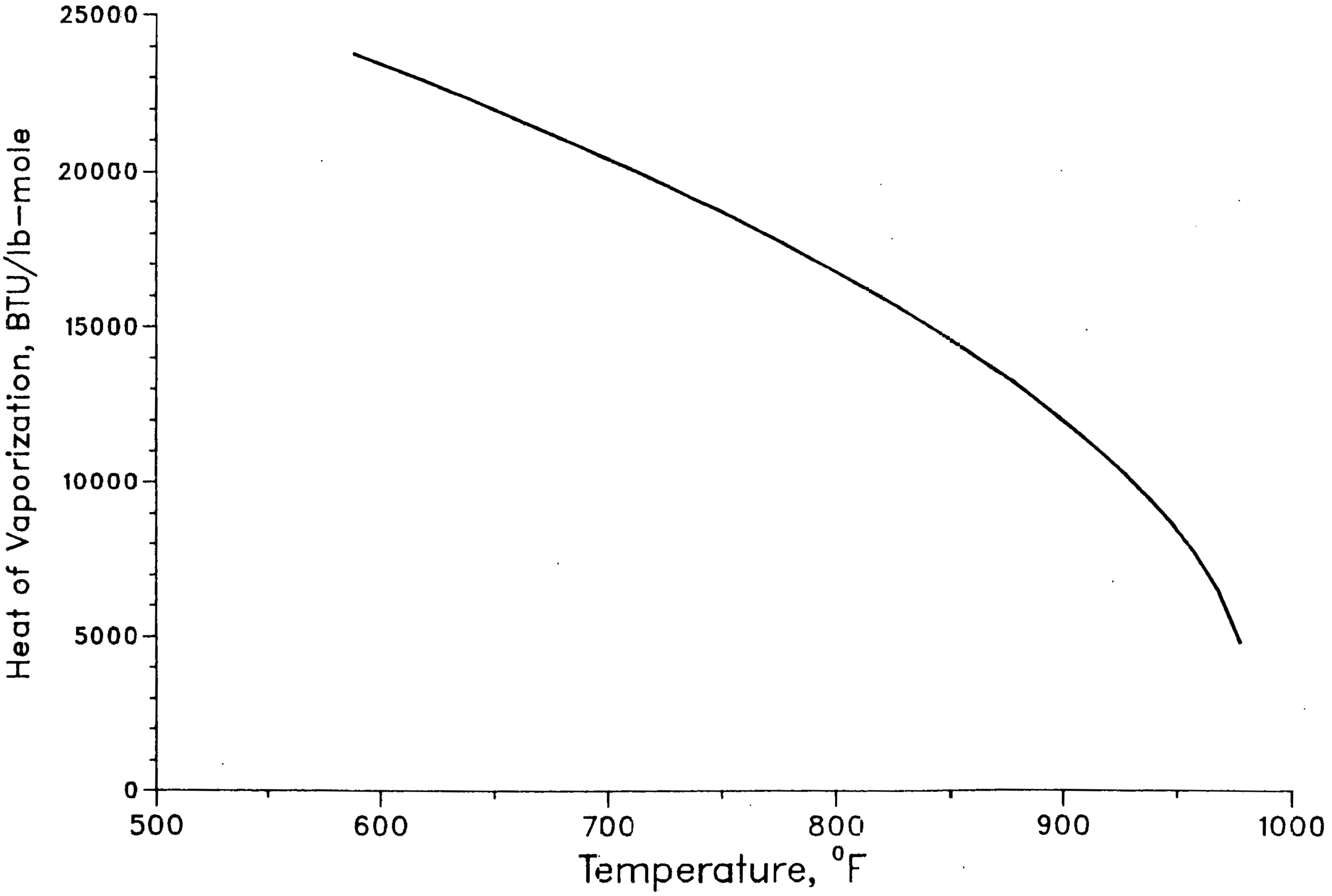

Figure 14. Heat of Vaporization vs. Temperature for Eastern Reference Shale Oil

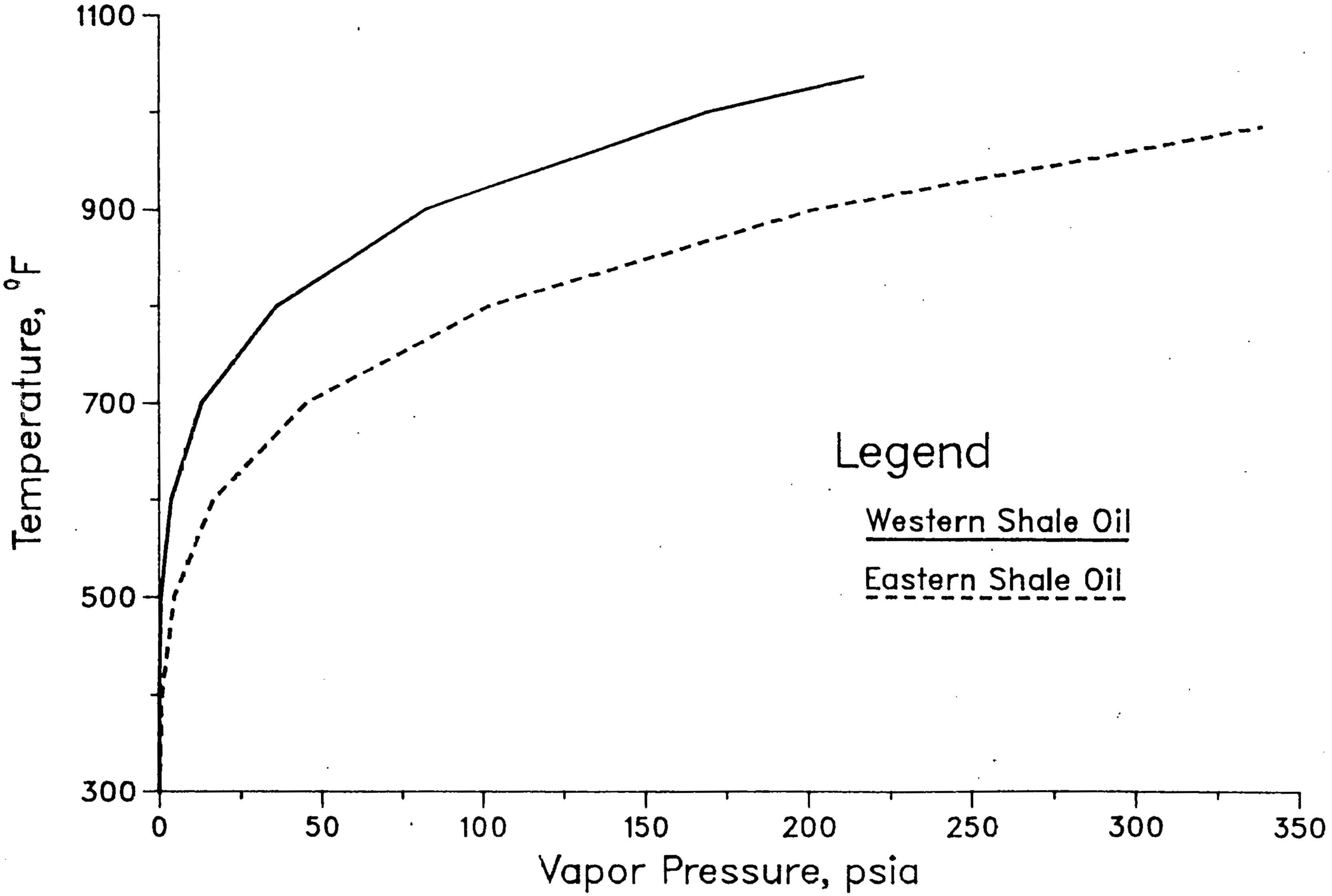

Figure 15. Temperature vs. Vapor Pressure for Reference Shale Oils

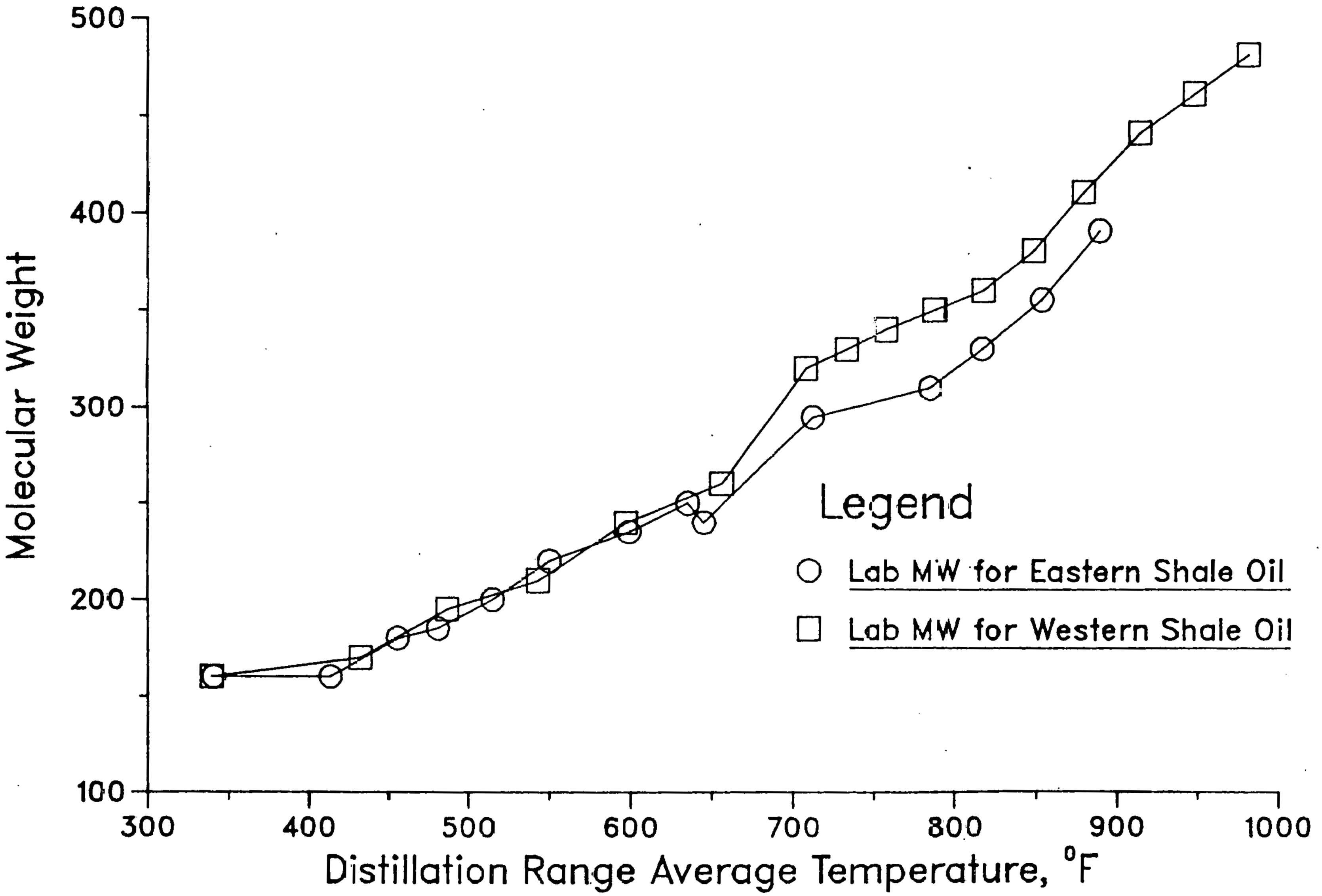

Figure 16. Comparison of Eastern and Western Reference Shale Oil Molecular Weights

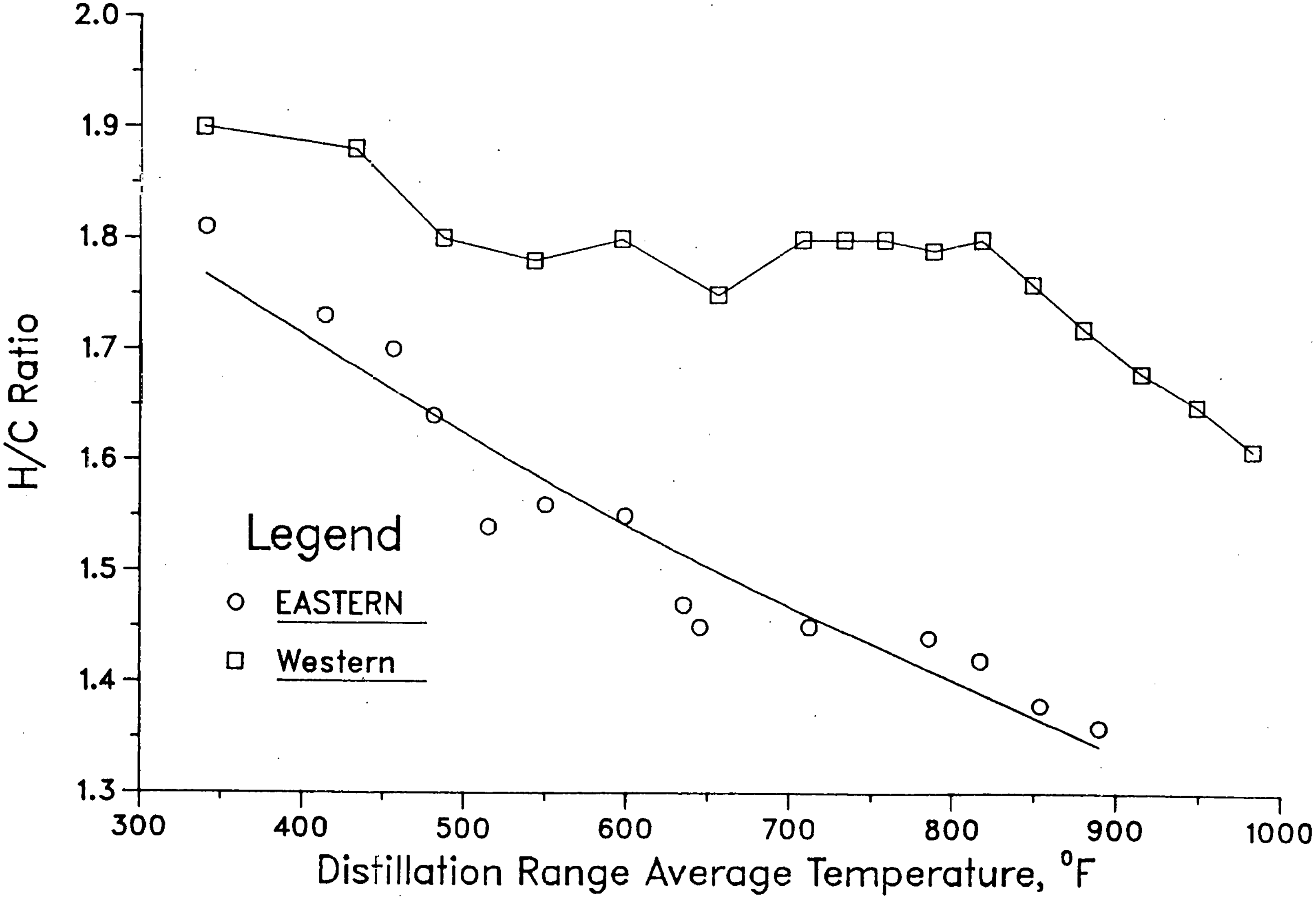

Figure 17. Comparison of H/C Ratios for Eastern and Western Shale Oil Fractions

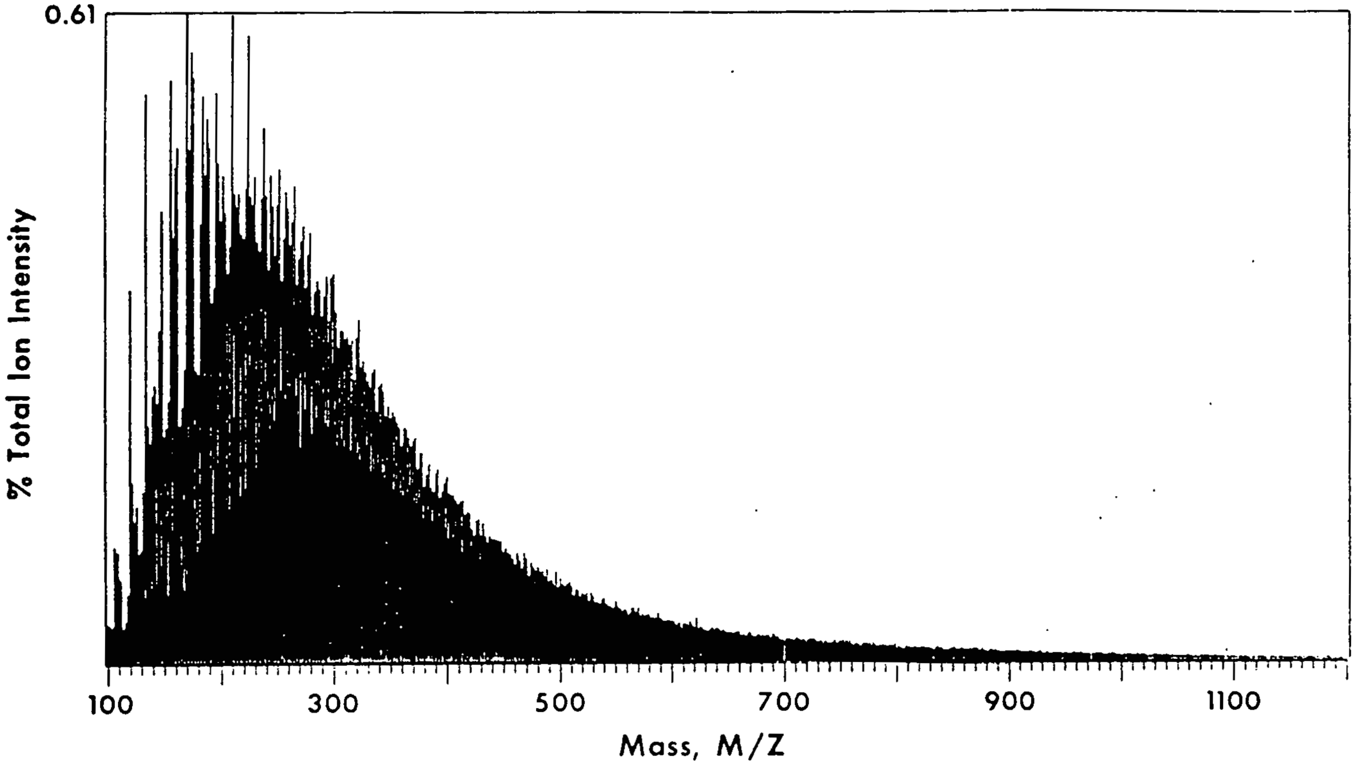

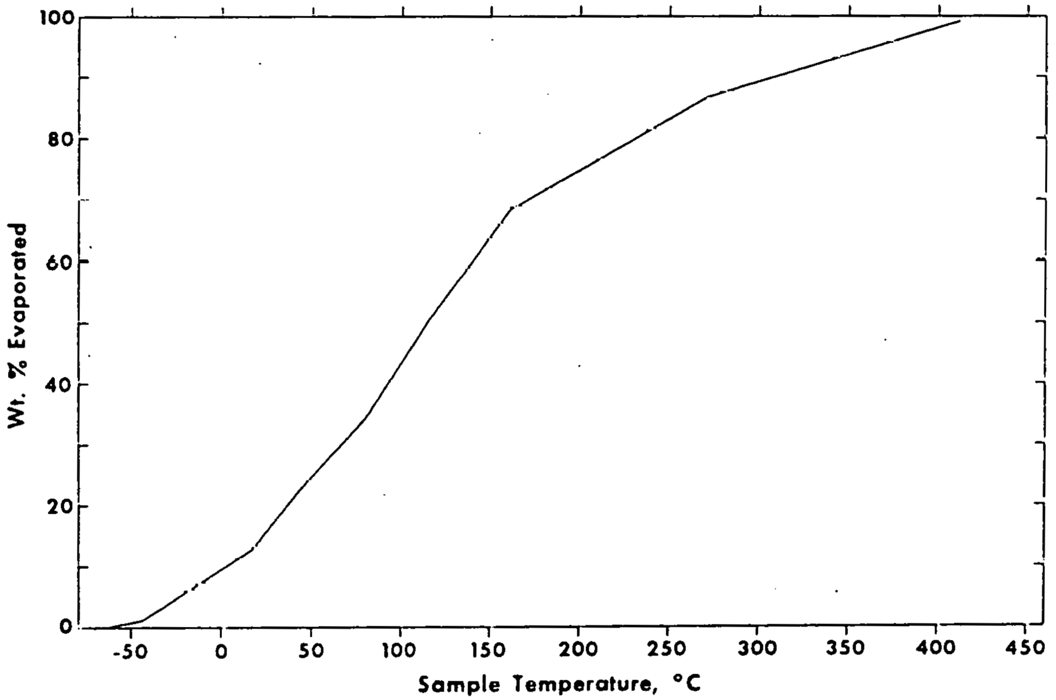

Figure 18. Field Ionization Mass Spectrum and Evaporation vs. Temperature for Composite Eastern Shale Oil

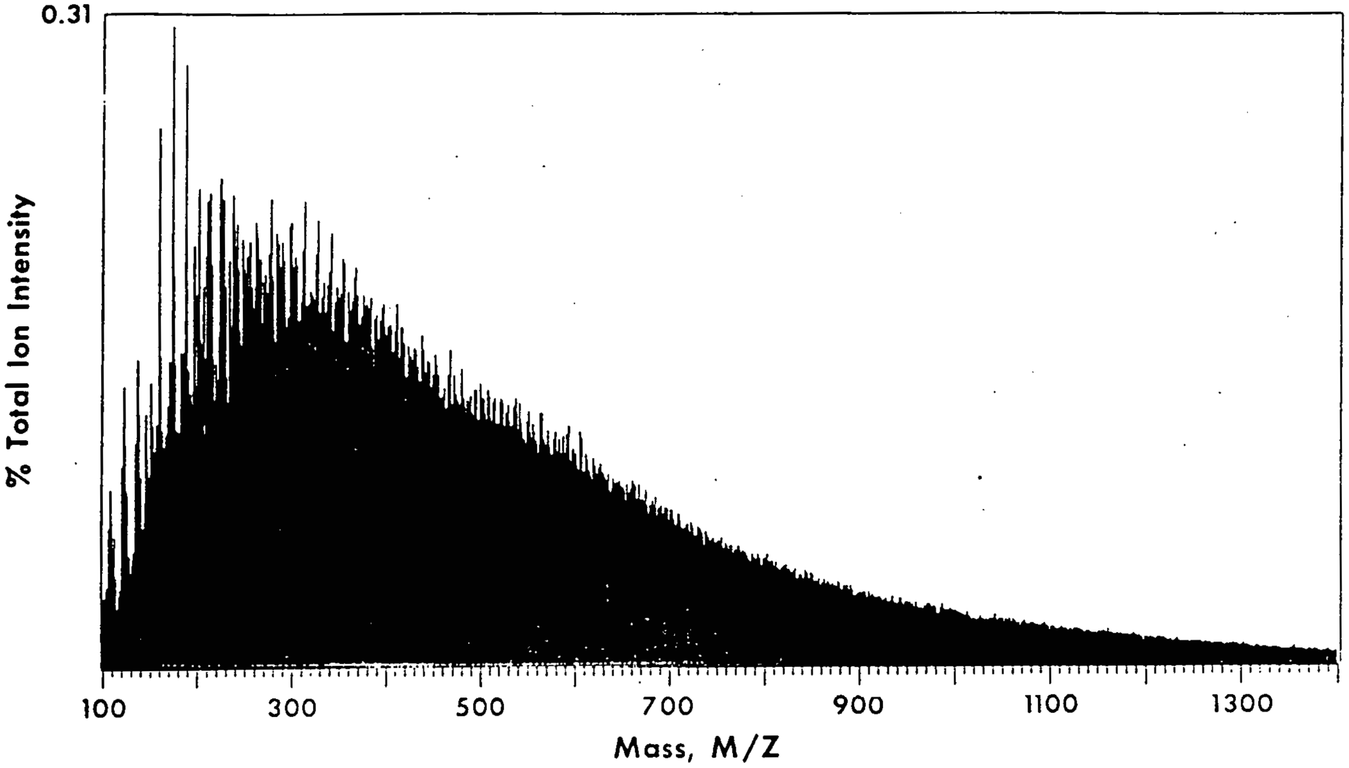

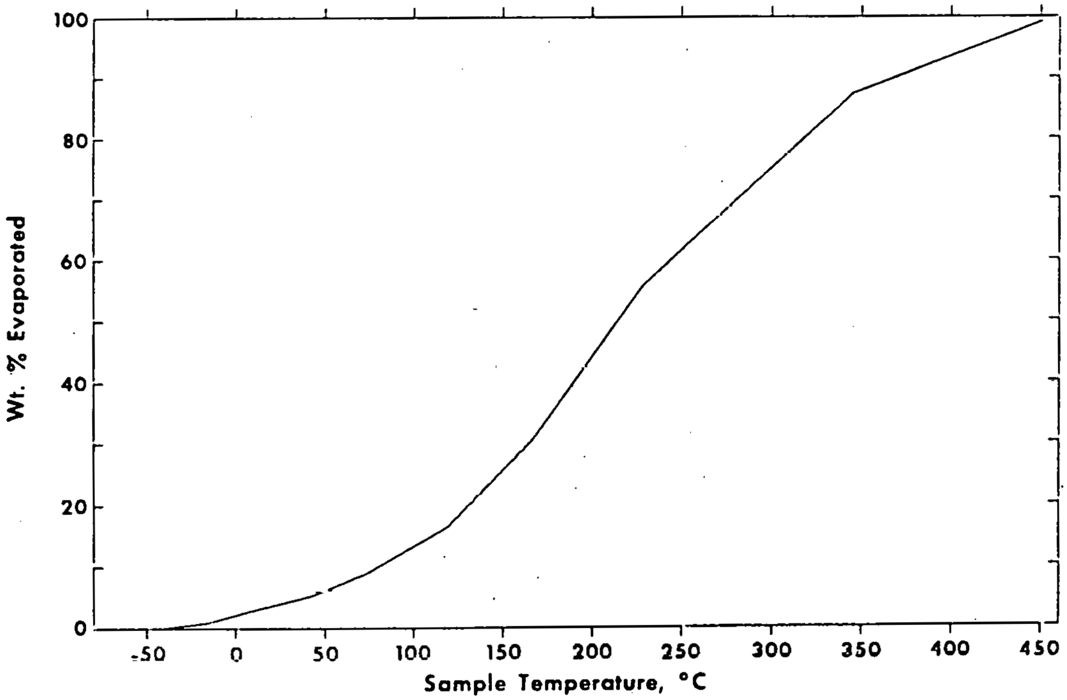

Figure 19. Field Ionization Mass Spectrum and Evaporation vs. Temperature for Composite Western Shale Oil

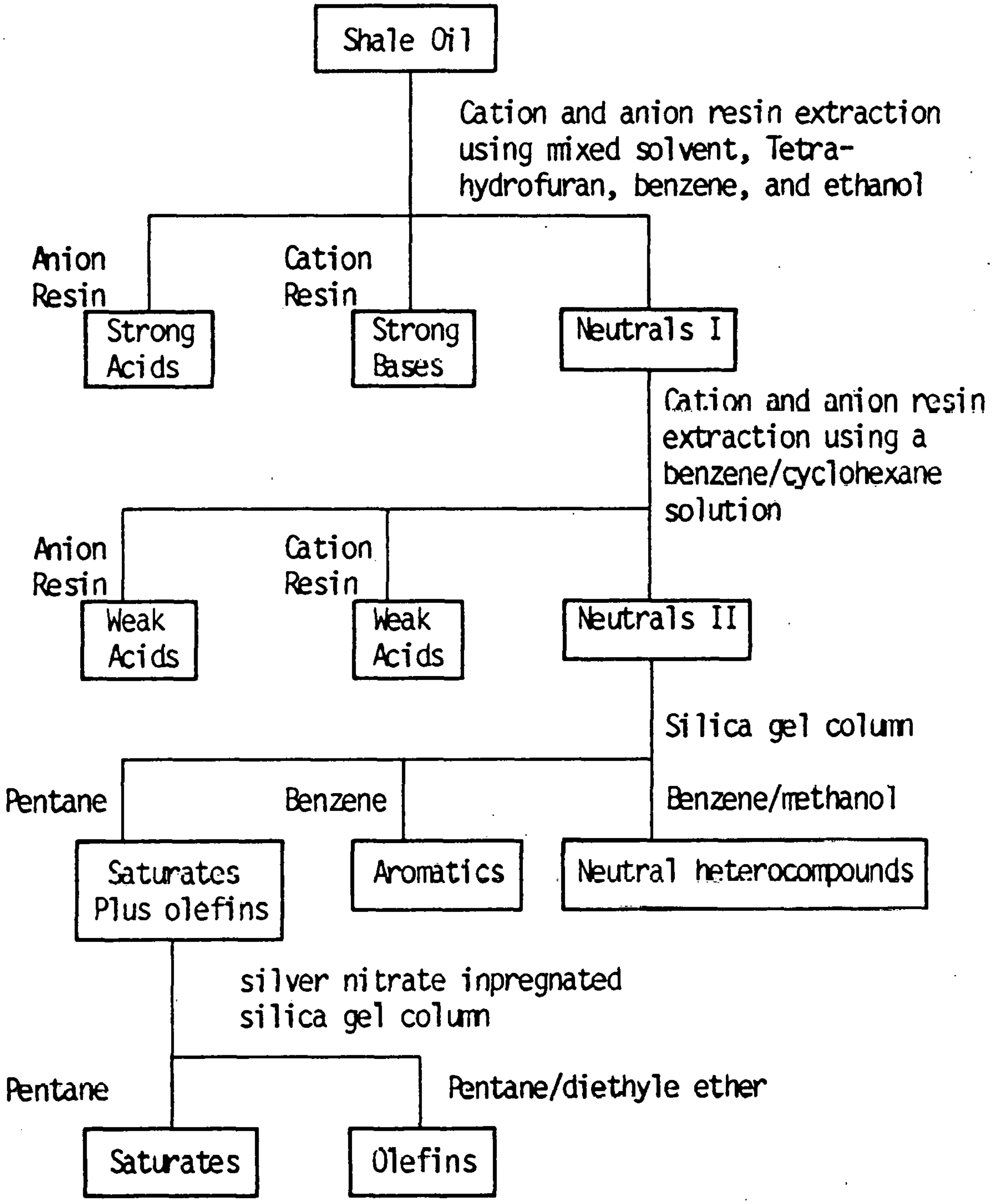

Figure 20. Chromatographic Separation Scheme Used to Fractionate Shale Oils

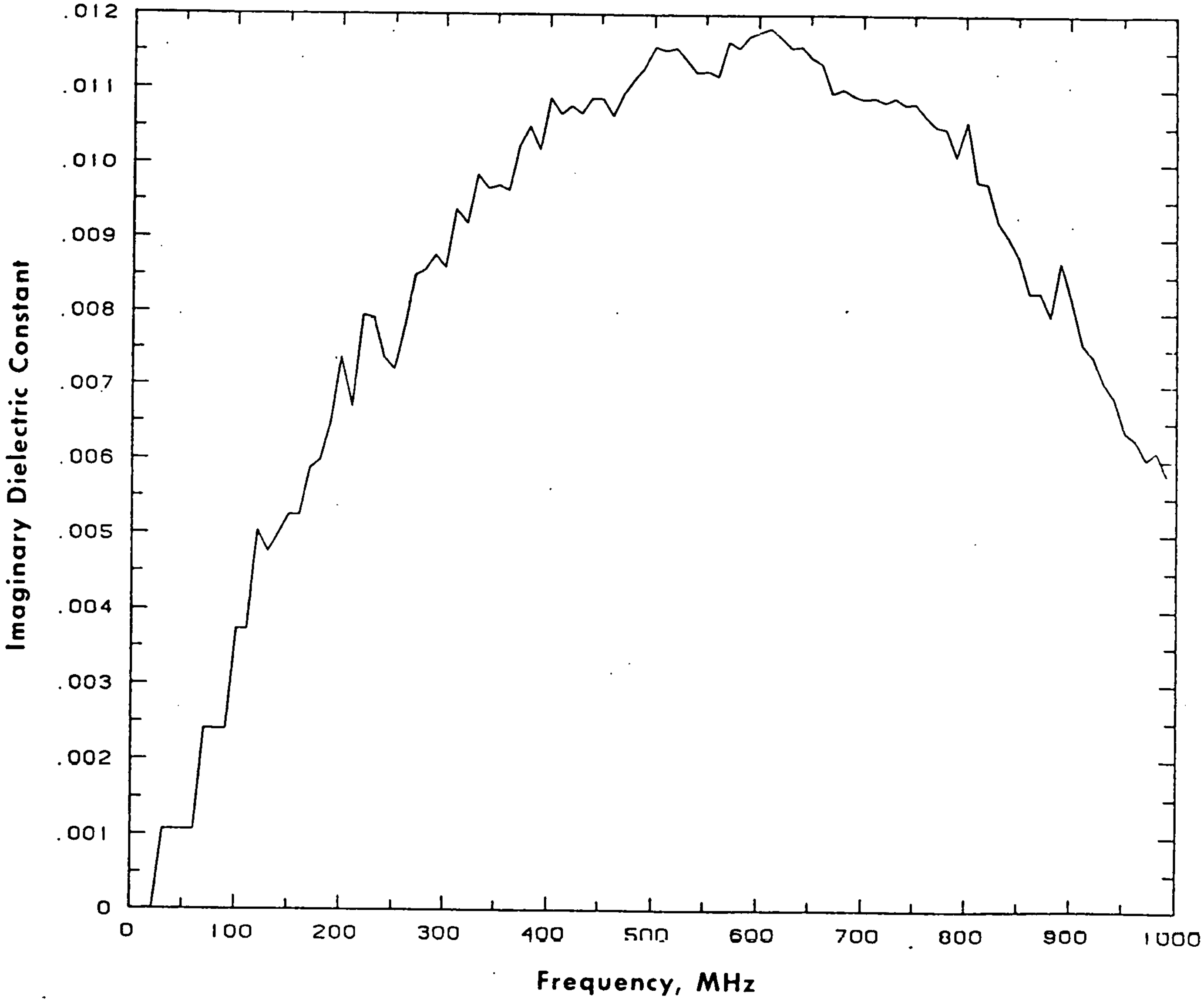

Figure 21. Imaginary Dielectric Response of Air in the Liquid Sample Cell

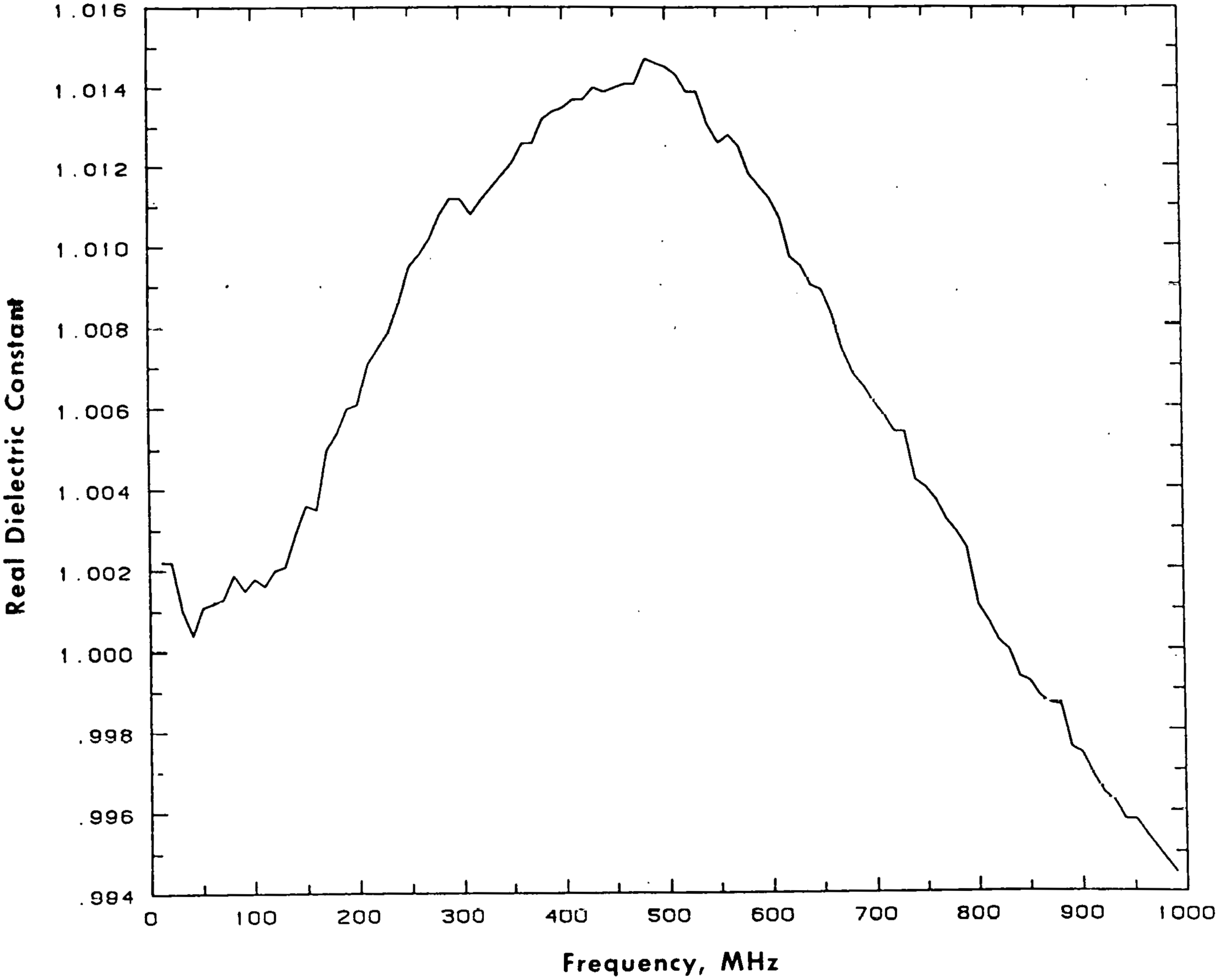

Figure 22. Real Dielectric Response of Air in the Liquid Sample Cell

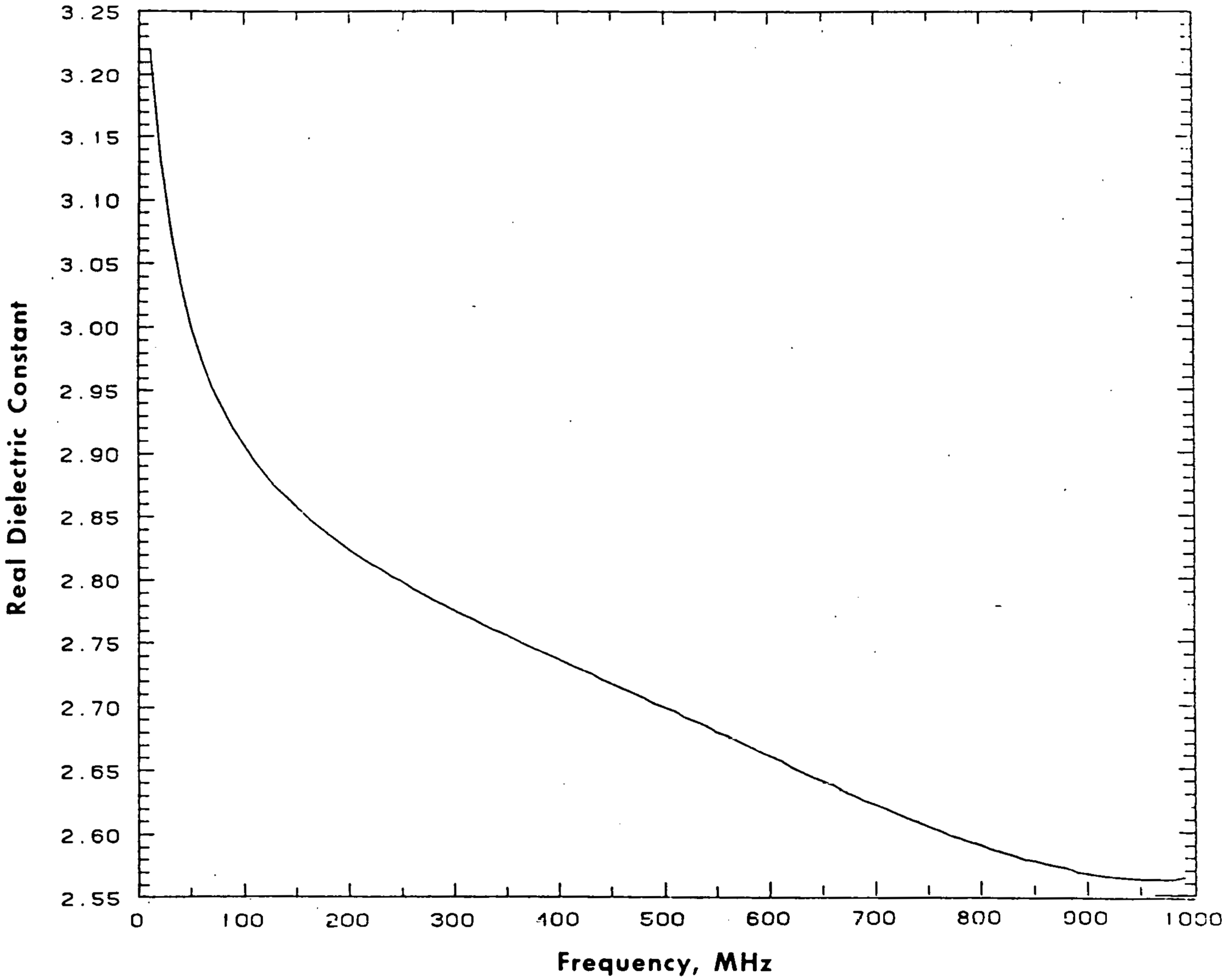

Figure 23. Real Dielectric Response of Composite Eastern Shale Oil

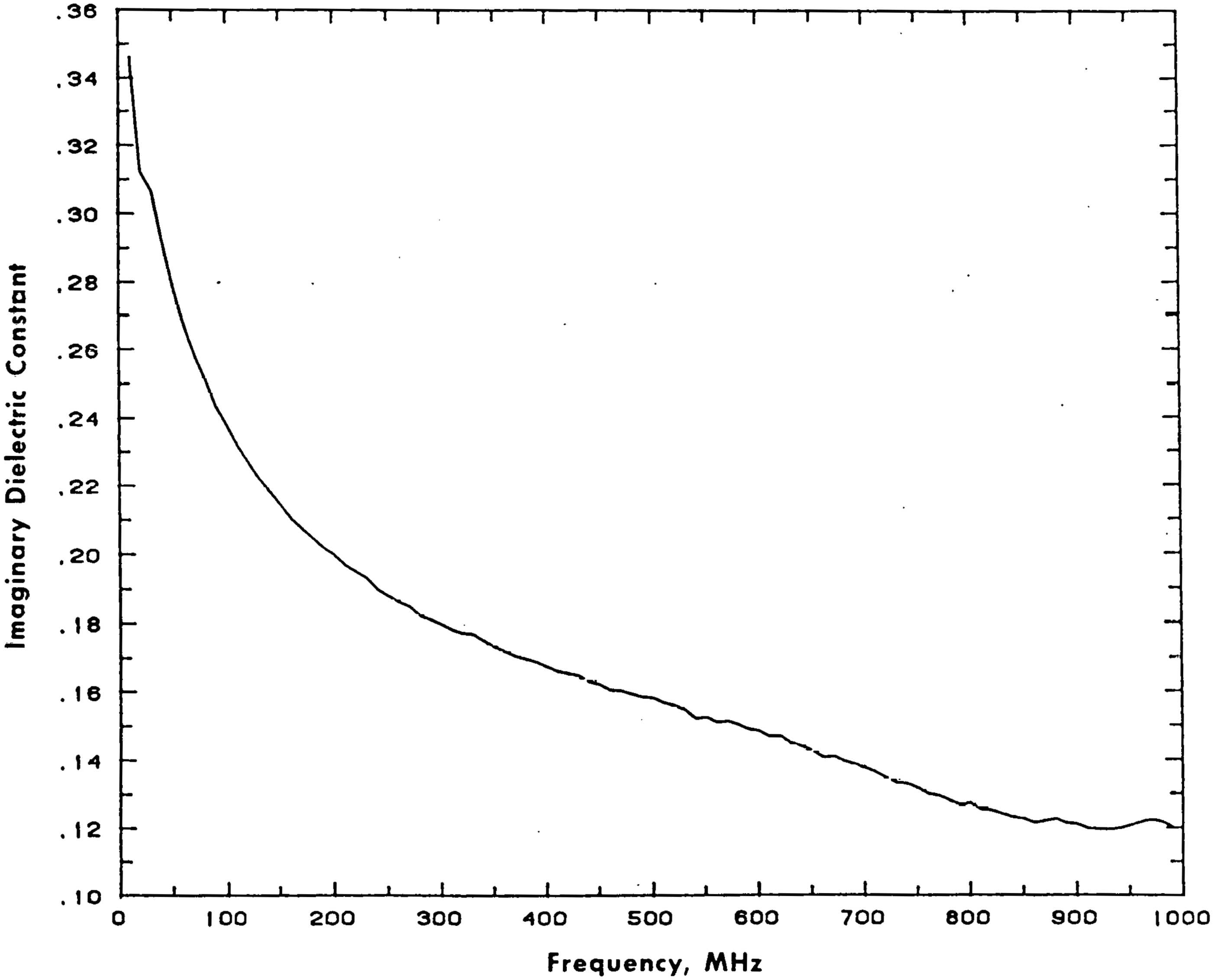

Figure 24. Imaginary Dielectric Response of Composite Eastern Shale Oil

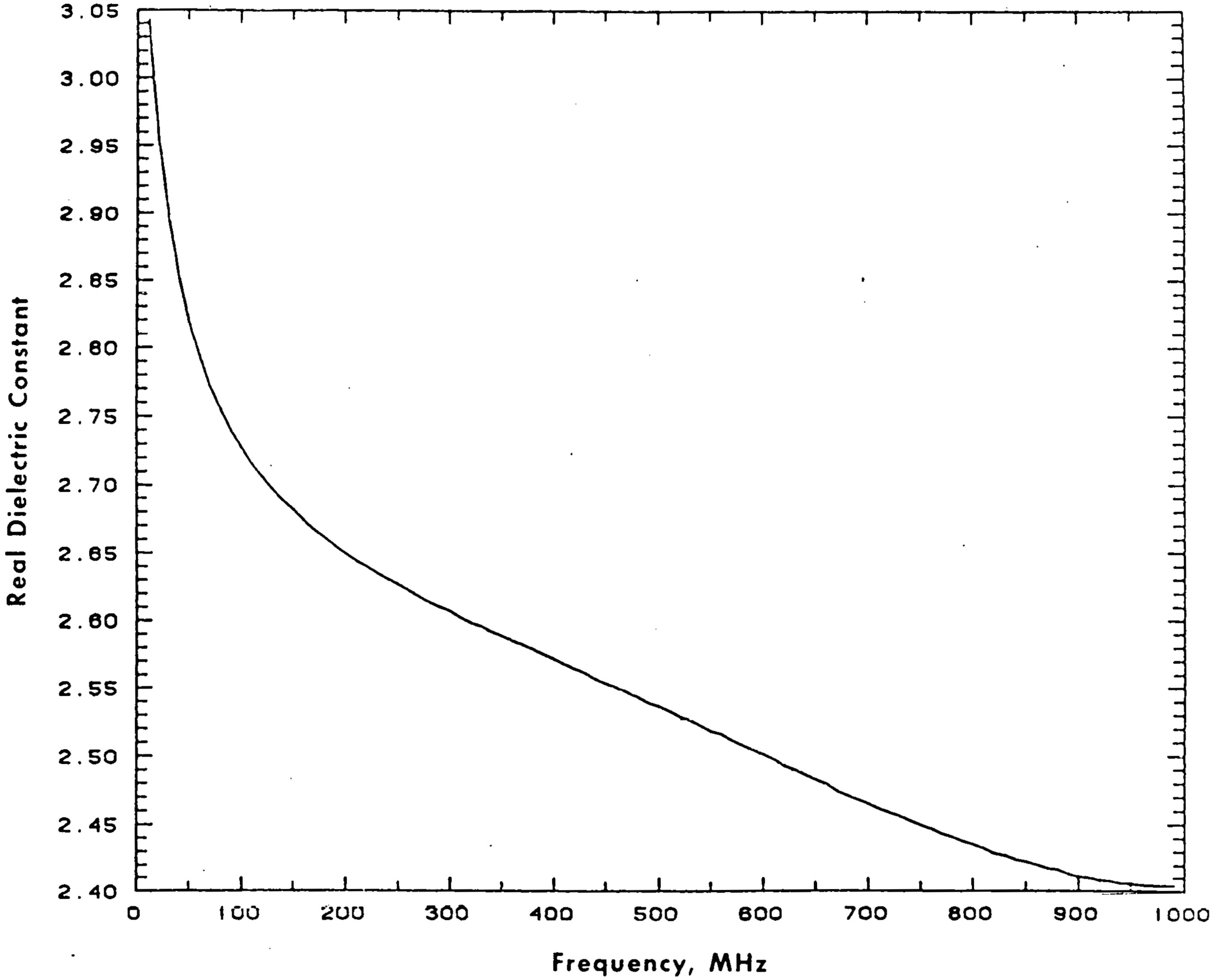

Figure 25. Real Dielectric Response of Composite Western Shale Oil

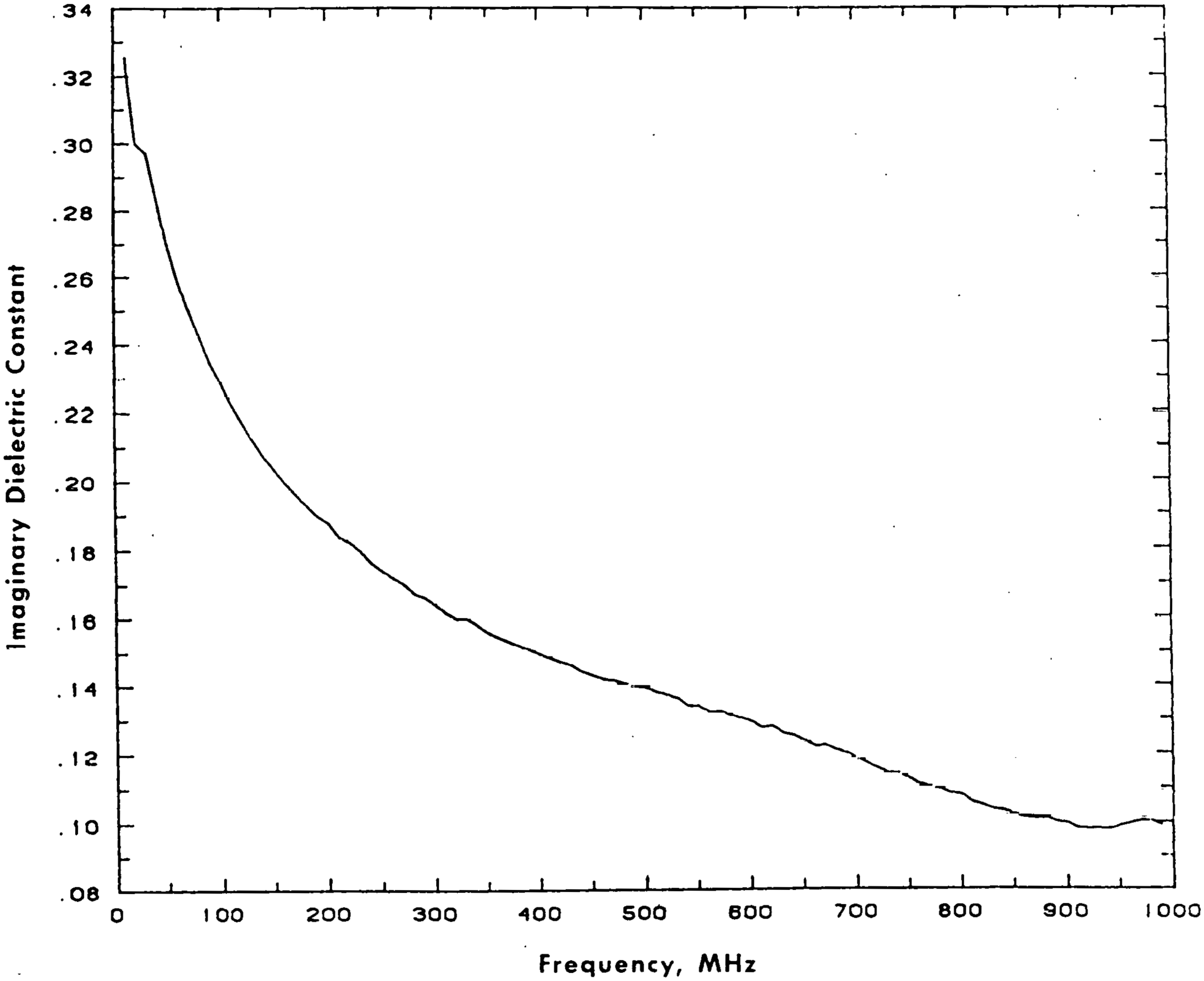

Figure 26. Imaginary Dielectric Response of Composite Western Shale Oil

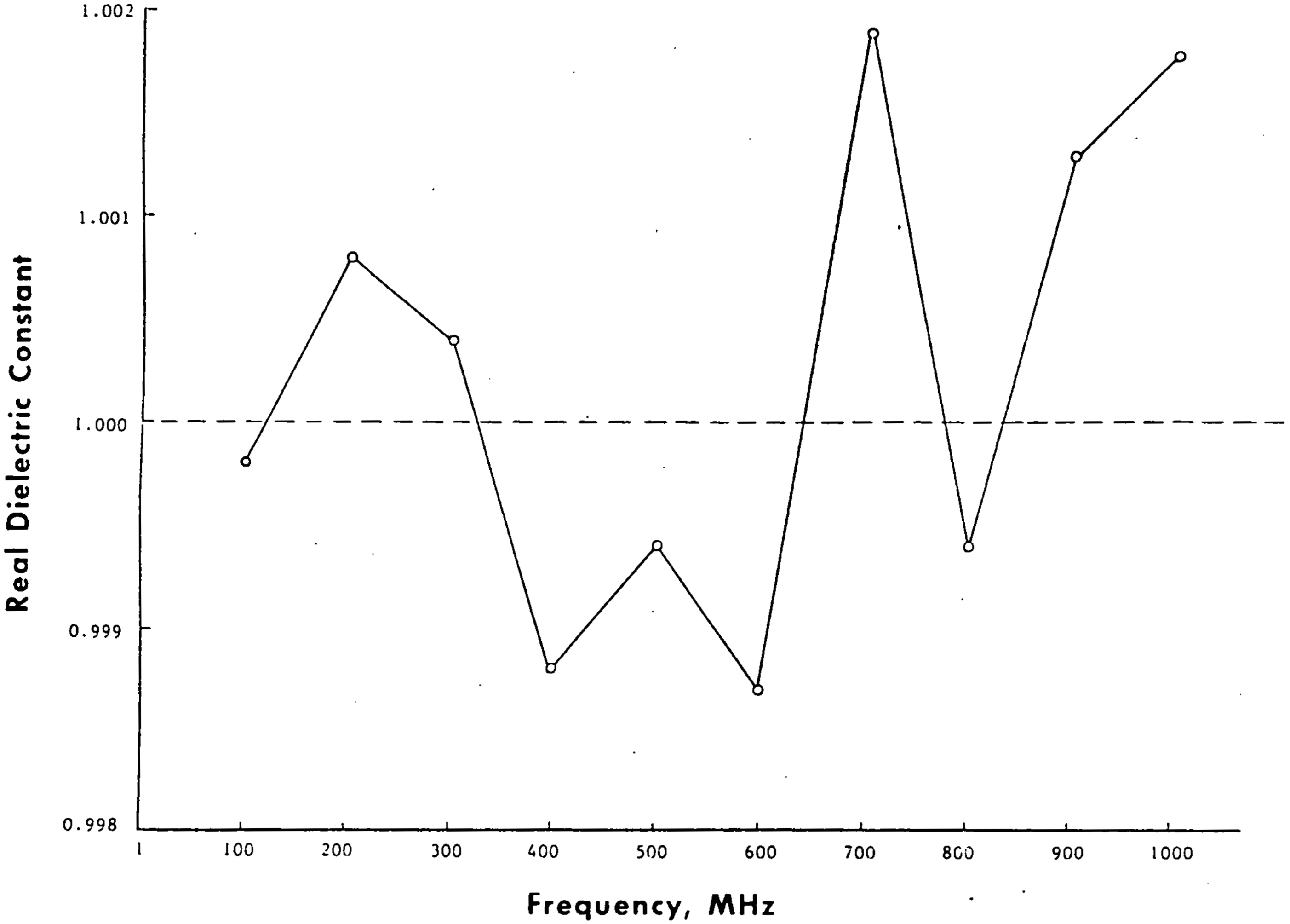

Figure 27. Real Dielectric Response of Air in the Solid Shale Sample Cell

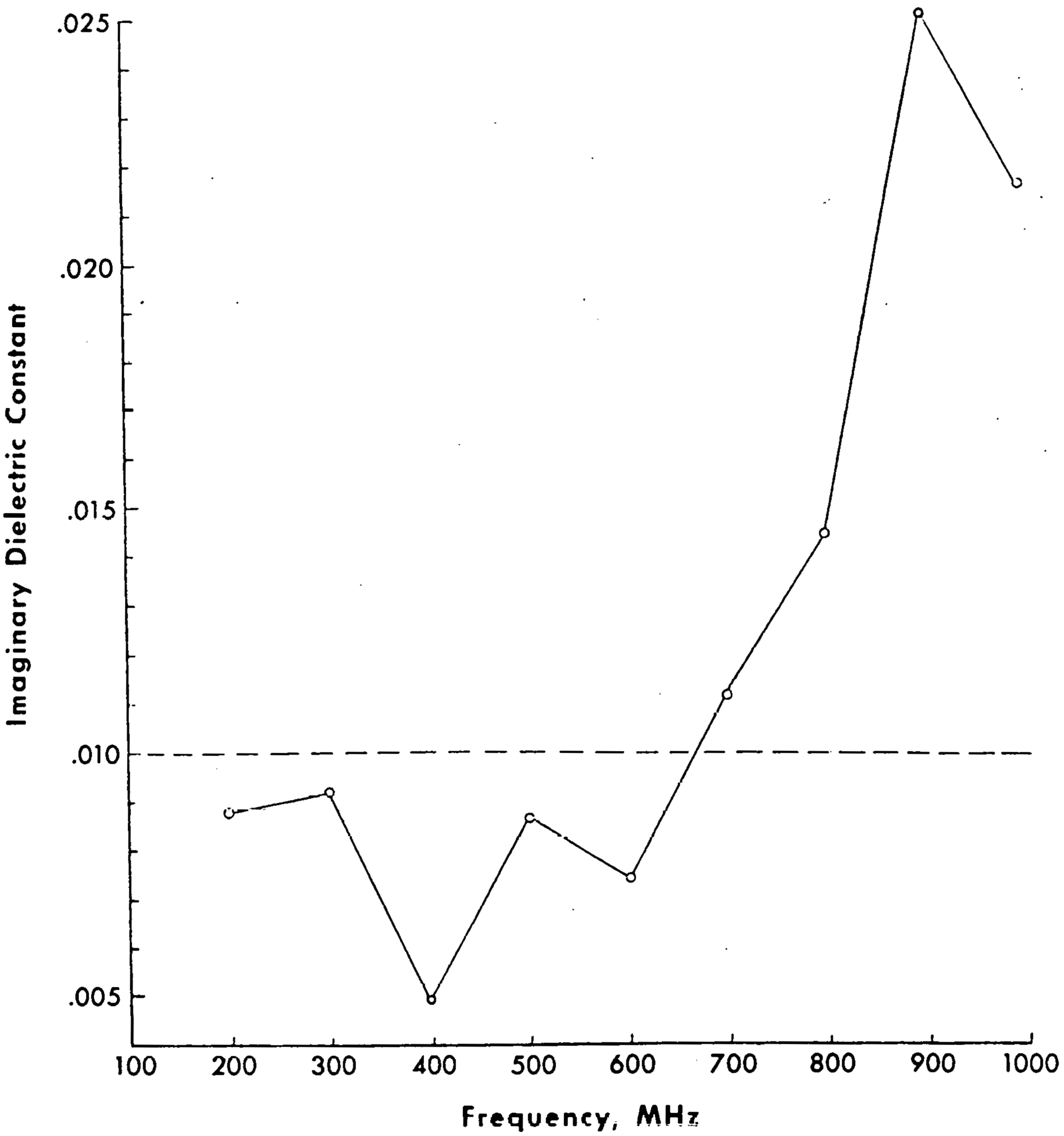

Figure 28. Imaginary Dielectric Response of Air in the Solid Shale Sample Cell

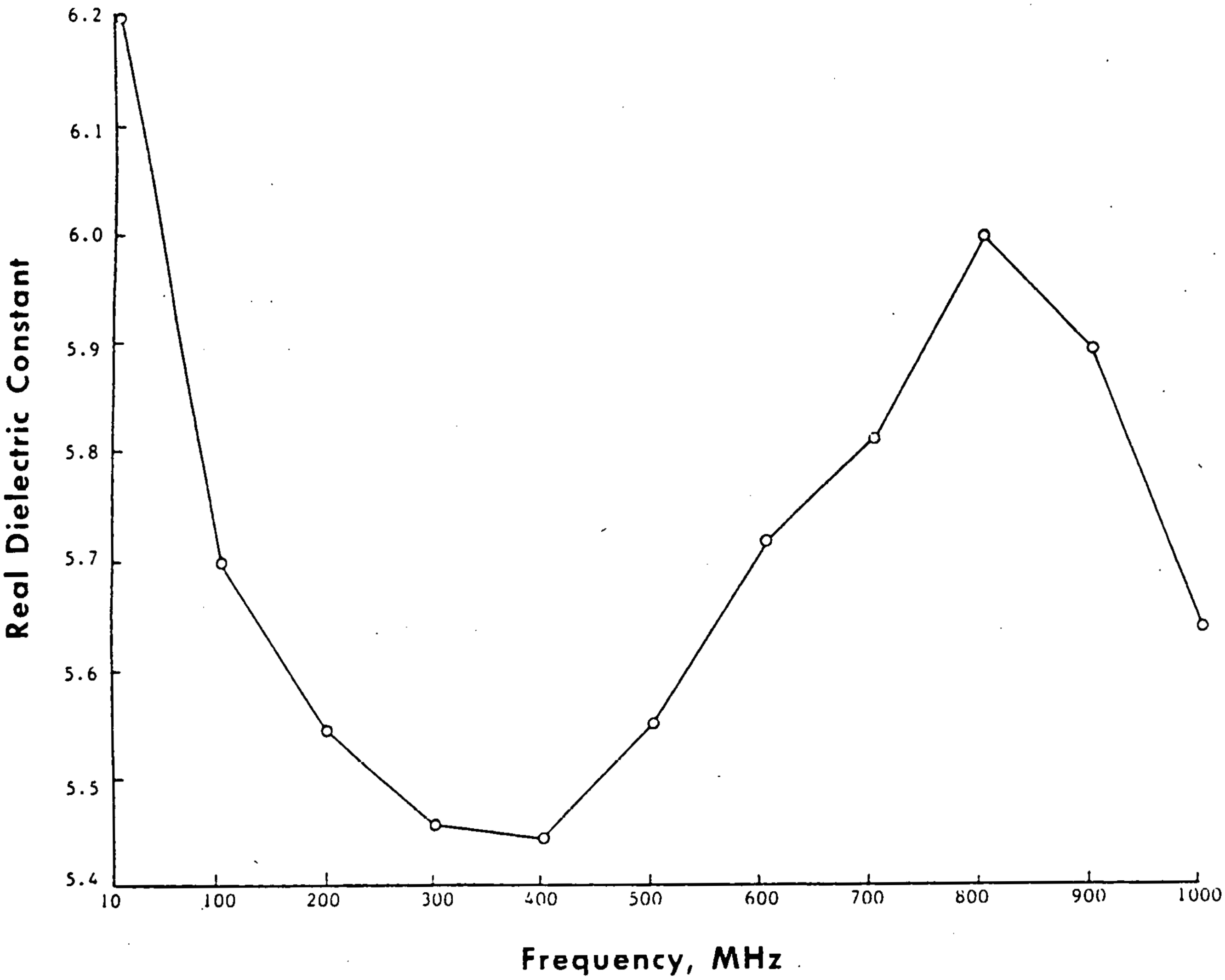

Figure 29. Real Dielectric Response of Western Shale: Sample Number 1

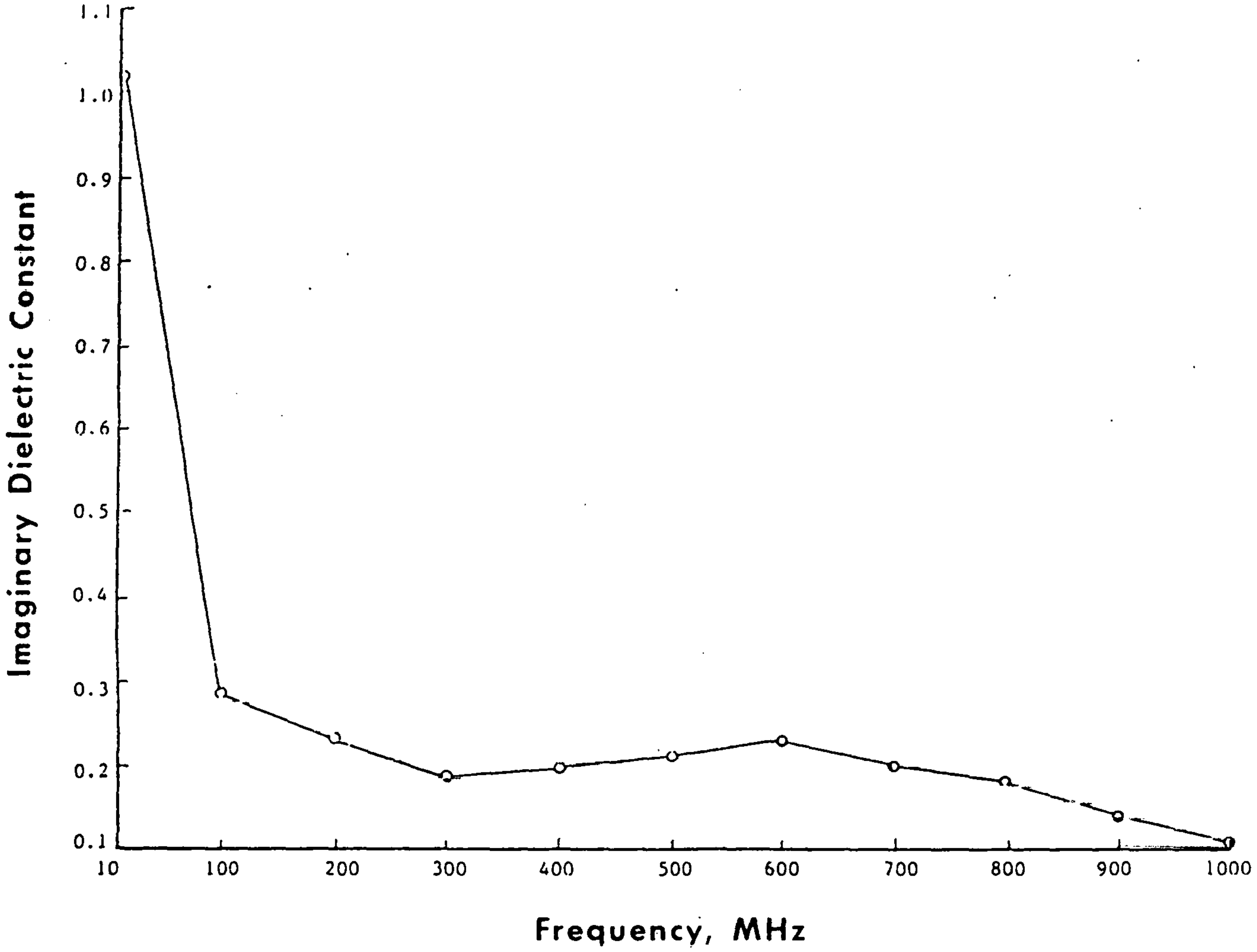

Figure 30. Imaginary Dielectric Response of Western Shale: Sample Number 1

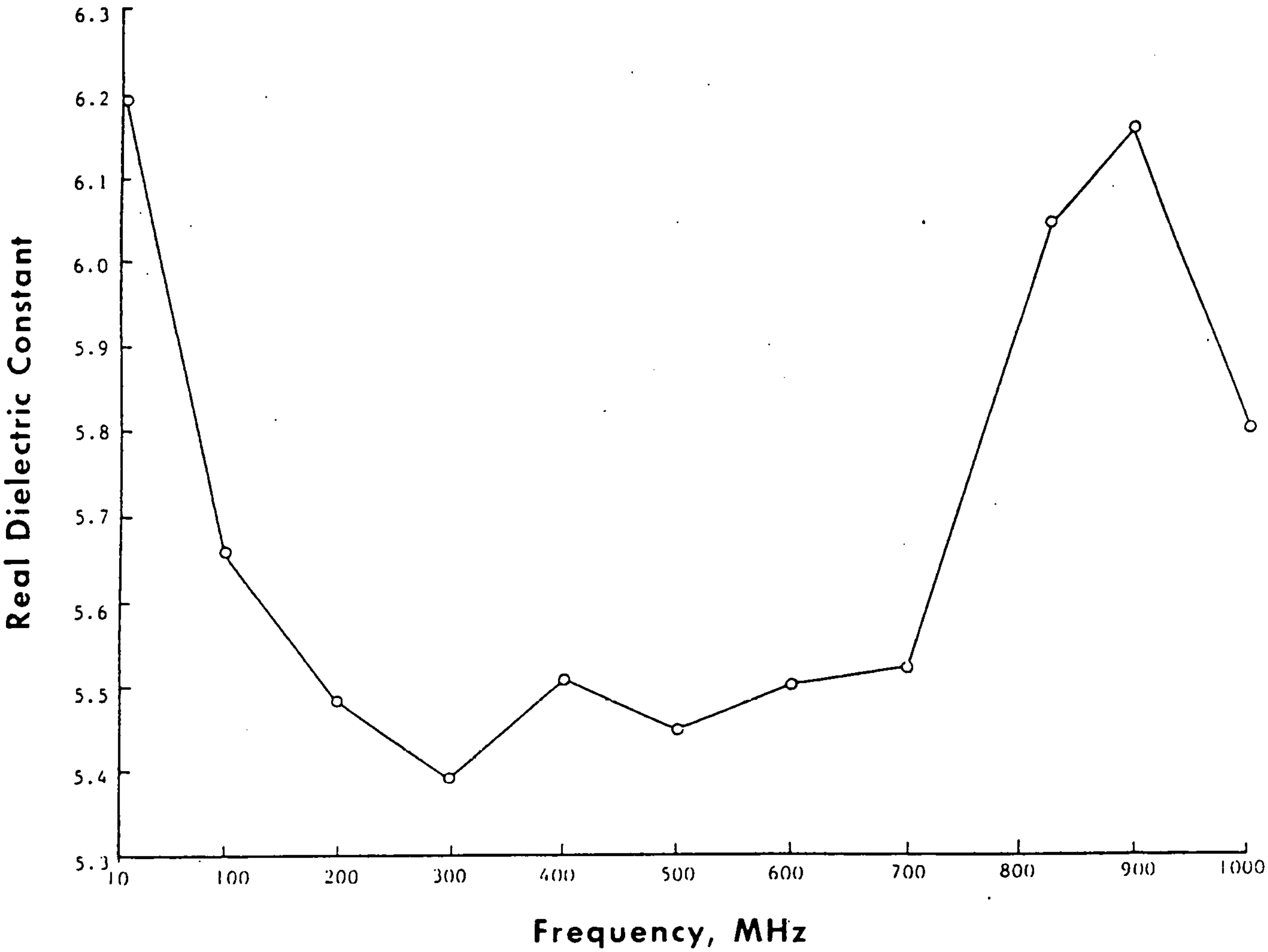

Figure 31. Real Dielectric Response of Western Shale: Sample Number 2

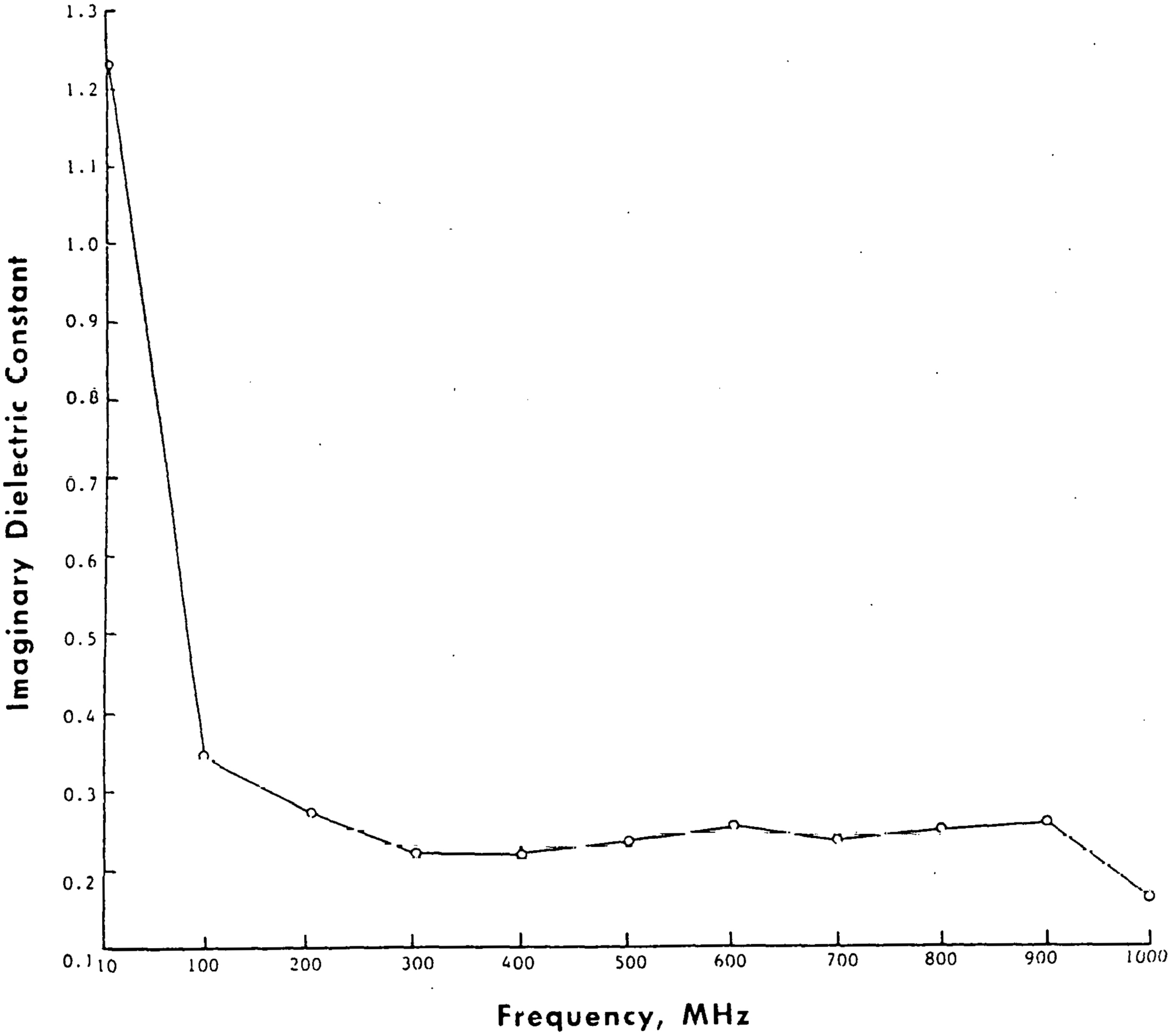

Figure 32. Imaginary Dielectric Response of Western Shale: Sample Number 2

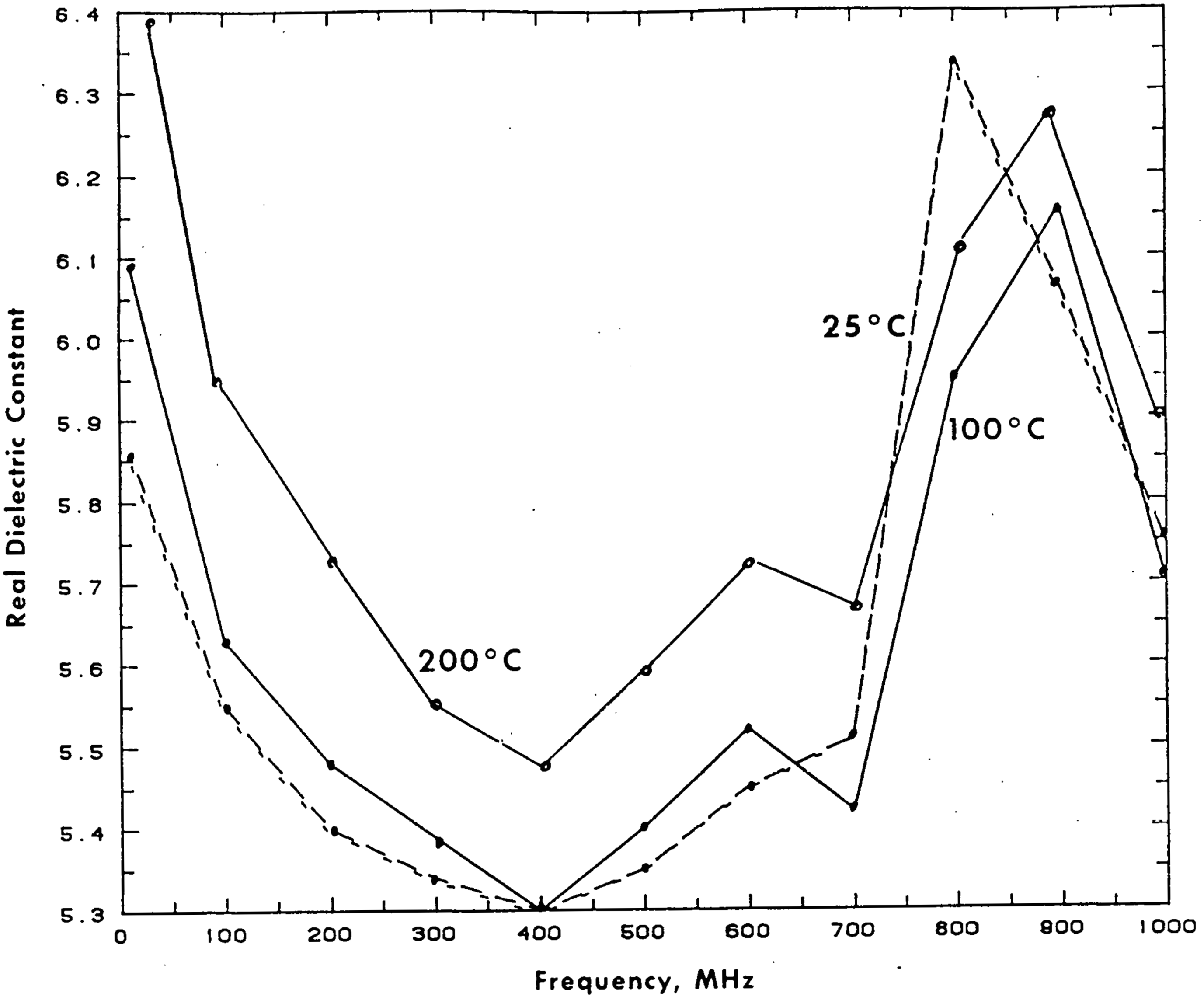

Figure 33. Real Dielectric Response of Western Shale at 25°, 100°, and 200°C

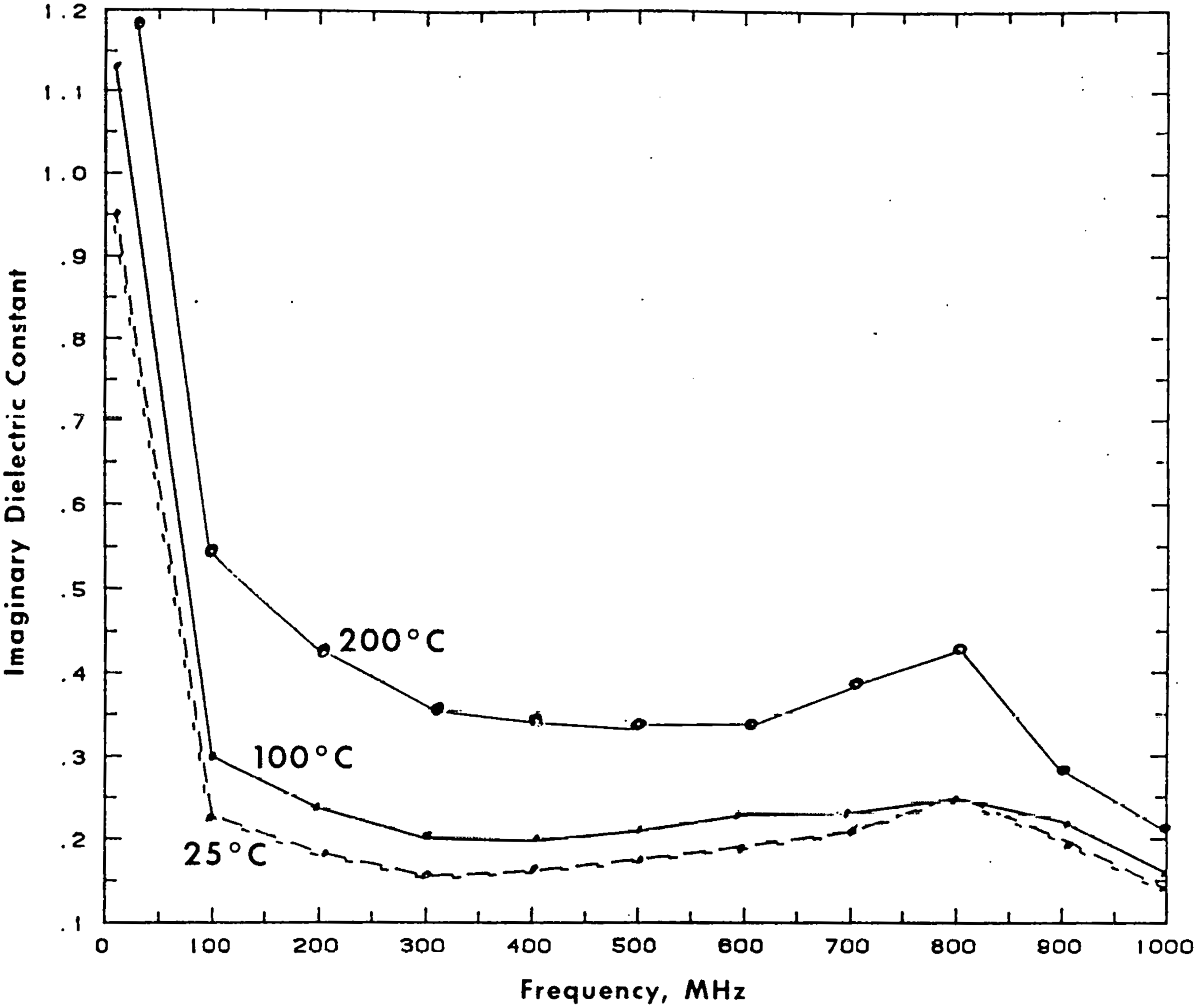

Figure 34. Imaginary Dielectric Response of Western Shale at 25°, 100°, and 200°C

APPENDIX B. PROCEDURES FOR CALCULATING CHEMICAL AND PHYSICAL PROPERTIES OF REFERENCE SHALE OILS

Molecular Weight

a) Riazi, Daubert (1980)

$MW = 4.5673 * 10^{-5} * T_b^{2.1962} * SG^{-1.0164}$

MW = molecular weight

T_b = mean average boiling point, °R

SG = specific gravity, 60F/60F

b) Kesler, Lee (1976)

$MW = -12,272.6 + 9486.4 * SG + (4.6523-3.2287*SG)*T_b$

$+ (1-0.77084 * SG-0.02058*SG^2) * (1.3437-720.79/T_b) * 10^7/T_b$

$+(1-0.80882 * SG+0.02226 * SG^2) * (1.8828-181.98/T_b) * 10^{12}/T_b^3$

MW = molecular weight

SG = specific gravity, 60F/60F

T_b = normal boiling point, °R

c) Twu (1984)

Use Figure 4 or iterative procedure from abstract.

d) API Technical Data Book (1985)

Procedure 2B2.1

$MW = 204.38 * \exp(0.00218 * T_b) * \exp(-3.07 * SG) * T_b^{0.118} * SG^{1.88}$

MW = molecular weight

T_b= mean average boiling point, °R

SG = specific gravity, 60F/60F

e) Adler and Hall

Use Figure 1

Critical Temperature

a) Riazi, Daubert (1980)

$T_c = 24.2787 * T_b^{0.58848} * SG^{0.3596}$

T_c = critical temperature °R

T_b = molal average boiling point, °R

SG = specific gravity, 60F/60F

b) Kesler, Lee (1976)

$$T_c = 341.7 + 811 * SG + (0.4244 + 0.1174 *SG) *T_b + (0.4669 - 3.2623 * SG) *10^5/T_b$$

T_c = critical temperature, °R

SG = specific gravity, 60F/60F

T_b = normal boiling point, °R

c) API Technical Data Book (1985)

Use API Procedure 4D1.1.

$$T_c = 186.16 + 1.6667 * Delta - 0.007127 * Delta^2$$

T_c = critical temperature, °F

Delta = specific gravity (60F/60F) * (VABP+100)

VABP = volumetric average boiling point, °F

d) Twu (1984)

Use Figure 1 or iterative procedure from abstract.

e) Brule, Lin, Lee, Starling (1978)

$$T_c = 429.138 + 0.886861 *T_b - 4.596433 * 10^{-4} *T_b^2 - 2.410089 *10^{-3}* API * T_b + 1.630489 *10^{-7}* T_b^3 -1.430628 * 10^{-8} * API^2 * T_b^2$$

T_c = critical temperature, °K

T_b = normal boiling point, °F

API = specific gravity, °API

Critical Pressure

a) Riazi, Daubert (1980)

$$P_c = 3.12281 * 10^9 * T_b^{-2.3125} * SG^{2.3201}$$

P_c = critical pressure, psia

T_b = mean average boiling point, °R

SG = specific gravity, 60F/60F

b) Kesler, Lee (1976)

$$\begin{aligned}
\text{Ln } P_c = {} & 8.364 - 0\ .0566/SG-(0.24244 + 2.2898/SG \\
& + 0.11857/SG^2) * 10^{-3} * T_b + (1.4685 + 3.648/SG + \\
& 0.47227/SG^{\ 2}) * 10^{-7} * T_b^2 - (0.42019 + 1.6977/SG^2) \\
& 10^{-10} * T_b^3
\end{aligned}$$

P_c = critical pressure, psia

SG = specific gravity, 60F/60F

T_b = normal boiling point, °R

c) Twu (1984)

Use Figure 3 or iterative procedure from abstract.

Critical Volume

a) Riazi, Daubert (1980)

$$V_c = 7.5211 * 10^{-3} * T_b^{0.2896} * SG^{-0.7666}$$

V_c = critical volume, ft^3/lb

T_b = mean average boiling point, °R

SG = specific gravity, 60F/60F

b) Brule, Lin, Lee and Starling (1982)

$$V_c = 3.01514 * MW^{1.02247} * SG^{-0.054476}$$

V_c = critical volume, ft^3/lb

SG = specific gravity, 60F/60F

c) TWU (1984)

Use Figure 2 or iterative procedure from abstract.

Critical Compressibility Factor

a) Ideal Gas Law

$$Z_c = \frac{P_c * V_c}{R * T_c}$$

Z_c = critical compressibility factor

P_c = critical pressure

R = gas constant

T_c = critical temperature

V_c = critical volume

Benedict-Webb-Rubin Orientation Parameter

a) Brule, Lin, Lee, Starling (1982)

$$BWR = 333.333 + 151.244 * (T_c/T_b) - 519.841 * (T_b/T_c) + 38.9063 * (T_b/T_c)^4 + 1255.01 * \text{Log}\,(T_b/T_c)$$

BWR = Benedict-Webb-Rubin orientation parameter

T_c = critical temperature, °R

T_b = normal boiling point, °R

Watson Characterization Factor, "K"

a) API Technical Data Book (1985)

Use API Figure 2B2.1

b) Kesler, Lee (1976)

$$K = T_b^{1/3}/SG$$

K = Watson characterization factor

T_b = normal boiling point, °R

SG = specific gravity, 60F/60F

Liquid Molar Volume

a) at 20°C, 1 atm

Riazi, Daubert (1980)

$LMV = 7.6211 * 10^{-5} * T_b^{2.1262} * SG^{-1.8688}$

LMV = liquid molar volume, cm^3/g-mole

T_b = mean average boiling point, °R

SG = specific gravity, 60F/60F

b) at Normal boiling point

Reid, Prausnitz, Sherwood (1977)

$LMV = 0.285 * 1.048 V_c$

LMV = liquid molar volume, cm^3/g-mole

V_c = critical volume, cm^3/g-mole

Enthalpy of Vaporization

a) Riazi, Daubert (1980)

$H_v = 8.48585 * T_b^{1.1347} * SG^{0.0214}$

H_v = heat of vaporization, Btu/lb-mole

T_b = mean average boiling point, °R

SG = specific gravity

b) Adler and Hall (1985)

Use Figure 1

At various temperatures from boiling point to critical temperature using the method of Reid, Prausnitz and Sherwood (1977) 212 (??).

$\Delta H_v = \Delta H_{vb} * Tr * (x+x^q)/(T_{br} * (1+x^p))$

ΔH_v = Heat of vaporization at desired temperature, Btu/lb-mole

ΔH_{vb} = Heat of vaporization at normal boiling point, Btu/lb-mole

Tr = reduced temperature at desired temperature (T/T_c)

T = desired temperature

T_c = critical temperature

T_{br} = T_b/T_c

T_b = Mean average boiling point

$x = T_{br} * (1-T_r)/(T_r * (1-T_{br}))$

$p = 0.13856$

$q = 0.35298$

Ideal Gas Heat Capacity at 0°F

a) Riazi, Daubert (1980)

$$C_p = 4.0394 * 10^{-7} * T_b^{2.6724} * SG^{-2.363}$$

C_p = ideal gas heat capacity, Btu/lb mole °F

T_b = volumetric average boiling point, °R

SG = specific gravity, 60F/60F

Isobaric Liquid Heat Capacity at 0°F

a) Kesler, Lee (1976)

$$C_p = -0.32646 + 0.02678 * K - (1.3892 - 1.2122 * K + 0.03803 * K^2) * 10^{-4} * T - 1.5393 * 10^{-7} * T^2 - C_F * [(0.084773 - 0.080809*SG -$$

$$C_F = [12.8/K-1) * (10.0/K-1 * 100]^2$$

$$(2.1773-2.0826*SG)*10^{-4} *T+(0.78649-0.70423*SG)*10^{-7} * T^2]$$

C_p = ideal gas heat capacity, Btu/lb mole °F

K = Watson characterization factor

T = desired temperature, °R

b) API Technical Data Book (1985)

Use API Procedure 7D2.2

Pitzer Acentric Factor

a) Reid, Prausnitz and Sherwood (1977)

$$W = \frac{-\text{Ln } Pc - 5.92714 + 6.09648*A^{-1} + 1.28862 \text{ Ln}A - 0.169347*A^6}{15.2518 - 15.6875*A^{-1} - 13.4721 *\text{Ln}A + 0.43577 A^6}$$

W = Pitzer acentric factor

$A = T_b/T_c$ °K/°K

T_b = mean average boiling point, °K

T_c = critical temperature, °K

P_c = critical pressure, atm

b) Kesler, Lee (1976)

$$W = -7.904 + 0.1352 * K - 0.007465 * K^2 + 8.359 * T_{br} + (1.408 - 0.01063 * K)/T_{br}$$

W = Pitzer acentric factor

K = Watson characterization factor

T_{br} = reduced normal boiling point, °R/°R

Fugacity

a) API Technical Data Book (1985)

Enthalpy

a) Kesler, Lee (1976)

Using equations and figures from Kesler, Lee, the enthalpy can be determined.

b) API Technical Data Book (1985)

Use API procedure 7B4.2

Solubility Parameter

a) API Technical Data Book (1985)

$$S = [(\Delta H_v - \frac{RT}{MW}) * \rho]^{1/2}$$

S = solubility parameter

ΔH_v = heat of vaporization at 25°C, cal/g

R = 1.9872 cal/g-mole °K

T - temperature, 25°C → 298.15°K

MW = molecular weight

ρ = density at 25°C, g/cm^3

Viscosity

a) API Technical Data Book (1985)

Use API Figure 11A4.1

Surface Tension

a) API Technical Data Book (1985)

Use API Figure 10A3.1

Thermal Conductivity

a) API Technical Data Book (1985)

Use API Figure 12A3.1

Liquid Vapor Pressure

a) API Technical Data Book (1985)

Use API Procedure 5A.10

Mean Average Boiling Point

a) API Technical Data Book (1985)

Use API Figure 2B1.1

Volumetric Average Boiling Point

a) API Technical Data Book (1985)

Use API Figure 2B1.1

Molal Average Boiling Point

a) API Technical Data Book (1985)

Use API Figure 2B1.1

Cubic Average Boiling Point

a) API Technical Data Book (1985)

Use API Figure 2B1.1

Heat of Combustion

a) API Technical Data Book (1985)

API Procedure 14A1.3

$$GHC = 17{,}672 + 66.6 * API - 0.316 * API^2 - 0.0014 * API^3$$

GHC = gross heat of combustion at 60°F, Btu/lb

API = API gravity

b) Adler and Hall (1985)

Use Figure 1.

DOE/MC/11076-2448 CHARACTERIZATION OF DOE REFERENCE OIL SHALES DOE